2015

Alternative Restraint Methods in Child Restraint Systems

Kazimierz Andrzej Czubernat
University of Windsor

ALTERNATIVE RESTRAINT METHODS IN CHILD RESTRAINT SYSTEMS

By

Kazimierz Czubernat

A Thesis Submitted to the
Faculty of Graduate Studies through
Mechanical, Automotive and Materials Engineering
in Partial Fulfillment of the Requirements for
the Degree of Master of Applied Science at the
University of Windsor

Windsor, Ontario, Canada

2015

ALTERNATIVE RESTRAINT METHODS IN CHILD RESTRAINT SYSTEMS

by

Kazimierz Czubernat

APPROVED BY:

_____

N. Zamani

Department of Mechanical, Automotive and Materials Engineering

Mechanical Engineering

_____

A. Edrisy

Department of Mechanical, Automotive and Materials Engineering

Materials Engineering

_____

W. Altenhof, Advisor

Department of Mechanical, Automotive and Materials Engineering

Mechanical Engineering

January 6, 2015

DECLARATION OF ORIGINALITY

I hereby certify that I am the sole author of this thesis and that no part of this thesis has been published or submitted for publication.

I certify that, to the best of my knowledge, my thesis does not infringe upon anyone's copyright nor violate any proprietary rights and that any ideas, techniques, quotations, or any other material from the work of other people included in my thesis, published or otherwise, are fully acknowledged in accordance with the standard referencing practices. Furthermore, to the extent that I have included copyrighted material that surpasses the bounds of fair dealing within the meaning of the Canada Copyright Act, I certify that I have obtained a written permission from the copyright owner(s) to include such material(s) in my thesis and have included copies of such copyright clearances to my appendix. The permission for reuse of Figure 1 on page 11 can be found in Appendix D.

I declare that this is a true copy of my thesis, including any final revisions, as approved by my thesis committee and the Graduate Studies office, and that this thesis has not been submitted for a higher degree to any other University or Institution.

ABSTRACT

This research focuses on methods to reduce the frequency of negative health events experienced by premature and low birth weight infants in child safety seats as well as methods to mitigate some of the risk of injury to an infant during both crash events and aggressive driving conditions. Simulations were carried out using a computer model of an anthropomorphic testing device within a child safety seat subjected to various aggressive driving conditions, a frontal impact, and a side impact. The performance of the system was based on neck angle, observed head acceleration and various loads in the neck of the infant dummy. Two different prototypes were investigated; a preemie positioning device and a head restraint system. It was observed that the preemie positioning device was able to reduce head accelerations by up to 13.2 percent in front and side impact simulations, while keeping similar levels of neck forces and increasing the amount of neck extension up to 20 percent. The head restraint system in turn provided a small increase of 3.2 percent in the neck angle observed and a reduction of 10.3 and 16.3 percent for the peak head accelerations and neck forces experienced in the frontal impact. Meanwhile a decrease of neck angle by 5.5 percent and increase in head acceleration by 14.2 percent with neck forces lowered by 7 percent at the lower neck joint in the side impact.

DEDICATION

I would like to dedicate this thesis to my loving parents, two sisters and younger brother. All of their love and support made the completion of my master's degree possible. I would also like to dedicate the thesis to all those who have impacted and supported me along my journey.

ACKNOWLEDGEMENTS

The author is incredibly grateful for his academic advisor, Dr. William Altenhof, who provided guidance and motivation throughout the duration of this research. His knowledge of vehicle crashworthiness and finite element modeling helped tremendously and his patience throughout the years will not be forgotten. The author would also like to thank the Auto21 Network Centres of Excellence for the funding provided to carry out this research. The contributions from the Woodbridge group and its members were crucial to the progression of this research. The guidance received from the staff in the Neonatal Intensive Care Unit at the Windsor Regional Hospital was also very beneficial to several aspects of the research that could not have been obtained otherwise. All of the contributions provided by all parties involved are greatly appreciated.

TABLE OF CONTENTS

LIST OF FIGURES

ABBREVIATIONS

ATD	Anthropomorphic Testing Device
BPM	Beats per Minute
CATIA	Computer Aided Three-dimensional Interactive Application
CMVSS	Canadian Motor Vehicle Safety Standards
CRS	Child Restraint System
FEM	Finite Element Model
FMVSS	Federal Motor Vehicle Safety Standards
HANS	Head and Neck Support
HIC	Head Injury Criterion
HRS	Head Restraint System
NICU	Neonatal Intensive Care Unit
PMHS	Post-Mortem Human Subjects
PPD	Preemie Positioning Device
USA	United States of America

NOMENCLATURE

a	Acceleration
HIC	Head injury criterion
t	Time

1. INTRODUCTION

Every year hundreds of thousands of lives are affected by road traffic accidents. In 2011, in Canada, there were 2006 fatalities, and 166 725 total injuries, of which 10 443 were serious injuries [1]. Among those, infants aged zero to four years had 16 fatalities with 2116 total injuries, 81 of which were serious injuries [1]. Although these young children are not a large portion of the fatalities and injuries, the accidents involving them are considered to be much more tragic for the families.

Child Restraint Systems (CRSs) have been found to greatly reduce the chance of severe injuries, when used properly, for this younger population. It has been found that the reduction in risk of death of 71 percent can be observed and the risk of injury is decreased by 67 percent [2,3]. Newborns and young children are more vulnerable in vehicles for a number of anatomical reasons and current CRSs are not well adapted for a certain newly born population. Preterm and low birth weight infants do not always have a suitable restraint method for them without the use of some form of adaptation. There are recommendations and guidelines to try and make sure these infants get home safely and in a timely manner, but there is no standardized restraint method or procedure to ensure all children are being prepared and tested the same way. These infants are at an increased risk of respiratory complications due to the low development at such an early age or such a small size.

The number of preterm infants born every year is increasing globally, with 15 million babies being born preterm in 2011, which accounts for more than one in ten infants [4]. These infants are responsible for a significant amount of medical costs incurred by the government, families and insurance companies in both Canada and the United States of America (USA). In Canada and the USA, roughly 30 thousand (2009) and 500 thousand (2007) premature infants, respectively, are born per year [5,6].

The purpose of this research is to develop a suitable restraint method for this vulnerable population that is growing in size every year. The research will focus on low birth-weight and preterm infants to provide safety in potential everyday driving conditions and in the event of accidents. The project is a joint effort between the University of Windsor, industry partners and medical staff at Windsor Regional Hospital

(WRH). This research will study the effects of two prototypes designed to adapt a CRS for prematurely born and low birth weight infants to improve the fit and potentially increase the safety of these infants while traveling in a vehicle. Aggressive driving conditions and crash scenarios will be investigated to evaluate the performance of these prototypes against each other and compared to the current status quo of a CRS with no standardized method to adapt the seat. This study will evaluate the performance of these prototypes in terms of head accelerations, neck loads, head positioning and other parameters to determine whether or not these proposed designs are a potential solution to the problem at hand.

2. LITERATURE REVIEW

2.1 Economic Burden

Several studies have been undertaken to determine the cost of these infants either on their own or relative to a healthy full term newborn discharged without complications from the hospital. A study containing a sample size of 193 thousand infants by Phibbs and Schmitt [7] determined that the earlier infants were born the more their stay cost on a daily basis. At 24 weeks gestational age the median cost among infants was $2356/day (for 92 days), whereas at full term (37 weeks gestational age), the cost associated with keeping a child at the hospital was $295/day (for two days). Another study by Muraskas and Parsi [6] found daily costs in Neonatal Intensive Care Units (NICU) to often exceed $3500 per child. It was also found that it was not uncommon for the entire duration of a child's stay to cost over $1 million. Russell et al. [8] found that the average cost associated with preterm infants was $1170 per day for 12.9 days and with full term infants was $315 per day for 1.9 days. It was also found that, although, the earlier the child is born the higher the cost associated with caring for that child in the hospital, the major burden on the healthcare system (or private insurance companies in the US) is still the near full term infants who account for 80 percent of all preterm births and 64 Percent of total hospitalization costs [8].

Society is often responsible for absorbing the economic burden generated by road traffic accidents. In 2004, traffic related accidents were the third leading cause of overall injury costs, accounting for 19 percent ($3.7 billion) of total cost of injury and economic

losses. It was the leading cause of indirect costs, accounting for 23 percent ($2.1 billion) of total indirect costs. Indirect costs consist of the value lost to society as a result of the injury. These could be, for example, the inability to go to work and perform regular tasks and contributing to the creation of products or wealth. In Ontario alone, motor vehicle incidents resulted in 400 deaths, 4805 hospitalizations, 1249 permanent partial disabilities and 126 permanent total disabilities in 2004 [9]. Children consist of a small portion of these fatalities and injuries and these figures indicate the strong need for proper safety mechanisms in vehicles.

2.2 Infant Anatomy

When dealing with infants of this size and early age it is important to keep in mind that the anatomical differences between these small infants and fully grown adults are significant. Not only do they differ in size, but also in body proportions, mass distribution and functionality.

Preterm infants do not fit into all CRS properly without additional padding or material added. Harnesses straps will often be too loose, harness strap slots could be too high above the infant's shoulders (will generally always lead to a loose harness if additional material is not provided for the infant) and the retainer clip may not be able to adjust to the appropriate height because of its size relative to the infant [10]. If a child doesn't fit properly within a CRS then the risk of injury and/or death is significantly increased because the seat is not restraining the infant and bearing the loads as it was designed to do.

The structural body of an infant is also much different than that of an adult in terms of bone structure, musculature and posture. In general, bones from young children are poorly mineralized and have a low elastic modulus [11]. This leads to large amount of deformation allowed in the bones of an infant when a smaller load is applied which is not desirable for the developing child. It could result in permanent deformation of crucial bones such as in the skull or ribs which would not allow for proper development of internal organs or could cause great injury to those organs. Not only are the infant bones softer, but the skulls are extremely flexible because instead of being one solid piece the skull bones are segmented into several smaller pieces that are not yet attached; making

the head of the infant much more susceptible to injury due to impact trauma [12]. At birth the head accounts for ¼ of the total body length, meanwhile the adult head is generally $1/7^{th}$ of the body length [12], this leads to a different mass distribution in the infant with a large proportion of the infant mass found in the head, one of the components not restrained by the CRS. All the muscles are generally present after 38 weeks gestational age [13], however, they have not yet had the chance to strengthen or grow in size. A full term infant is born at 37 weeks gestational age and preemies, prematurely born infants, are born before the 37 weeks have been completed. As a result, low birth-weight newborns and preemies lack the proper muscle strength in the neck to support the head and slow down or reduce violent head movement [12,13].

There have been several studies which set out to determine the mechanical properties of the human neck to determine injury thresholds and failure points. Most of the literature available on the mechanical properties of the neck has been completed using full grown adults. However, there are a handful of studies that have analysed the perinatal and pediatric spine in both the tensile and bending loading conditions [14-16]. Luck et al. [15] studied the biomechanics of the cervical spine on post-mortem infants aged between 20 weeks gestation and 14 years. The cervical spine was stripped of any musculature or ligamentous tissue prior to any mechanical testing. Tensile testing was completed to failure for 3 separate segments of the infant neck (O-C2, C4-C5, and C6-C7). Minimum, average and maximum ultimate failure loads observed, for all neck segments, corresponded to 142 N, 205.5 N and 360.5 N respectively. These minimum, average and maximum values were obtained from only those specimens aged 0.4 months or less in order for the loads to be representative of the target population being studied. Ouyang et al. [16] also studied biomechanics of the cervical spine, however, the test subjects ranged from 2-14 years of age. The results from both studies [15,16] were consistent when considering the same age group in children. However, both of these studies differed significantly when compared to the results obtained in the study by Duncan [14], where, five fully intact post-mortem newborn foetus' were loaded until disseverment took place (the location for disseverment was always the neck). The Post-Mortem Human Subjects (PMHS) were hung between two parallel bars below the biparietal diameter of the head and an apparatus consisting of a hook was mounted just above the ankles of the infant to

attach weights. The spinal column of the PMHSs, in 3 out of 4 cases, gave way before complete decapitation; indicating that the life of the child is compromised before complete decapitation. The minimum, average and maximum loads experienced by the neck at failure are 400 N, 470 N and 540 N respectively. The forces experienced for failure to occur here are nearly twice as large as those seen by Luck et al. [15]. This indicates that, although musculature is underdeveloped and weak, ligaments and muscles still play a very important role in the load bearing capacity of the preemie cervical spine. Similar findings were found in a study, on the muscular and ligamentous cervical spine in adults, by Van Ee et al. [17]. The study was completed in 3 phases and in phase 1 tensile testing was performed on the ligamentous spine to determine its tensile properties and failure thresholds. In phase 2, a combination of post mortem dissection of the neck and MRI scanning of live volunteers was used to determine the muscle geometry of the 50^{th} percentile male. The obtained geometry was then used along with previous research to determine mechanical properties of the muscles in the neck. Phase 3 consisted of creating a validated ligamentous neck model based on the experimental results obtained in phase 1. After that model was developed, the musculature was added to the model (in the form of 172 discreet nonlinear spring elements) based upon the geometry obtained from phase 2 and material properties for the musculature obtained from the study by Myers et al. [18]. When a tensile load was applied without neck musculature the load in the neck corresponded to the tensile load applied to the system. The tensile limit was the lowest for the lower neck segments, 1800 N instead of 2400 N for the upper neck segments. However, when the musculature was present a tensile load of 1800 N applied to the structure the forces experienced in the neck segments ranged from a maximum of 640 N in the upper segments to -150 N (compression) in the lower neck segments. With the musculature present the load applied at failure corresponded to 4160 N and caused failure at the upper neck segments. These findings confirm that the neck musculature significantly increases the load bearing capacity of the cervical spine (228 percent increase in infants and 231 percent increase in adults).

2.3 Injury Mechanisms

Because of the nature of the infant anatomy (ligamentous laxity, un-ossified vertebrae, large relative mass of the head and weakness of the musculature in the neck) and of the CRSs (only torso is restrained while head and limbs are free to move) it should be anticipated that most, if not all, injuries should occur at the head or cervical spine region. Myers and Winkelstein [19] and Roche and Carty [20] confirm this in their review of published research looking into the mechanisms and tolerances of injury. However, Scheidler et al. [21] and Howard et al. [22] determined that head impact was the leading cause of injury among infants. The head of the infants is also soft and segmented as mentioned earlier and can be easily damaged when impacting the seat in front of the child, the side of the CRS or even the side wall of the interior cabin. Although it was found that head impact was the leading cause of injury in infants it was also noted that when head impact is present that is not the only location for injury. There is also an enormous amount of data that suggests neck injuries are among the top injury mechanisms in infants with the highest rate of morbidity and mortality [23-28]. Although there are so many studies that suggest that upper cervical spine injuries are much more common in children, some still try to dispute this and claim that lower neck injuries are just as common if not more common among the neck injuries seen in today's youth [29-31]. However, they also comment that as the age of the child decreases the tendency is more upper neck injuries than lower neck injuries (when children are less than 8 years old). Therefore, it is widely accepted that young infants are at a greater risk of upper cervical spine injury than lower cervical spine injury. Nitecki and Moir [31] and Nightingale et al. [28] found that injuries to the cervical spine in these younger infants were generally dislocations, hyperextensions and ligamentous disruptions. These injuries are considered to be caused by tensile loading of the neck and excessive neck flexion.

2.4 Airway Management

All newborns, preterm or not, are required to be in a CRS upon discharge from the hospital when travelling by car. However, it has been found, that preterm and full-term infants are at risk of oxygen desaturation (a reduction in the amount of oxygen carried in the blood, healthy levels are between 95 and 100 percent oxygen saturation), bradycardia

(a slower than normal resting heart rate, fewer than 60 beats per minute (BPM) in adults and under 100 BPM in infants, who have a normal resting BPM of 120-160), and apnea (the cessation of external breathing or no movement of the muscles used in inhalation and unchanged volume of the lungs) when in a CRS or a seated position [32-39]. Those studies found that a range of 12 percent to 30 percent of infants monitored within a child seat experienced at least one "respiratory complication" (oxygen desaturation, bradycardia and apnea) while the majority of those who experienced at least one event experienced more than one. Bull and Engle [33] stated that an increased frequency of oxygen desaturation, apnea or bradycardia may expose the infants to slowed neurological development (potentially affecting capability to socialize and learn in school in later years). It is proposed that the CRSs be adapted to the smaller infants using rolled towels either side of the infant and between the seatbelt webbing and the crotch of the infant. Merchant et al. [36] studied 50 preterm and 50 full term infants. It was found that premature infants are at an elevated risk for apnea, bradycardia, and oxygen desaturation and that even after the use of blanket rolls, 24 percent of preterm infants still do not fit securely within a suitable CRS. Mean oxygen saturation levels decreased from 97 percent (92-100 percent) in a supine position to 94 percent (87-100 percent) after 60 minutes of being placed within their CRS. Prolonged periods of oxygen saturation below safe levels could be harmful for the development of the infant. Twelve percent of premature infants were found to have episodes of apnea and bradycardia during the monitoring period while term infants did not experience any. In a slightly smaller study by Kinane et al. [35], 34 infants were studied in a CRS and compared with infants in a car bed. Half of the infants spent 10 percent of the study time with oxygen saturations below 95 percent while one third spent 20 percent or more of the time below that mark. Six of the 34 infants spent half of the study time with oxygen saturation levels below the recommended levels. Salhab et al. [40] also tried comparing the incidence of adverse respiratory events when a child is in a CRS compared to when it is in a car bed. The study analyzed 151 infants in both a CRS and a car bed with slightly stricter criteria (longer duration and lower oxygen saturation levels needed) to determine whether children are more at risk in a CRS or a car bed. Oxygen desaturation was defined as an oxygen saturation of less than 88 percent lasting for ten seconds or more while apnea was defined as an interruption of breathing

for twenty seconds or more; or less than twenty seconds accompanied by bradycardia, and bradycardia was defined as a heart rate of less than 80 BPM for 5 seconds or more. Fifteen percent of infants (23) had an event in the car seat and six percent required intervention from a nurse (repositioning, suction or oxygen administration). These studies show that newborn infants, and especially prematurely born infants, require constant monitoring in a CRS because they are at an increased risk of adverse respiratory events and are not always able to recover from them on their own.

As a result of these reports, indicating infants not maintaining oxygen levels or experiencing apnea and bradycardia, investigations have been undertaken to attempt to determine whether or not these conditions pose any serious risks for the infants involved. Tonkin et al. [41] evaluated 43 infants who were referred to a cot monitoring service after apparently life threatening events. This was done over the span of 18 months between July 1999 and December 2000 in the Auckland region of New Zealand where there are approximately 15000 births per year. Only one infant was preterm and the rest were full term with normal growth. Seven of these infants, including the preterm infant, were found blue in their CRS and when placed in the position of the original episode the heads flexed forward causing the jaw to press down against the chest. It is also possible that more similar cases were found and unreported; therefore, the numbers presented are not necessarily inclusive for that region. Cote et al. [42] performed a similar study to determine the incidence of sudden deaths in infants occurring in sitting devices and whether premature infants account for a significant number of these deaths. Data for the retrospective study was obtained from the coroner's office for the entire province of Quebec (Canada). Data for 508 deaths was obtained but 409 of those were unexplained. Seventeen deaths occurred in a sitting device with ten of those being unexplained. Premature infants were not found in excess in the group of children found dead in a sitting device, however, children below one month of age were found to be at an increased risk of dying unexpectedly in a sitting device. Three of the seventeen cases were children who were known to be at an increased risk of airway obstruction. Tonkin et al. [41] and Cote et al. [42] have found that younger children (less than one month of age) are at an increased risk of unexpected death in car seats when compared to

those infants found in a laying position and that the longer infants are in a sitting position the more the risk is increased.

Studies have also been performed to try and identify the mechanisms or events responsible for the various respiratory complications associated with infants in a sitting position. Among those, Reber et al. [43], studied the effect of chin lift on airway dimensions during sedation, using magnetic resonance imaging, on ten children aged between two and eleven years. The diameter of the pharynx (portion of the throat behind the mouth and nasal cavity; serves as passage for both food and air) was measured in three different places and areas were also considered (because of the varying front to back and side to side diameters) comparing two scenarios with the head in the same position relative to the tabletop and torso but with tape keeping the mouth closed for one set of measurements. Chin lift, which resulted in mouth closure, increases the diameter of the pharynx at all measuring points in all children and could serve as a good mechanism to prevent airway obstruction or collapse. Wilson et al. [44], studied the effect of neck posture on maintaining an open airway. The study consisted of nine infants, examined at the time of their autopsy, weighing between 760 and 3500 grams and having survived between 1 hour and 3 months after birth. The upper airway was cleaned, the esophagus (tube or passage connecting the pharynx to the stomach) was tied closed low in the neck and soft cannulas were inserted and tied to the trachea (tube or passage connecting the pharynx to the lungs) and one of the nostrils (while the other nostril and mouth were sealed with adhesive tape. Both cannulas were connected to manometers and a syringe was also attached at the tracheal cannula in order to inflate the airway initially and slowly release the pressure. This experimental setup can be seen in Figure 1 (a). The pressure was initially 15-20 cmH_2O and was lowered until airway closure was observed (when the tracheal pressure was not being transmitted to the manometer in the nose. When this occurred the pressure recorded was termed the closing pressure. The nasal pressure was then returned to atmospheric pressure by opening the three way tap in the cannula and tracheal pressure was increased using the syringe until there was a sudden equilibrium between the tracheal and nasal pressures to determine the opening pressure. It was found that opening pressure was larger than closing pressure, indicating that once the airway has collapsed there is a small amount of adherence between the walls of the airway and

that it is harder to reopen the airway than to maintain it open. When the degree of neck angle remained constant, turning the head or changing the positioning of the child did not significantly affect closing pressure. The angle (degree of neck flexion or extension) is measured between two lines; one line passes through the outer edge of the eye and the ear canal while the other line represents the longitudinal axis of the infant's trunk and is shown using orange annotations in Figure 1. At a neutral neck angle of 90 degrees the mean closing pressure was -0.7 ± 2.0 cmH_2O (indicating that pressure at or below this small negative value generally induced airway collapse). Neck extension beyond 90 degrees made the airway more resistant to collapse (closing pressure of -5.2 ± 0.8 cmH_2O for neck angle of 120-130 degrees) and neck flexion below a value of 90 degrees was found to induce upper airway closure (closing pressure of $+7.4 \pm 0.6$ cmH_2O for neck angle of 60-70 degrees). This information can also be obtained from the graph in Figure 1 (b). Peak inspiratory pharyngeal pressures can reach -0.6 cmH_2O during average tidal breaths and -1.5 cmH_2O during a periodic sigh [45-48]. This means that without the assistance of the muscles used to keep the airways open the transmural pressures experienced during regular breathing would be enough to induce airway collapse unless the neck is in extension. However, the muscles are active in infants during transport home and so these conditions do not guarantee airway collapse. Neck flexion is still undesirable because neck angles below 90 degrees will increase the risk of airway collapse.

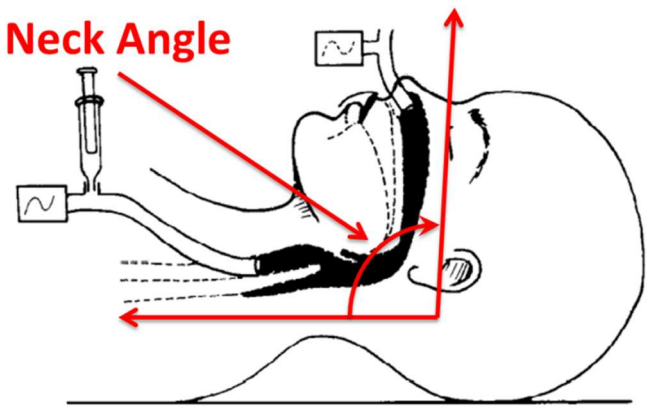

(a)

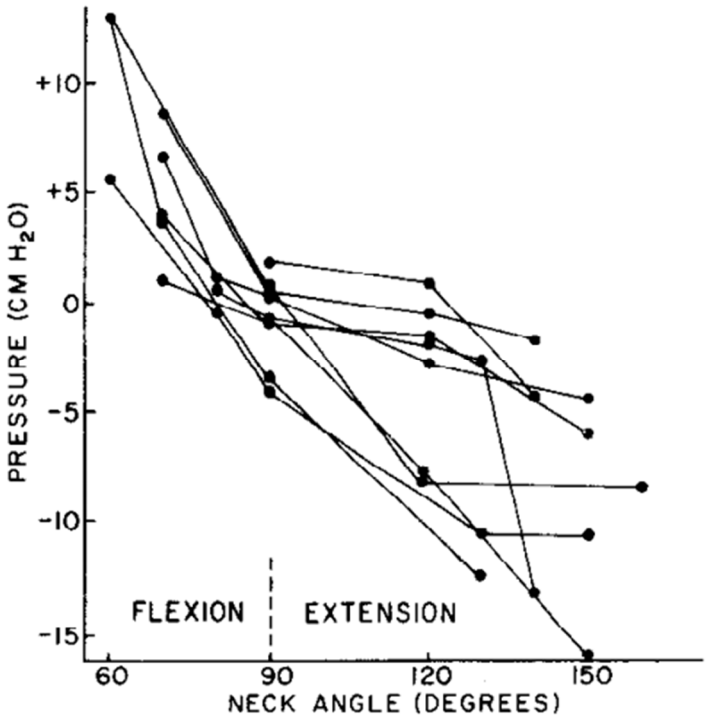

(b)

Figure 1 – Study by Wilson et al. [44] (a) experimental setup used (b) closing pressure as a function of neck angle.

Because of the respiratory risks associated with using a CRS the American Academy of Pediatrics recommends the implementation of a car seat challenge prior to discharge from the hospital [49]. Children are monitored prior to discharge in a CRS to try and

identify the infants with respiratory complications that could be dangerous while travelling in a vehicle. Although the recommendation has been around for several years to try and monitor infants there are no hard set regulations on how long to monitor the children being discharged, what information should be monitored, and what is considered a failure of the test [13,33,36]. In most cases the children are monitored for a period between 60 and 120 minutes. Oxygen levels, heart rate, respiratory rate and apneic events are generally monitored [50]. Towels are rolled and placed to either side of the child and in the crotch region to try and adapt the child to the CRS. Thresholds for failure need to be identified and made uniform across all hospitals with some data to back up the numbers used for that threshold.

2.5 Related Research

2.5.1 A Brief CRS History & Background

CRSs have been around for a long time. The first introduction for a restraining device designed for infants was in 1898. The design was not a sitting device of any kind, but instead consisted of a bag with a drawstring that you could place the child inside and attach to the seat to prevent the infant from moving around and falling off the seat while the vehicle was in motion. However, restraining devices did not start being used as safety devices until the introduction of the first child seat designed for safety in the 1960s. However, when first introduced to the market there was no interest in buying them because of a lack of knowledge regarding their importance in the event of a crash. All of the US states required a child to be restrained in a CRS by 1995, with the process starting in the mid-1980s [51]. There are several different types of restraint systems that are/were widely available such as the T-Shield harness, the Overhead Shield, a 3-point harness and a 5-point harness [52].

The T-Shield restraints have harness straps attached to a “T’ shaped rubber piece. This seat is no longer being manufactured because of its lack of adaptability to smaller infants who cannot use it because the shield would come up too close to the head and neck and could cause safety issues in the event of a car accident [52]. The overhead shield consists of shoulder and crotch belts with a large plastic bar used to restrain the lap portion of the infant. This type of CRS is also not suitable for smaller infants because of

lack of adjustability and the potential for head injuries when contacting the shield during an impact. The 3-point harness consists of two shoulder belts and a crotch belt and is slightly easier to operate than a 5-point harness but does not provide as much support for the body. The 5-point harness is by far the most versatile and widely used for infants in rearward facing CRSs because of the wide range of infants it can secure. In addition to the two shoulder belts and the crotch belt, there are two belts that secure the infant at the hip level. This configuration also provides more support for the infant in the event of side impacts. Figure 2 shows three of the four mentioned types of CRS, however, the 3-point harness is identical to the 5-point harness with the exception that it has no straps going to either side of the hips.

(a) (b)

(c)

Figure 2 – Different types of child safety seats: (a) T-Shield Harness, (b) Overhead Shield, and (c) 5-Point Harness.

2.5.2 Recent Research

Work has been completed to try finding a solution to some of the aforementioned complications via clinical trials and computer simulations of proposed solutions. Shorten et al. [53] studied 12 children between the ages of ten months to eight years of age who were found to be at risk of airway obstruction because of sedation and inability to use the muscles that would normally prevent the obstruction. Two different positioning techniques were used in order to try and correct this issue by increasing the diameter of pharynx. A sniff position (placement of the head of the child that provides a small level of neck extension to keep the airway open) pillow and a simple foam insert were used. The sniff position pillow is placed under the neck and serves to keep a neutral or slightly extended neck angle, while the foam bolster was simply placed behind the shoulders to elevate them. The sniff position pillow generated a significantly greater degree of atlanto-occipital (joint between the uppermost segment of the neck (atlas) and the bottom segment of the skull (occipital bone)) extension as well as a significantly greater diameter of the pharynx. However, both positioning techniques showed no signs of airway obstruction or oxygen desaturation. Although that study did not concern infants/children in the appropriate age group, it is important to note that shoulder elevation does not have the same effect as supporting the spine to increase the neck angle. Tonkin et al. [54] created an insert for a CRS that allowed for the infant's head to rest in a more neutral position. The insert consisted of a piece of foam that had a slit in the crotch area to accommodate the belt as well as an opening at the head to allow the head to rest further back than the torso. The insert had a similar concept to the shoulder elevation technique in the study by Shorten et al. [53] and aimed to reduce the amount of oxygen desaturation and prevent the narrowing of the upper airway. Seventeen preterm infants were monitored in a CRS both with and without the foam insert for a period of 30 minutes in each configuration. The introduction of the insert contributed to a wider airway opening, fewer events of desaturation (less than 85 percent blood oxygen levels), bradycardia (less than 90 BPM), and arousal. It was also concluded that oxygen desaturation has several factors and that head/neck flexion is a significant contributor to the problem. A follow up study by McIntosh et al. [55] using a very similar insert studied 78 full term infants (39 with the insert and 39 without) during sleep while restrained in a CRS. A moderate

desaturation event was classified as a fall in oxygen saturation of 4 percent lasting longer than or equal to 10 seconds and the insert did not change the rate of moderate desaturations occurring. However, the rate of obstructive apnea and the severity of desaturation events were improved. Although certain pillows and positioning devices have been investigated to determine their potential to prevent respiratory difficulties faced by the infants, it is recommended that only firm padding or very thin padding be used behind a child's back [56]. Soft padding, pillows, and soft foams will compress on impact and introduce some slack to the harness system generating impact forces when the child is thrown against the loose harness in the event of a crash [56]. In order to further investigate the potential use of an insert to combat the respiratory difficulties these vulnerable infants experience it would also be necessary to investigate the performance of such an insert under crash conditions.

Computer models are an economic and practical method to investigate the effects of a crash on occupants of a vehicle. In order to complete these numerical investigations mathematical models of the human body need to be created along with the system which will be restraining them. There are several computer models available based on anthropomorphic testing devices (ATDs), which can also be referred to as crash test dummies. There are three popular newborn ATDs along with one dummy representing a preemie. The newborn ATDs consist of the Civil Aeronautical Medical Institution (CAMI) newborn, the P0 and the Q0. Among those three, the CAMI and the P0 are both very simple and cannot be used to accurately predict the behaviour of an infant in crash simulations [57]. The Q0 is representative of a 6 week old infant with a mass of 3.4 kilograms [58]. It was designed for crash configurations and is able to measure head, chest, and torso accelerations as well as upper neck forces and moments. It is by far the most advanced of all of the newborn dummies but it is too heavy to be considered for an appropriate prediction tool for preemie behavior. Bondy et al. [57] developed a finite element model of a preemie/low birth weight infant. The model, shown in Figure 3, consists of 17 parts; of which seven are neck segments joining the head to the torso with seven translational and 8 rotational joints. The model was lighter than that of the Q0 with a mass of 2.5kg and also had more joints. The geometry was obtained from a Nita Newborn mannequin provided by the NICU at the WRH and the important geometric

parameters such as head circumference, chest circumference, and length among others were compared with measurements taken on infants at the NICU. Biomechanical properties for the neck were obtained from the studies by Ouyang et al. [16] and Luck et al. [15] and the dummy model was validated with respect to studies of the biomechanics of infant falls, shaken baby syndrome and the Q0 ATD.

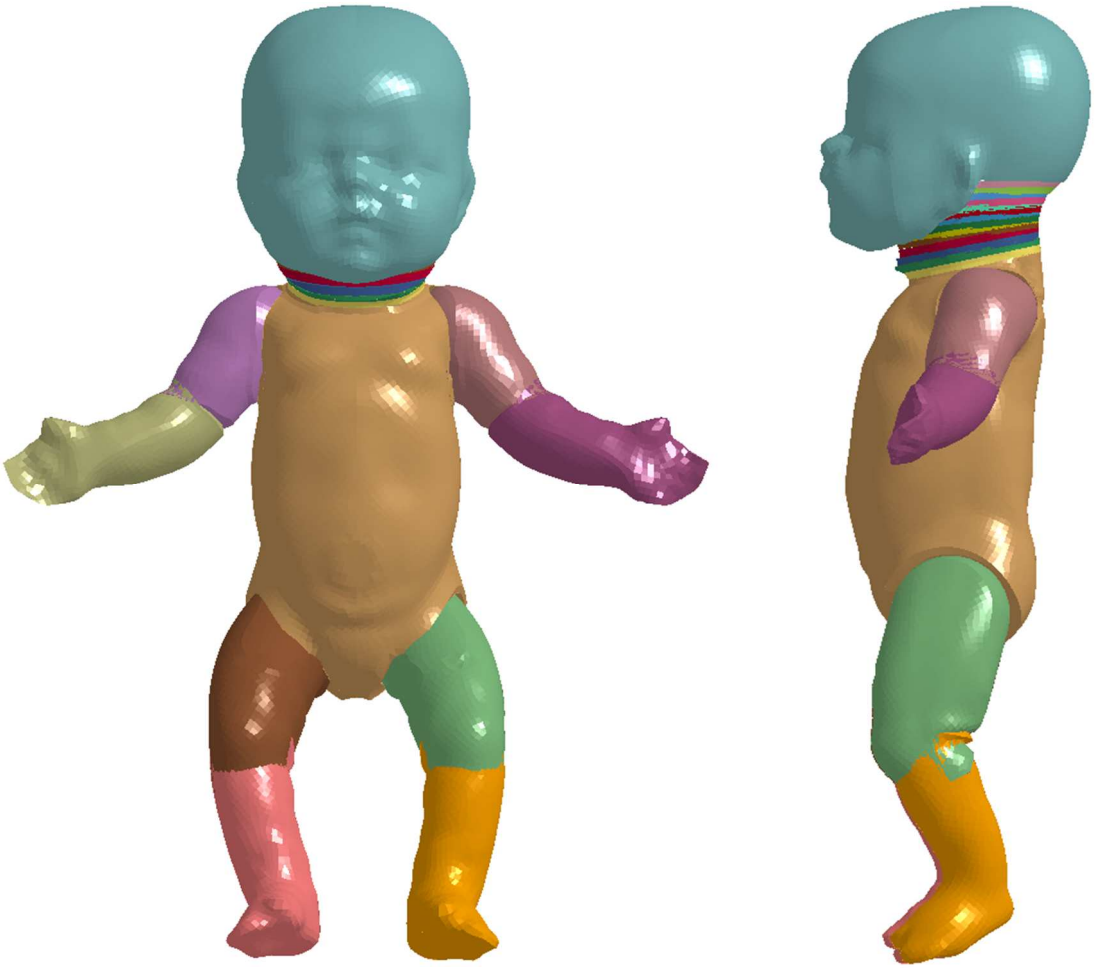

(a) (b)

Figure 3 – Infant ATD model created by Bondy et al. [57] (a) front view and (b) side view.

Chen [59], worked on the development of a restraint device for low birth weight infants and assessed the effects of such a device on the performance of the CRS in frontal crash, side crash and aggressive driving conditions. Aggressive driving conditions, in this

study, represent driving scenarios resulting in a more dynamic environment which heightens the potential for vehicular related injuries. These driving scenarios, which will be discussed in more detail later in the document, are not considered to be dangerous to full grown adult passengers but could introduce health risks for younger travellers who are unable to counteract the motions induced by such conditions. Existing crash input data was used along with data collected using accelerometers mounted in a CRS to obtain the acceleration profiles used for the aggressive driving conditions. The aggressive driving conditions are similar to those use by Stockman et al. [60,61]. In those studies the driving scenarios were meant to simulate the conditions leading up to a crash, so a sharp turn or sudden braking. The insert, shown in Figure 4, was designed with three different geometrical profiles to modify the neck angle when the child is in a resting position. There were also three different foam materials analyzed based upon material testing of 10 different foam specimens. Geometry and material were chosen based upon neck angles, head accelerations and neck forces observed in the various configurations. Those results were also compared to the results with the child in the CRS with no insert present to determine the impact of the insert on the functionality of the CRS. The insert was generally not found to decrease the peak head accelerations significantly; however, it did reduce the head accelerations after the initial peak, indicating that the insert does provide some damping for the system. Neck angle was improved across all scenarios and the head always returned to a favorable resting position after the disturbance was applied to the CRS.

(a) (b)

Figure 4 – Preemie positioning insert from a (a) front view and (b) side cut away view.

2.6 Head and Neck Restraints

In racing applications drivers generally make use of a five point restraint system alongside a head and neck support (HANS) device. The HANS device is restrained to the torso by the shoulder harness and seatbelt. The forces experienced that act to stretch the neck are reduced by 80 percent with the use of this device [62]. There are several safety benefits that come from the HANS in terms of head excursion (to reduce the possibility of hitting something in the vehicle) and head accelerations as well. A similar product for younger infants would be greatly beneficial since they lack strength in the neck muscles and have a larger portion of their body mass in the head than at an adult age. Kapoor [63] investigated the effects of implementing this device in a CRS with several ATDs representing three year old children. Two of the three dummies showed a reduction in head acceleration of between twenty and forty percent and all three dummies showed a reduction between forty and eighty percent in upper neck forces experienced.

3. FOCUS OF RESEARCH

The literature shows that keeping preemie babies in the hospital for extended periods is a great burden on the health care system in Canada and parents or their insurance companies in the United States. The number of prematurely born infants is also on the rise. Premature infants are still spending too much time at the hospital and there have been no significant recent advancements to try and speed up the process of these infants being discharged earlier. It is in the best interest of everyone to send the infants home as soon as possible; not only from a financial point of view for the families, the government, and insurance companies, but also for the health of the infants.

Although there has been some work done previously on the testing of a positioning device by Tonkin et al. [54], there is no data to suggest that the insert, produced by that research group, was tested physically or simulated in crash conditions. This is very important because the preemie infants are already at an increased risk of head and neck injury because of their underdeveloped neck musculature and disproportionate head size relative to their bodies. Not only must the clinical side be proven to be beneficial, but, the integrity of the ability of the CRS to protect the infant in the event of a crash must be considered as well.

This research is a continuation of the work done by Chen [59] on the development of a preemie positioning device (PPD). Although preliminary simulations were completed, several material models were validated and tested against each other, and several different geometries were investigated, some limitations remained. The simulations were implemented using a CRS larger than those intended to be used by the target population and the PPD prototype was designed to conform perfectly to the shape of the virtual dummy, leaving no room for variation in infant size and restricting the prototype to only one size of child. Numerical simulations will use the finite element model of the low birth weight infants generated by Bondy et al. [57] with some minor modifications to change some of the possible outputs and their coordinate systems.

Based on the lack of standardized clinical procedure for the car seat challenge, the need to get the infants who are healthy enough home safely and the promising

preliminary results shown in early developments of the PPD, the current research will focus on the following:

i. Generating adequate PPD geometry in order to fit a variable range of premature or low birth weight infants. Considering input from the Woodbridge Group (as an industry partner) and nursing staff at the Windsor Regional Hospital (WRH) NICU to satisfy all conditions that need to be met from all points of view.

ii. Investigating the performance of the updated CRS geometry and PPD geometry on the performance of the entire system. The performance will be based upon aggressive driving conditions and crash scenarios. The intended outcome for the PPD is to decrease the frequency and severity of airway complications by keeping the neck posture at a neutral and slightly extended angle.

iii. Investigating certain designs/configurations that could serve the same purpose as the HANS device, for restraining the head in the event of a collision to minimize neck forces and head accelerations. The desired outcome here would be to investigate the possibility of reducing the stresses induced on an infant's body during a crash event without adding too much bulk or complexity to the system or changing the positioning of the body.

4. PROTOTYPE DEVELOPMENT

4.1 PPD Development at the NICU

Initially the PPD geometry needed to be reconsidered. Previously in the study by Chen [59], 3 different geometries were considered, which provided a different neck angle in the resting/initial position. These geometry changes affected a small region near the neck and head and only changed the inner profile of the PPD. However, the outer geometry was not adapted to the type of CRS that is most often used by preemies, an infant only child seat.

The minor changes needed for the first iteration of the prototype consisted of trimming excess material in the region of the head and slightly reducing the overall thickness of the PPD for the child to sit a little closer to the seat back. The back profile of the PPD was modified to fit within the infant only child seat and the dimensions for the cut-out were slightly modified to avoid excess material around the head of the infant, while the shape of the cut-out remained consistent with the original design, which adhered to the dimensions of the NITA newborn doll obtained from the NICU. The PPD conformed very well to the shapes it was designed to fit because they were based on coordinates of over 100 thousand points on both the surfaces of the Nita Newborn mannequin and the CRS shell. The point cloud was obtained from a white light scanning process used by InspectX, a provider of coordinate measuring and optical metrology services based in Windsor. These points were then used to generate surfaces for the CRS and the mannequin to then generate appropriate geometry for the PPD. Those changes were implemented and the first physical prototype can be seen in Figure 5. Once a physical prototype was created, by the Woodbridge Group, a visit was scheduled at the WRH NICU to test the fit of the PPD with human subjects and to get some feedback on the design from the perspective of workers specialized in the care of these low birth weight or premature infants.

The first trial of the PPD was done using a CRS provided by the University of Windsor that had no back padding or cloth cover present. The infant used in the trials was almost ready for discharge and was approaching a weight of approximately 2.5 kg. The child was considered to be slightly larger than the average child at discharge. The PPD proved to fit very well within the CRS and provided ample support for the child while allowing for favorable positioning in the head and neck region. However, according to the manufacturer, if any of the padding associated with a safety seat is removed the guarantee for the seat provided by the manufacturer is void. Bull et al. [56] also discourage the use of padding inserted behind an infant during vehicular travel to prevent any slack being introduced in the seatbelt in the event of a crash. However, the PPD is being investigated as a medical device to prevent airway complications and the seatbelt is routed through the PPD which will not allow for the padding to remove itself from the CRS and generating slack that way. In addition, according to preliminary results by Chen [59] and results observed later in this study, the foam is not compressed significantly behind the torso but mainly behind the head; meaning that there is little slack generated in the seatbelt. This is to be expected because of the nature of the infant's heavy head compared to the rest of the body. As a result of the need for the manufacturer's padding, the PPD was then tested within a CRS provided by the family. Figure 6 shows the setup with the child inside the seat without the manufacturer's padding installed. The infant fit well within the prototype and the feedback from the nurses about the general positioning of the child was favorable with some room for improvement. Since the fit of the cut-out conformed to the baby's body so well there was some concern that the insert would not be able to accommodate all infants coming from the NICU because of the variability in size, most importantly in the head. The variation in the head can be quite large and such a tight fit for the roughly average infant selected for the fit test would not work for all children. The tight fit also prevented the range of motion of the child's head within the PPD. It is important for the infants to have some moving space primarily because of the possibility of the infant regurgitating its last meal and it is also important for the children to develop some musculature by moving the head around from side to side.

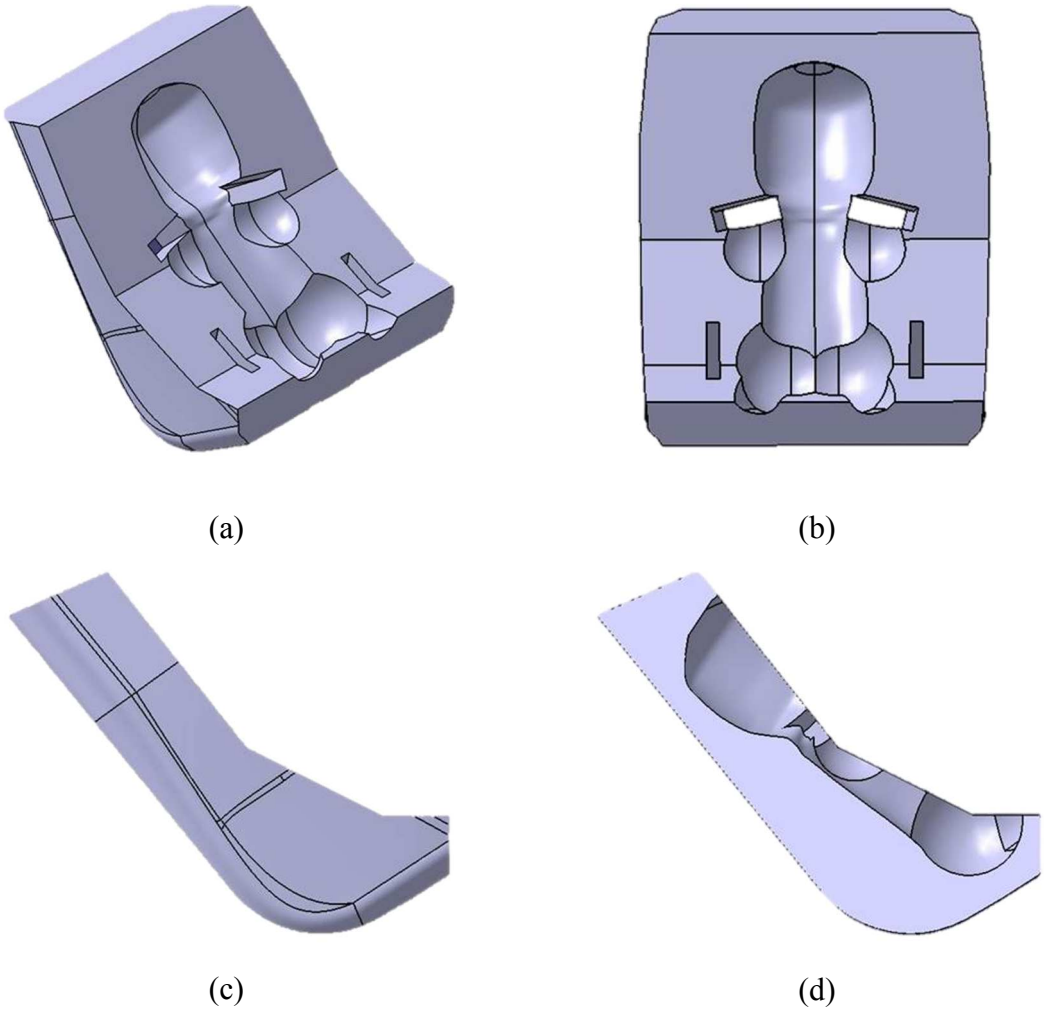

Figure 5 – First physical PPD prototype (a) isometric view (b) angled view of the front (c) side view and (d) side section view.

In order not to void the manufacturer's warranty, the original padding needed to be installed and the PPD needed to be checked for proper fit with that padding. Figure 6 (b) shows the deformation of the prototype when inserted into the CRS (it is most visible at the top center and bottom center of the positioning device). The PPD had to be forced into the CRS when the manufacturer's padding was present and as a result an infant could be placed in the device in this configuration because of the significant reduction in width of the entire cut-out profile.

(a)

(a)

Figure 6 – Physical testing of first prototype (a) with infant inside and no CRS padding (b) with CRS padding and no infant inside.

Based on the various observations and recommendations made by all parties present at the prototype demonstration, revisions were made to the three dimensional geometry of the PPD. The updated geometry took into account the various important aspects presented earlier and the changes made can be seen in Figure 7. The infant from this visit was slightly smaller than the child from the first visit and was not yet ready for discharge. However, with the parents' consent it was placed within the CRS al the same. The CRS with PPD installed proved to be a very soothing environment for the child as it was not disturbed while being inserted and did not become agitated in any way. Three millimetres of material was removed perpendicular to the entire cut-out profile to create extra space for the use of a small blanket or cover between the child and the PPD. The head space was elongated by 6.5 cm to accommodate the infants with larger heads and a chamfer was introduced to allow more room for side to side movement of the child's head (which is important in the event of regurgitation). When taken to the NICU again for observation

and feedback, the response of the nursing staff was very positive. No new concerns were raised by anyone in attendance and the prototype was considered ready for physical as well as virtual testing.

(a) (b)

Figure 7 – Updated PPD geometry (a) in a CRS with padding (b) in a CRS with padding and infant inside.

4.2 Head Restraint System Design

Because of the significant benefits introduced by a HANS device in racing applications along with the positive impact of a HANS device on young children observed by Kapoor [63], a method to introduce a similar safety enhancement to premature and low birth-weight infants. This was attempted with the goals of no increase in difficulty of use/installation of the entire safety system for the child and with the intention to keep the additional cost to implement the measures (if they are successful) minimal.

Several designs were considered with different methods of restraining the head, different types of materials used together, however all of the proposed designs seemed

too complicated to be manufactured at a low cost that would be beneficial to the family. Some of the devices required close fits to the infant which seemed impractical because of the short lifetime of such an item, due to the quick growth experienced by these infants in the early stages of life. Others proved to be slightly impractical because of the required method of restraint and potential risk of suffocation introduced by the restraint method. The initial proposed design was intended to eliminate the need for the chest clasp to keep the straps over the child and replace it with a cloth-like connection to reduce the amount of hard objects in the vicinity of the child. However, after some preliminary results using a spandex-like material obtained from the literature it was deemed to be impractical because it increased the risk of the child slipping out of the harness restraints. This was a concern because the shoulders of newborns are general very malleable and unable to carry any load because they are design to pass through the mother's pelvis. A graphical representation of this initial prototype idea can be found in Figure 8. This first investigated design was not intended to mitigate head accelerations but allow for a better force distribution across the torso of the infant instead of having the loads concentrated at the chest through a hard chest clasp. After some further research into past prototype designs and literature on the subject it was found that the effects of wearing a simple hoodie on the response of the head and neck during a crash event had not been investigated. Initially when considering this, a whole body suit was envisioned with reinforcement ribs going along the back and around the head to mitigate some of the head movement and attempt to attenuate the head accelerations. This idea was considered to be impractical because of the requirements of a tight fit and complex manufacturing methods for a suit that would only be used for a very short period of time. However, hooded sweaters for infants are fairly common and if the hood was fastened and provided a relatively good fit it could potentially prevent some of the head extensions experienced by the infant in both crash configurations. Not only this, but many infants are already leaving to go home wearing one piece outfits that do include a hood and it would not be too much to ask parents to try and buy tops or whole outfits with hoods instead of those without.

Figure 8 – Initial alternative restraint method considered.

The “hoodie” or “Head Restraint System (HRS)” was designed based on the geometry of the infant dummy model previously developed by Bondy et al. [57]. The surfaces of the dummy head and torso were offset from the initial design by three millimetres. These offset surfaces were then joined by a new generated surface to best represent the geometry a hooded top might have. However, the HRS did not come far down the torso or cover the arms as any regular hooded piece of clothing might. This was done to reduce the computational time associated with regions that would not greatly affect the results obtained.

The material chosen for the HRS was taken from a validated material model of seat trim used in the upholstery of a seat in a vehicle. This material was chosen as a result of its strength and durability being somewhat greater than clothing yet not too excessive to inhibit body movement. The experimental testing conducted on the material consisted of tensile tests using a MTS Criterion Model #43 universal testing machine equipped with a 50 kN MTS load cell. Since the material was non-isotropic the seat trim was loaded in the axial and transverse directions to determine the properties in both orientations. The elastic

modulus and Poisson's ratio in the axial direction are 7.43 MPa and 1.4 respectively, while in the transverse direction they are 8.17 MPa and 1.8 respectively. The density of the seat trim material is 10 kg/m^3. The tensile tests were reproduced numerically and the material model was simplified using an isotropic material model that was able to reproduce the response of the material adequately for the preliminary study to be carried out on the HRS, using the weaker of the two directions to keep the results in a conservative range. Although this simplification was implemented the numerical results matched closely to the experimental data with average stiffness in the axial direction being 2.40 N per mm (numerical) and 2.75 N per mm (experimental) while the stiffness in the transverse direction are 2.66 N per mm (numerical) and 2.70 N per mm (experimental). The HRS was modeled using the *MAT_FABRIC material card, which invokes a special membrane element formulation and is suitable for large deformations. The parameters elastic modulus and Poisson's ratio for the approximated isotropic material are 7.43 MPa and 0.38, respectively, and a fully integrated Belytschko-Tsay membrane element formulation was used. The average stress/strain response of the seat trim can be found in Figure 9 and was computed from the elastic moduli obtained from the seven experimental tensile tests. An automatic surface to surface contact algorithm with penalty formulation was used to define the contact between the dummy and the HRS. A static coefficient of friction of 0.424 was used along with a dynamic coefficient of friction of 0.25. These values were obtained through testing of the sliding behaviour or the cloth on aluminum. The fabric was mounted on a block of wood and attached to a load cell and pulled across different surfaces to determine the force required to initiate movement and the continuous resisting force while moving at a constant velocity. Although this was not a perfect representation the contact present within the model, the interaction with aluminum was more comparable to the contact in the model than the contact studied between the cloth and other materials found within the seat when performing the testing. The meshed geometry of the HRS can be seen in Figure 10.

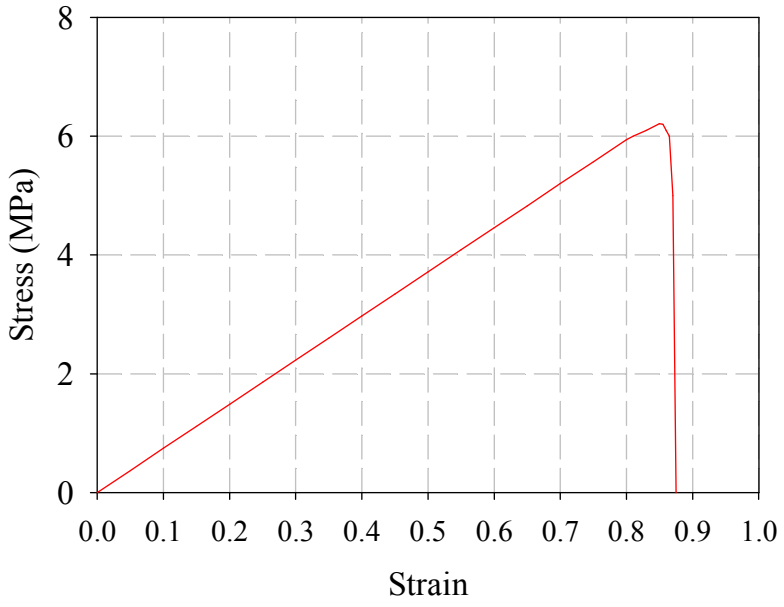

Figure 9 – Stress/Strain Response of the seat trim.

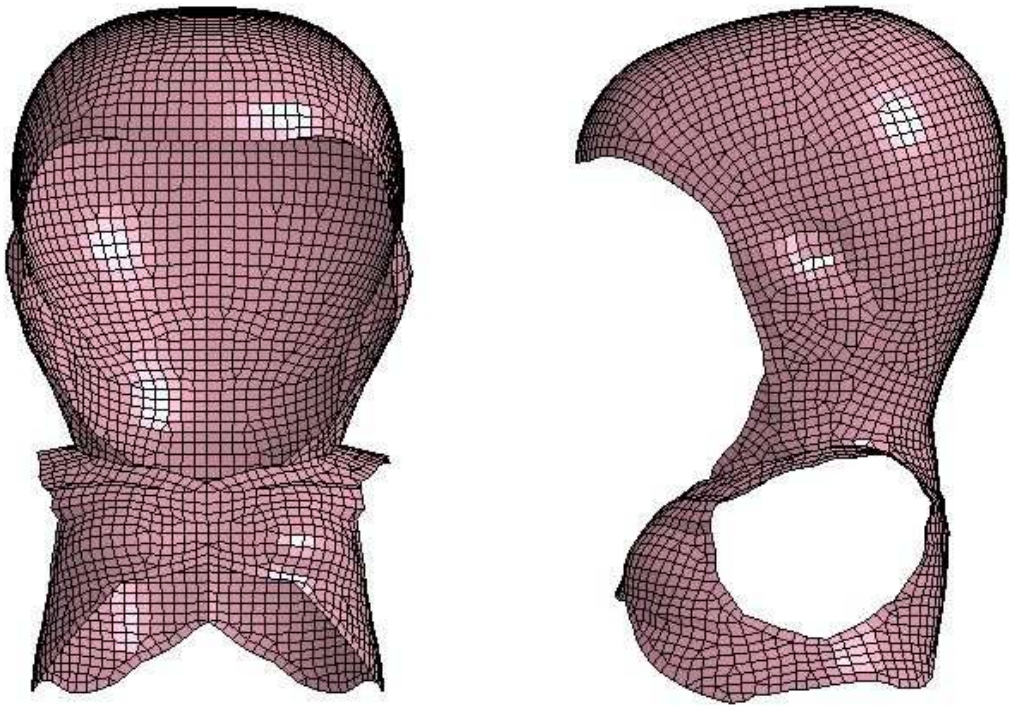

(a) (b)

Figure 10 – HRS design (a) front view and (b) side view.

5. MODEL DEVELOPMENT

The entire model was created and analyzed using Dassault Systèmes' Computer Aided Three-dimensional Interactive Application (CATIA), Altair's Hyperworks and LSTC's LS-DYNA and LS-PrePost software. Figure 11 illustrates the entire model and all of its components with the global coordinate system indicated in orange. The seat back is angled at 45 degrees relative to the XY plane, the positive x axis is directed from front to back of the CRS (or towards the front of the vehicle the CRS is in) while the y axis is directed from the infant's left to right and the positive z axis is pointed upwards.

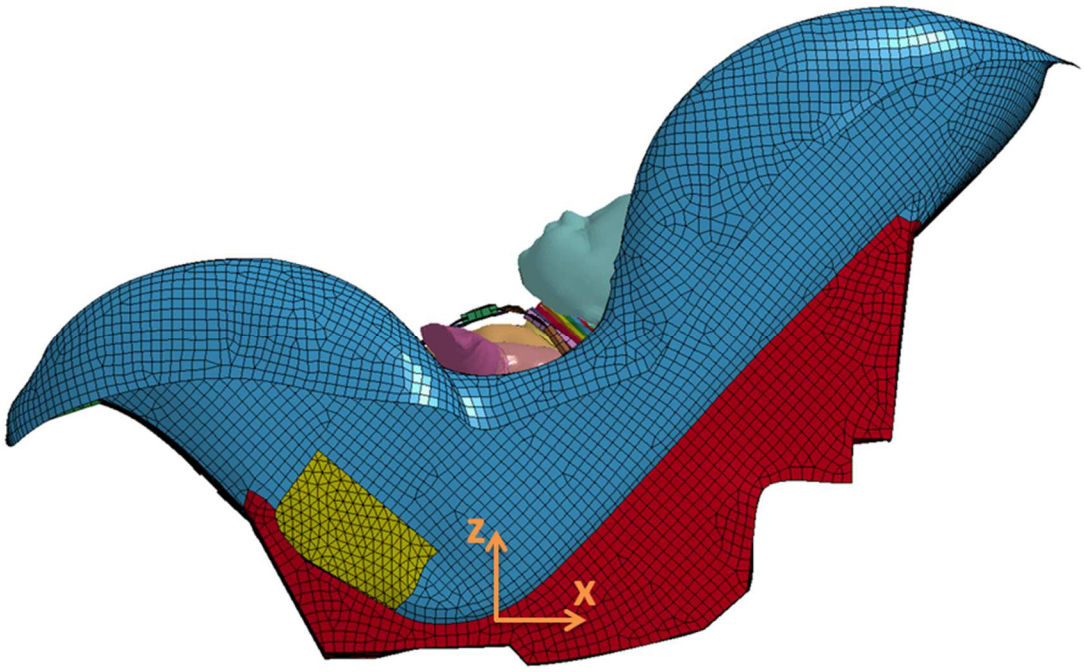

(a)

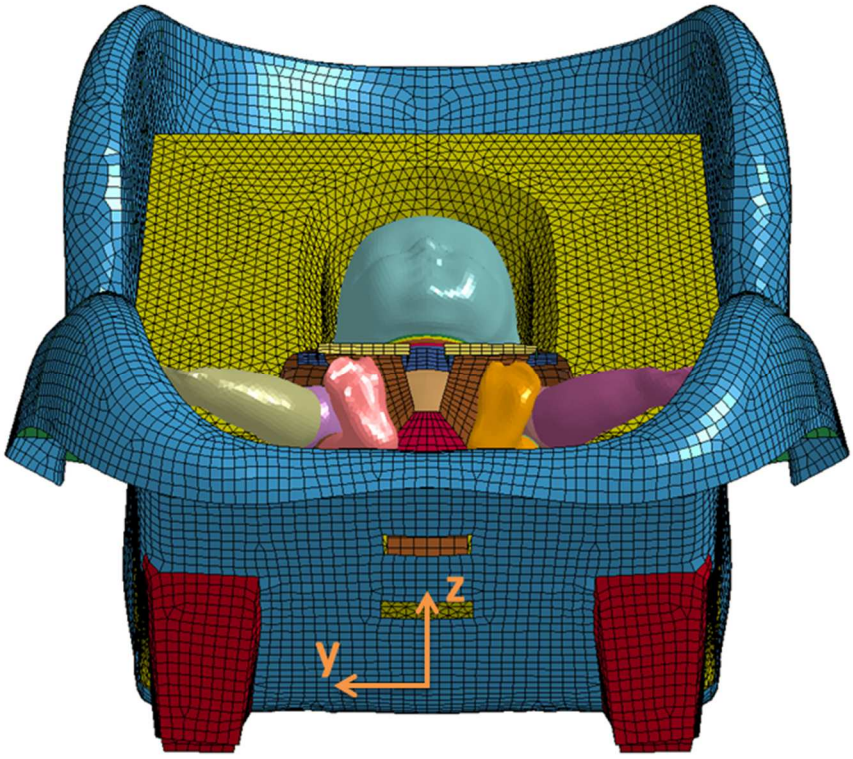

(b)

Figure 11 – Entire model with coordinate system shown from a (a) side view, and a (b) front view.

5.1 Updating CRS geometry

CRS geometry needed to be updated from the larger CRS used in the previous work by Chen [59] to reflect the most commonly used type of child seat used by preterm and low birth-weight infants. Surface geometry was obtained from a point cloud that was converted to be used within the finite element model (FEM), this is the same procedure and set of data as that described earlier in section 4.1. Some areas of the seat were not able to be scanned and included into the point cloud because of the orientation of the surfaces or the distance from the scanner. The missing surfaces of the CRS corresponded to the reinforcement ribs that provide a significant amount of structural rigidity to the seat. These surfaces were incorporated into the model using the data that was available from the point cloud along with physical measurements taken to finish the rest of the structure. Certain small features were omitted from the design because they were not important to the running of the simulations or the safety performance of the seat.

The two larger ribs, extruding from the bottom of the CRS, were modeled as rigid entities because they consisted of a thicker cross section and had reinforcement ribs running from side to side. Another reason for modeling the ribs as rigid is that when a compressive load of 2000 N was applied to the seat negligible deformation was observed in these two large ribs while it was evident that the seat wings were deforming significantly. The final meshed geometry can be found in Figure 12, with all of the colors indicating different shell thicknesses being used. The red portion of the seat corresponds to the rigid entities while the blue and green are the deformable portions with different thicknesses. The material used for the deformable portions of the CRS was originally developed and validated by Kapoor [63] by extracting material samples for tensile testing from the CRS and then a full component compressive test was conducted experimentally on a hydraulic Tinius-Olsen testing machine. This whole component compressive test was then reproduced numerically to obtain the necessary parameters for the material card. The *MAT_PIECEWISE_LINEAR_PLASTICITY card was used to model the behaviour of this material as an elasto-plastic material with a density of 800 kg per cubic metre, and elastic modulus of 842 MPa, a Poisson's ratio of 0.3 and a yield stress of 8.764 MPa (with the ability to define stress/strain data for the plastic behaviour). The stress/strain response of the CRS material can be found in Figure 13.

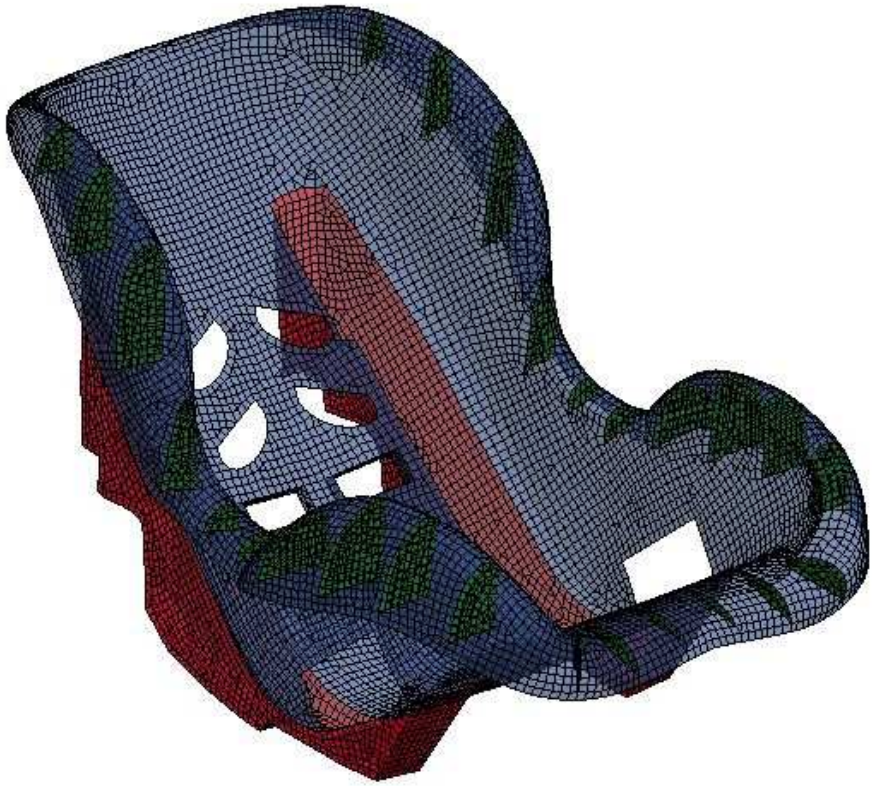

Figure 12 – Meshed final seat geometry.

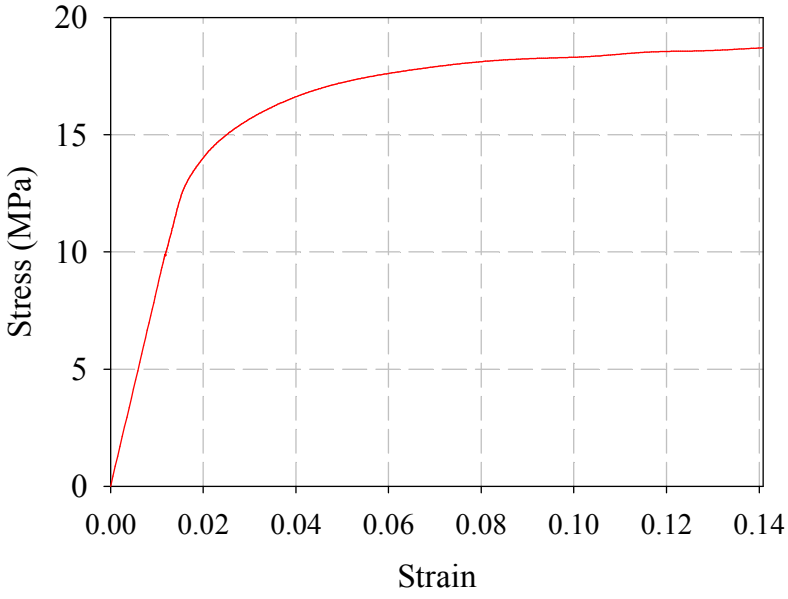

Figure 13 – Stress/strain response of the CRS polypropylene outer shell.

5.2 Updating Dummy

The ATD model for low birth weight infants developed by Bondy et al. [57] was used because of the lack of existing models for infants of that size/weight (less than 5 lbf). Some limited physical models exist, such as the APRICA dummy (physical dummy presented at the thirtieth international workshop for Injury Biomechanics Research), but that dummy is only a physical model and its performance has not been evaluated or peer reviewed by any body of scientific peers and is not recommended for use by its authors. Since the dummy was already generated there were only some simple modifications brought to the model in order to change some of the data that is possible to be extracted and some surfaces were added for various contact conditions.

When considering neck forces for evaluation in vehicular crash, resultant forces are a good way to compare across different configurations when doing a relative performance. However, tensile and shear forces alone would also be very interesting to know to compare the model to the actual physical thresholds that are documented in the open literature, such as the results presented by Luck et al. [15] and Duncan [14]. The previous configuration of the ATD finite element model had the neck segments outputting forces and moments in the global coordinate system which made it hard to identify the tensile load from the shear forces in the neck or determining the orientation of the moments in the constantly moving neck segments. A local coordinate system was added to each of the neck segments, as shown in Figure 14, to facilitate the process of obtaining the tensile and shear loads without the need for manipulation of the output data. This tensile data, in turn, can easily be used to compare with values from the literature.

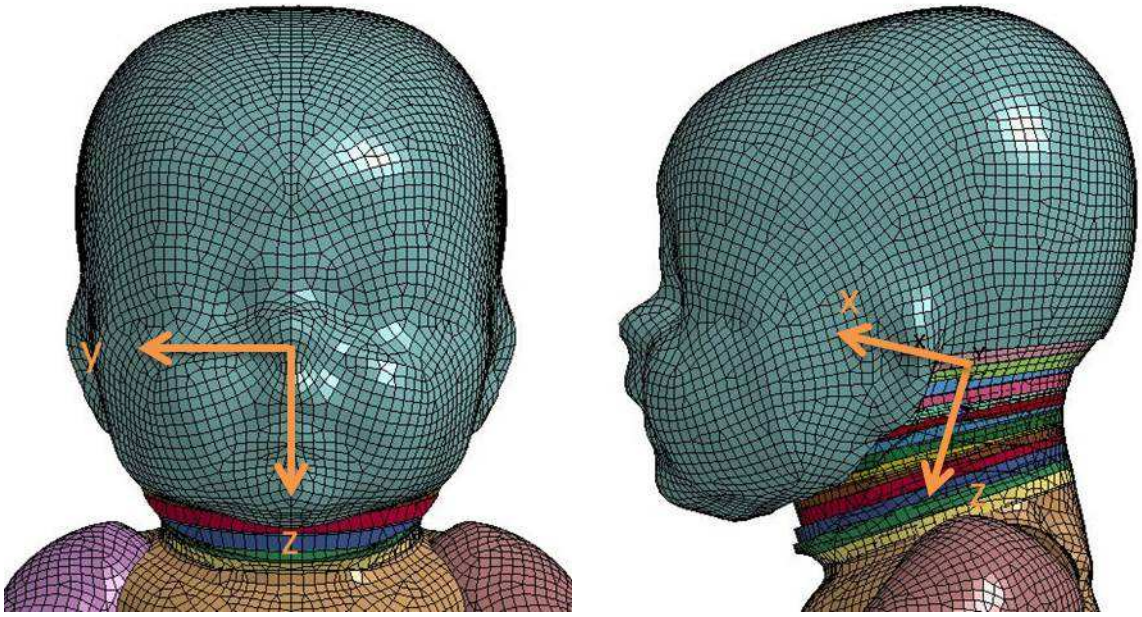

(a) (b)

Figure 14 – ATD head and neck with neck segment local coordinate system from a (a) front view, and a (b) side view.

Contact with certain portions of the dummy proved to be problematic in early simulations because of the large number of parts as well as their configurations. Firstly, the neck is composed of 14 parts, in the form of discs, which initially are all aligned and form a somewhat continuous surface with their sides. However, when an acceleration impulse is applied to the system, the neck segments move and create gaps for the seatbelt to potentially slide into causing contact issues. Secondly, the HRS would be prevented from sliding up too far off the torso in the event of a crash simulation by the armpit. There was no appropriate surface that could be used as the armpit of the child. The upper arms and torso do not have a contact algorithm preventing them from penetrating each other because that would not be an accurate representation of real life behaviour of the arms. As a result the area representing the armpit is a wedge in between the upper arms and torso that once in contact with the HRS cannot provide accurate kinematics of the system because once there is pressure applied the arms will be pushed upwards considerably (which is not the case when loading the armpit). Both areas of concern were addressed by introducing cylinders within the neck and through the torso at the level

of the shoulder joint to simulate the contact that was required. The cylinders were modeled as rigid bodies, however, in order to prevent them from adding any mass while still having appropriate contact characteristics the *CONSTRAINED_RIGID_BODIES keyword command was used. This merges two rigid bodies together and allows the possibility of the inertial properties of the slave part to be ignored if the master part uses the *PART_INERTIA keyword. An illustration of the cylinders inserted for contact purposes can be found in Figure 15; where one half of the dummy is transparent and the other half of the dummy is hidden.

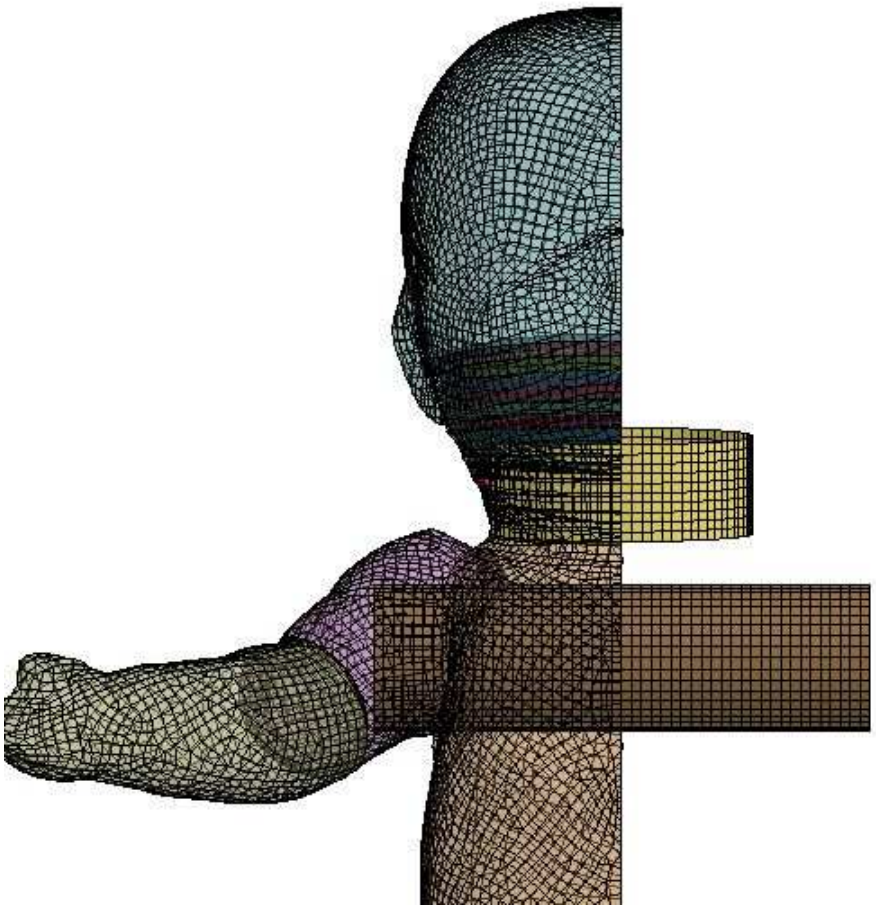

Figure 15 – Cylinders inserted into the dummy for contact surfaces.

5.3 Seatbelt

The seatbelt restraining infants in CRSs is a 5 point harness. Several different approaches were taken when trying to model the seatbelt. The entire system consists of the seatbelt webbing, the chest clasp and the abdomen clasp. The chest and abdomen clasps were both modelled as rigid entities and did not require any change of setup and geometry. The problems/difficulties with the restraint system were generated by the seatbelt webbing itself.

Initially the seatbelt webbing consisted of simple webbing using seatbelt elements and slip rings to attempt to accurately model the behaviour of a seatbelt during tightening. In this configuration, all of the seat belt ends in the abdomen and crotch section were constrained to not move relative to the CRS and only the shoulder straps were tightened via the metal clasp found behind the seat. Problems arising from this configuration included improper belt tightening, with the seatbelt having difficulty sliding through the slip rings properly when incorporated into the entire model. Test simulations were previously conducted with only the seatbelt elements and slip rings, which allowed proper sliding between the seatbelt elements and the slip ring, however, once incorporated into the model the behaviour was not consistent with previous trials. As a result, there was too much slack in the system and the infant ATD was not appropriately restrained. Another issue with this configuration was the contact definitions between the seatbelt edge and the neck as well as the seatbelt edge and the belt slots within the PPD, at both the shoulders and the pelvis. The issue in the neck region arose from the multiple neck segments present and the gaps generated when the ATD was disturbed and the belt becoming wedged between two neck segments or simply not detecting contact surfaces, parts or elements defined and sliding inside of the neck region. The issue associated with the contact interface between the belt and the PPD was the difference in material properties and the inability of a “Nodes to Surface” or “Surface to Surface” contact algorithm to solve the contact conditions alone. However, it is undesirable to have two contact algorithms between the same entities and contact algorithms on their own did not provide good results. Figure 16 shows the original seatbelt webbing along with the PPD and the infant ATD to help visualize the areas of concern described above as well as the routing method of the 5-point restraint system. The chest clasp consists of several parts

and is seen as the blue and yellow entities found together in proximity to the chest. The abdomen clasp, where all belts are fastened, is the pink entity in the crotch region. The 2 dimensional *SEATBELT_SHELL elements, which cannot be visualised with the mesh as quad elements in LS-PREPOST, are depicted by the yellow and green entities either side of the abdomen clasp. The brown quad elements are the regular shell elements that account for the majority of the seatbelt and are modeled using the *MAT_FABRIC card with a density of 890.6 kg/m^3, an elastic modulus of 2.07 GPa and a Poisson's ratio of 0.3. Isotropic material behaviour was also assumed based on the material validations carried out by Kapoor et al. [64]. The elements consisted of quadrilateral shell elements using fully integrated Belytschko-Tsay membrane elements with a thickness of 1.24 mm. The stress/strain response of the seatbelt webbing can be found in Figure 17.

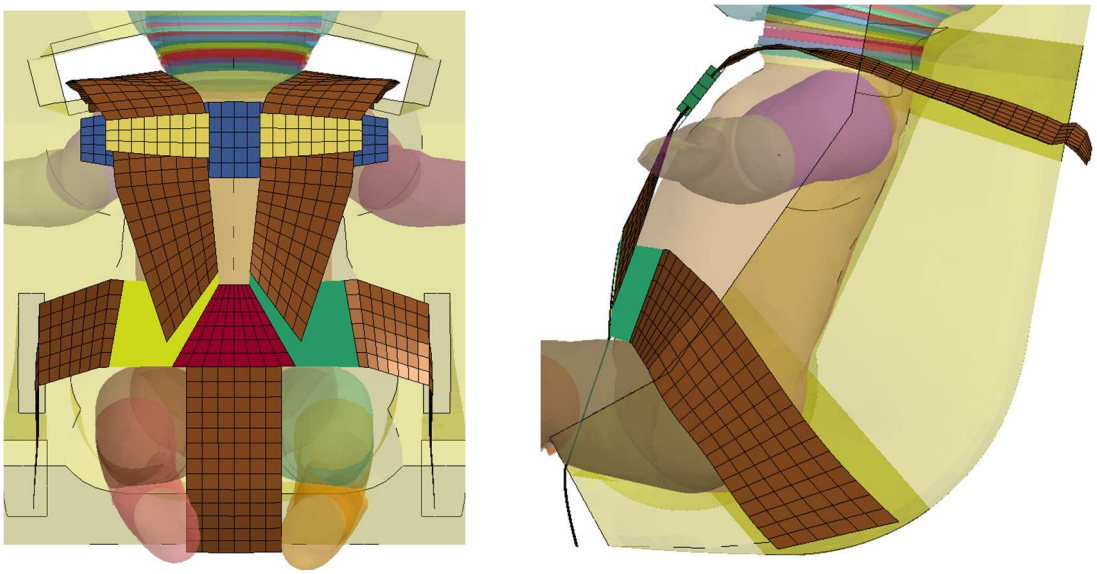

(a) (b)

Figure 16 – Seatbelt setup with seatbelt elements and slip rings from a (a) front view and a (b) side view.

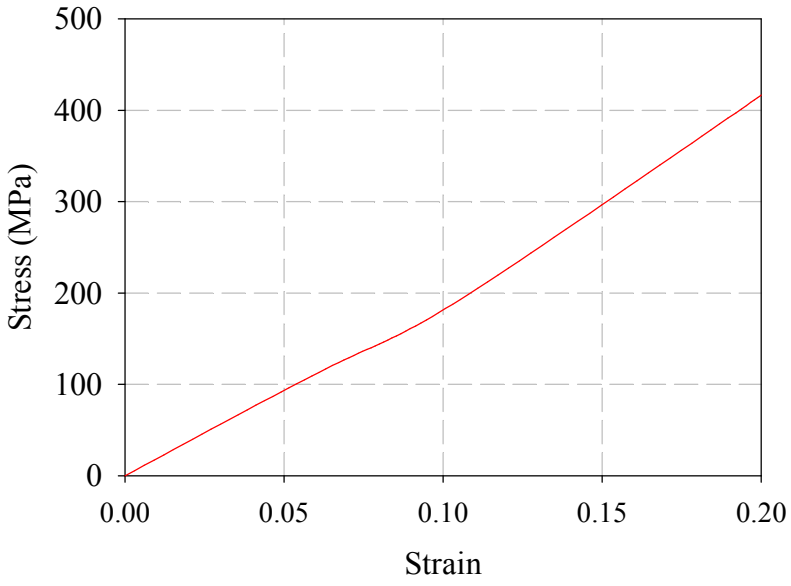

Figure 17 – Stress/strain response of the seatbelt webbing.

In order to overcome some of these difficulties several modifications were made by simplifying, adding or removing parts. The first difficulty, the slip rings not working properly, was overcome by replacing all of the *SEATBELT_SHELL elements with regular shell elements, identical to the elements being used everywhere previously shown in brown. Because of this change, the tightening method for the seatbelt needed to be updated accordingly. Instead of only applying a displacement for tightening to the metal clasp at the end of the shoulder straps, the abdomen straps also needed to be tensioned to remove any slack from the seatbelt in that region. In order to do this a row of rigid elements was added to each strap end at the side of the infant ATD (the loading methods will be described later). The contact issue between the seatbelt edges and the neck/PPD slots was corrected with the addition of soft solid pentahedron elements added to the seatbelt in the areas of interest to create a better contacting surface. A soft foam material, with the same properties as the PPD (will be discussed in greater details in the following section), was utilized to minimize the addition of weight to the system and the flexibility of the seatbelt. The added elements added 0.85 g to the entire system which had a mass of 4.09 kg. This addition was considered to be insignificant when considering the entire system. The added pentahedron elements added a surface for contact between the

problematic areas and prevented the belt from becoming wedged between two neck elements when openings were created. Although a rigid cylinder was previously added to the ATD to try and combat this issue, both options were considered simultaneously and the addition of elements to the seatbelt seemed to provide a better solution to the problem. Figure 18 shows the added pentahedron elements as well as the change in element formulation from two dimensional seatbelt elements to shell elements using the fully integrated Belytschko-Tsay membrane. The blue component corresponds to the chest clasp, the orange component corresponds to the abdomen clasp, the green components corresponds to the added pentahedron elements, the red components correspond to the rigid belt tensioners, and the grey component corresponds to the seatbelt webbing.

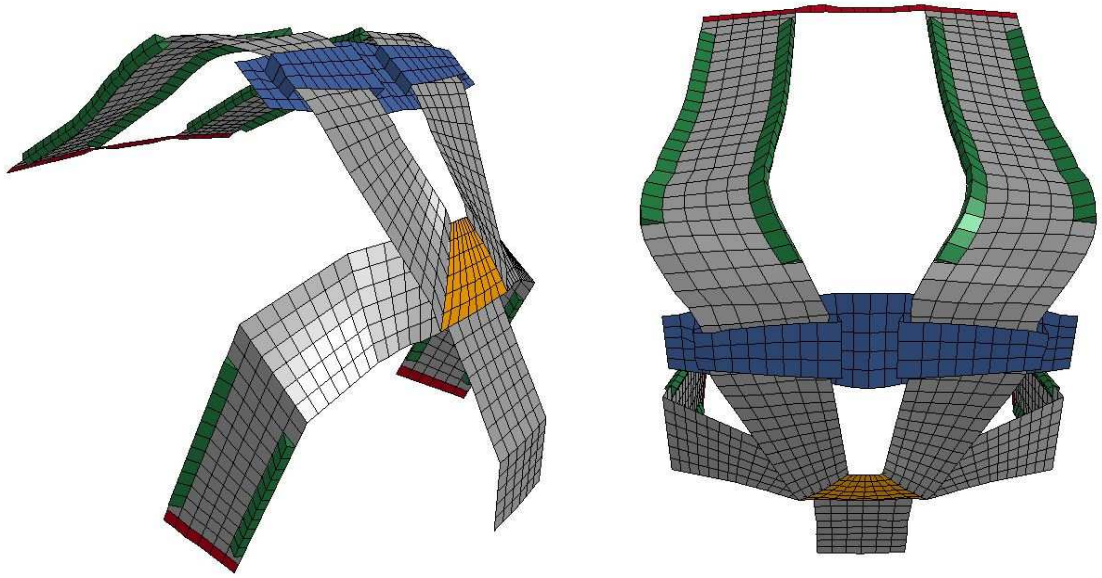

(a) (b)

Figure 18 – Updated seatbelt design and configuration (a) Isometric view (b) Top view.

5.4 PPD

The PPD was meshed using tetrahedral elements because of its complex shape and need to be modeled as a solid entity. The foam material used for the PPD was selected based on a parametric study completed by Chen [59]. Compression tests were completed using foam blocks for 10 different foam specimens and 3 candidates were chosen for

comparison; one of the stiffest foams, one of the softest foam and one of the foams in the middle range. The foams were also considered based upon their different characteristics and upon recommendation from the Woodbridge Group. After the parametric study, the foam that provided the best possible performance to meet the criteria (neck angle, head accelerations, neck forces and moments) was chosen and was used in this study with the updated PPD geometry and configuration. *MAT_LOW_DENSITY_FOAM was used to model the PPD because it represents highly compressible low density foam and allows for the input of a stress/strain response to model the appropriate behaviour. The density of the foam used is 60.2 kg/m^3 and the elastic modulus is 117.7 kPa. Aside from the general material properties there is a possibility for defining several other parameters, of which the hysteretic unloading factor and shape factor were used. The presence of the hysteretic unloading factor results in an unloading curve that lies beneath the initial loading portion of the curve and allows for energy dissipation in the foam. The foam used for the PPD had a hysteretic unloading factor of 0.005 and a shape factor of 3. The stress/strain response of the foam can be found in Figure 19.

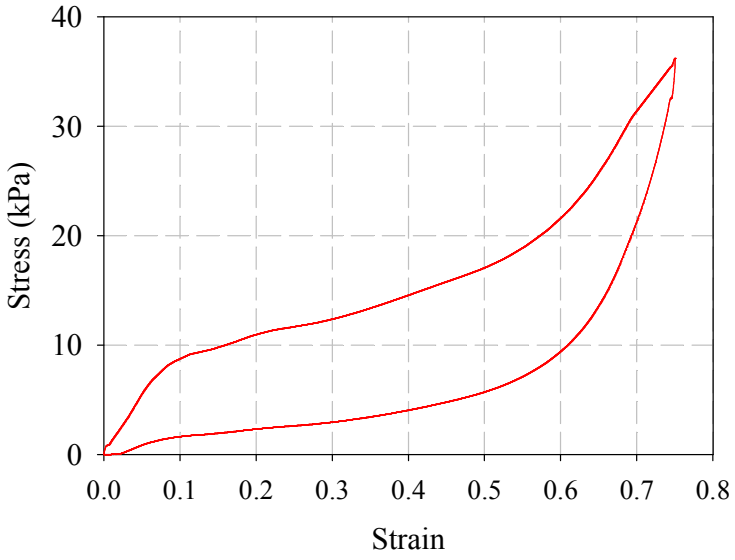

Figure 19 – Stress/strain response for the foam material used in the PPD.

When running early versions of the crash simulations there was a negative volume problem observed. To combat this issue the *CONTACT_INTERIOR keyword was used

alongside the use of some artificial stiffness applied to the foam in the larger deformations of the foam. The *CONTACT_INTERIOR keyword is intended for use with foam hexahedral and tetrahedral elements. It introduces a contact algorithm between the inner surfaces of the solids to try and eliminate the occurrence of negative volumes. There are a few parameters that can be modified; the penalty scale factor for the contact algorithm, the level of compaction reached before this contact algorithm becomes active and the type of algorithm used to calculate the contact. The default penalty scale factor of one was used along with an activation factor of 0.7 (meaning that the interior contact is activated at 30 percent crush) and a contact formulation of type two, which is designed to control both the shear and compression modes. The activation factor was gradually increased to the value of 0.7 obtained while checking the model results to see if any significant changes to the model resulted. For the artificial stiffness, the initial behavior of the foam remains unchanged, however, at the larger compressions the foam behave as a stiffer entity to prevent the negative volumes form occurring. The point where artificial stiffening is introduced is decided by the engineer since it is simply implemented by changing the data in the stress/strain response to a point where the problem of negative volumes is removed.

A combination of both methods was used in the simulation because neither of the two methods was able to provide adequate results on their own. When using these methods to prevent negative volumes the final behaviour of the modified behaviour must be monitored so that it is not modified too significantly with the introduction of the artificial stiffening or interior contact. When neither of the two methods was being applied the foam appeared to be crushing to 95-100 percent of its initial thickness in the region behind the head. After artificial stiffening and internal contact were applied the compression was reduced to 85-90 percent in that same region. This was not considered to significantly affect the results of the simulation, because, this issue was mainly encountered in the frontal crash scenario and the initial through thickness of the PPD directly behind the head where problems were arising was small; between 2 cm and 3 cm. Therefore, the largest observed reduction in crush possible would be 0.5 cm which would not greatly affect the kinematics of the simulation.

6. SIMULATION PROCEDURE

The simulation consisted of two events; the first was the tightening of the seatbelt and application of gravitational loads, and the second was application of a disturbance to the system (disturbances consisted of crash events and aggressive driving acceleration pulses). Both events were simulated in a transient analysis instead of through dynamic relaxation because of the lack of an accurate representation of the response the system should have had when subjected to belt tightening procedures.

The initial belt tightening events were achieved by applying a displacement using the *BOUNDARY_PRESCRIBED_MOTION_RIGID card in a local coordinate system that only allowed movement relative to the CRS and not the global coordinate system. The belt displacement was applied over 0.09 seconds and an additional 0.01 seconds were allowed for the system to relax temporarily before the crash or aggressive driving disturbances were applied. The portion of the seatbelt that passes over the shoulder is has a displacement of 30 mm in the negative Z direction while the two abdomen straps are pulled down 18 mm in the local Z direction Although dynamic relaxation was not used, global damping was added to the system to manually impose the similar conditions to those seen in dynamic relaxation. There was also a brief pause, where no loads were applied to the system, when everything was allowed to come to rest before the disturbance for the main event was applied. The local coordinate system had the same orientation as the global system, as seen in Figure 11 on page 32. The amount of tension applied to the belt was approximated qualitatively via trial and error, determining when all of the slack in the belt was gone with different displacements. The displacements were applied to the belt ends, depicted in red in Figure 18 above. The previously mentioned belt tightening and preloading will be presented and discussed in greater detail in Figure 20 on page 47.

The main events of interest were the front and side impacts along with the aggressive driving conditions. The disturbances for these events were applied in the form of displacements (for the crash events) and accelerations (for the aggressive driving events), also through the *BOUNDARY_PRESCRIBED_MOTION_RIGID keyword. These

displacements and accelerations were applied to the portion of the CRS modeled as a rigid entity, as denoted by the red portion of the CRS in Figure 12 on page 34.

The aggressive driving events generally lasted significantly longer than the crash events. The crash events lasted 0.15 seconds while the aggressive driving events lasted between four and ten seconds. Due to the very small time step required to properly run the simulation, time and mass scaling needed to be invoked to keep the simulation time at a reasonable level for the aggressive driving conditions. Time scaling consists of scaling down the time taken to complete a simulation by simply scaling down the time in all cases present to condense the whole event into a smaller timeframe. Mass scaling, on the other hand, is a technique implemented by the software to reach a desired time step to complete the simulation in a timely manner. Both techniques can be problematic if used too extensively or unreasonably because it can cause a previously quasi static problem to have dynamic effects because the time of the event was shortened so much or a much larger mass was accelerated.

However, even though these methods could be problematic, the use of these methods were justified by the fact that the accelerations experienced in a crash event reach somewhere in the vicinity of sixty to seventy g's while the aggressive driving conditions never reach more than 1 g. Since relative performance was of interest whatever small changes would be experienced, would translate to all configurations and the relative performance would remain unaffected. The animations obtained from the simulations were carefully looked over in order to check for any abnormal behaviour of the ATD or any excessive violent shaking of the system. Mass was only added to the elements within the model that did not meet the desired time step and the amount of mass added was 189 g while the physical mass of the entire system was 4.09 kg, which represents 4.62 percent of the entire model. A parametric study of different amounts of mass scaling was performed in order to determine what an appropriate amount of mass scaling would be without adding a significant amount of kinetic energy to the system. Table 1 shows the results from the parametric results and how the DT2MS variable was chosen in the *CONTROL_TERMINATION card. Trials one through four were run simultaneously to determine how significantly different values of DT2MS affected the simulation run time, and the amount of mass added. After all 4 trials were completed a

value was chosen for DT2MS to drive down the simulation time without greatly affecting the simulation results. Table shows the effects of increasing the value of DT2MS on the mass of the system as well as on the total run time for the simulation. Smaller values of DT2MS add less mass to the system and consequently require more time to complete simulations. However, choosing a DT2MS value that is too large will significantly drive down your simulation time but will add excessive amount of mass which could lead to inaccurate results in any form of dynamic loading. As an example, Trial 4 showed an addition of mass of 30.1 kg while the mass of the entire original system is 4.09 kg.

Table 1 – Different amounts of mass scaling and the resulting changes to the simulation.

Trial	DT2MS (s)	Mass Added (kg)	Simulation time
1	0	0	26 hr 13 min
2	-2.14×10^{-6}	0.263×10^{-3}	21 hr 28 min
3	-5.35×10^{-6}	0.7484	8 hr 51 min
4	-1.7×10^{-5}	30.1	3 hr 15 min

Both of the proposed prototype designs need to be evaluated and compared to the status quo. The comparison will be done by simulating all of the different restraint configurations in all of the different loading conditions. Performance will be evaluated in a frontal crash, side crash, braking, roundabout and sharp turn condition.

6.1 Crash Conditions

Both the front and side impact were obtained from the work carried out by Kapoor [63]. Crash tests were carried out by Transport Canada according to the Canadian Motor Vehicle Safety Standard (CMVSS) 208. Accelerometers were mounted in the vehicle and two CRSs were also used with a dummy installed to collect all of the pertinent head accelerations, chest accelerations and neck forces. A numerical model was

then generated and validated to obtain an appropriate displacement curve to simulate the experimental configuration. Figure 20 shows a graphical representation of the inputs into the model including the displacement profiles applied to the CRS for the frontal and side impact conditions. The front crash displacement profile is applied in the negative x direction and the side crash displacement is applied in the y direction. The front and side impact conditions were chosen because they have standard performance criteria and test methods to evaluate the performance of vehicles and occupant safety devices. The front and side impact also generally cause more harm (both financially and physically) than the various other types of collisions (rear impact, rollover, etc.).

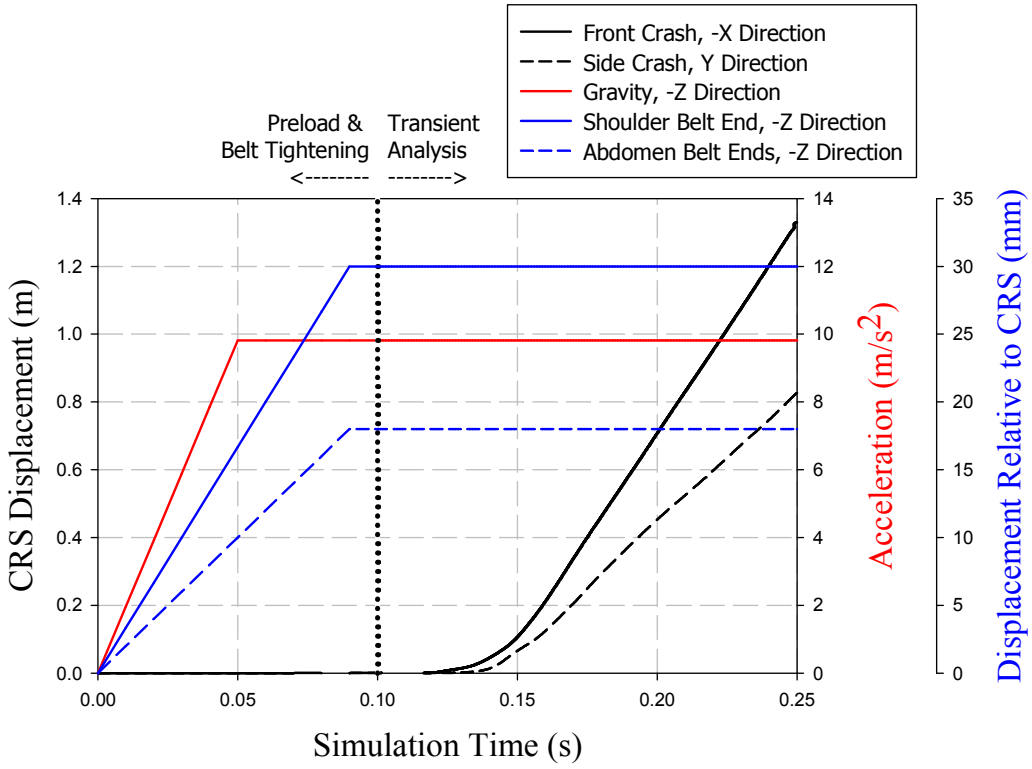

Figure 20 – Displacement profiles for the front crash event and the side crash event.

The first 100 ms consists of the preloading of the system by applying the gravitational acceleration to the system (depicted in red above), the tensioning of the seatbelt by pulling the ends (shown in blue above). Gravity is ramped up to the 9.81 m/s^2 and the abdomen and shoulder straps are "pulled" downwards (-Z direction) to remove any slack from the system. During this stage of the simulation damping is applied to the

entire system to remove and transients that could potentially affect the response of the model during the application of the events of interest (crash and aggressive driving). The kinetic energy levels are brought down to below 10% of the energy in the system to reach a quasi-static state. At that point the main event can begin to be simulated, as is shown above with the CRS displacement only beginning at 100 ms. Additionally, at this time damping was removed from the system to simulate a truly transient response. The aggressive driving conditions were modeled in the same way however acceleration was applied instead of displacement. The acceleration profiles representing the various aggressive driving conditions can be found in Section 6.2 below.

6.2 Aggressive Driving Conditions

The CRS would also be evaluated under different aggressive driving scenarios. In-vehicle road tests were carried out by Chen [59] to determine the accelerations experienced by a CRS in these driving conditions that would be experienced by the travelling infants. Three events were carried out in one vehicle with two CRSs installed and mounted with accelerometers to extract input data for the numerical simulations. All testing configurations followed SAE J211 norms and all data acquired was recorded for both CRSs in order to compare the results between the two. The three driving events consisted of a hard braking, roundabout turn, and a sharp turn. The SAE J211 document provides guidelines and recommendations for the measurement of impact tests. The document outlines various minimum sampling frequencies when using data collections tools as well as limits to the filtering of the data to remove any noise from the system.

6.2.1 Braking

The braking event was meant to simulate a scenario where a sudden stop was required. The starting vehicle velocity was approximately 40km/h and a full braking load was applied until a complete stop was achieved [59]. The acceleration was recorded for the duration of the braking event in all directions but only the acceleration in the x direction was of significance and was applied as a disturbance. Figure 21 shows the acceleration applied to the system to simulate the braking event.

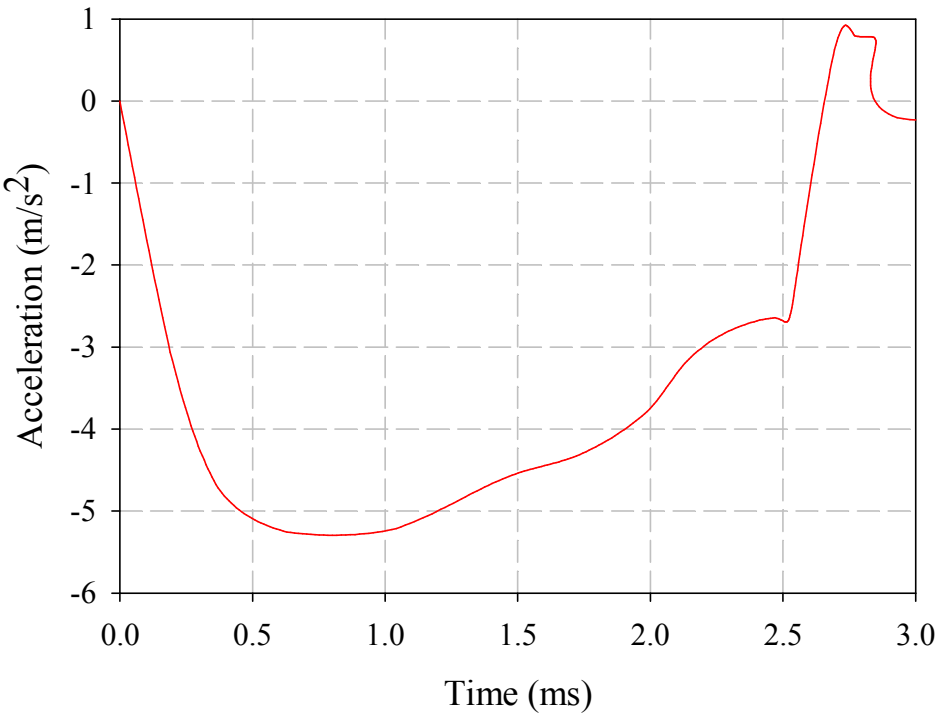

Figure 21 – Acceleration versus time for braking scenario.

6.2.2 Sharp Turn Event

Unlike the braking event, the "sharp turn" event was monitored in all three directions because of the nature of the driving conditions. The entered a corner at a speed of approximately 30 km/h with an exit speed of approximately 20 km/h [59]. The turn also involved a small bump or curb to drive over, which created the need for all three directions of acceleration to be measured. Figure 22 shows the responses for all three loading directions, the X direction, the Y direction and the Z direction in the global coordinate system as seen on page 32.

(a)

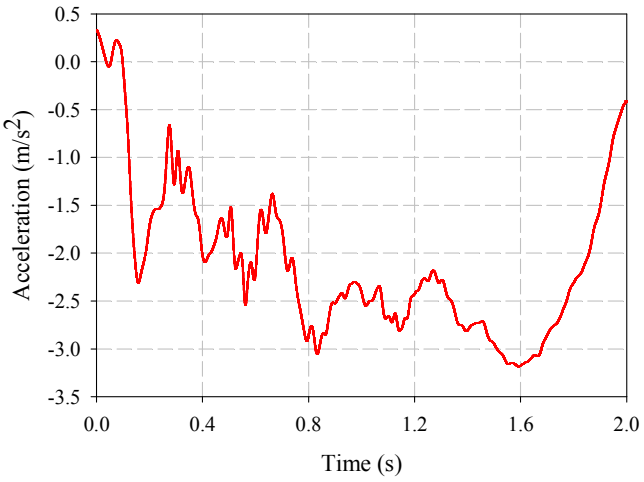

(b)

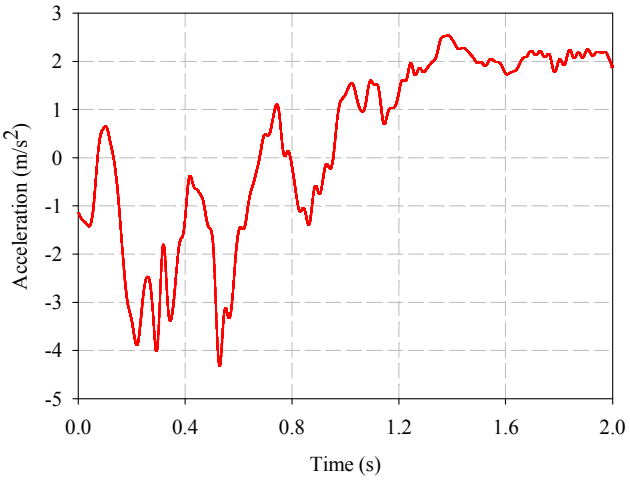

(c)

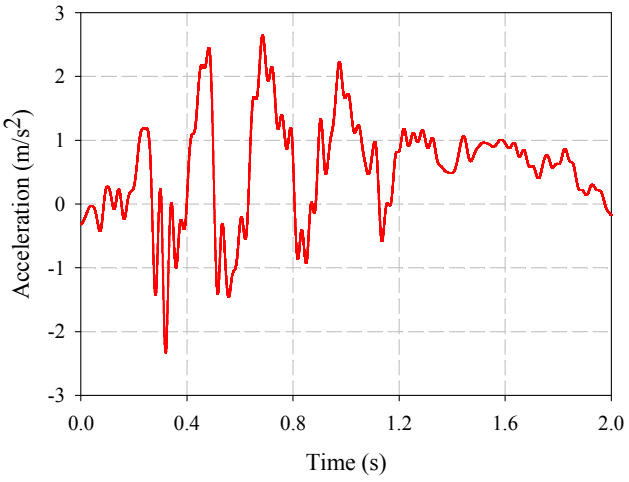

Figure 22 – Acceleration versus time for sharp turn scenario (a) X direction (b) Y direction (c) Z direction.

6.2.3 Roundabout event

The roundabout turn provided a unidirectional lateral acceleration; it was applied in the Y direction of the model. The driving speed within the roundabout was approximately 35 km/h and the radius of the roundabout was 8 meters [59]. The whole event lasted over 10 seconds, however only the first few were taken into account since it is a ramped input with a plateau. This simulation could represent an entry into a roundabout, an on/off ramp for any highway, or any other situation that requires a smooth rounded entry or exit.

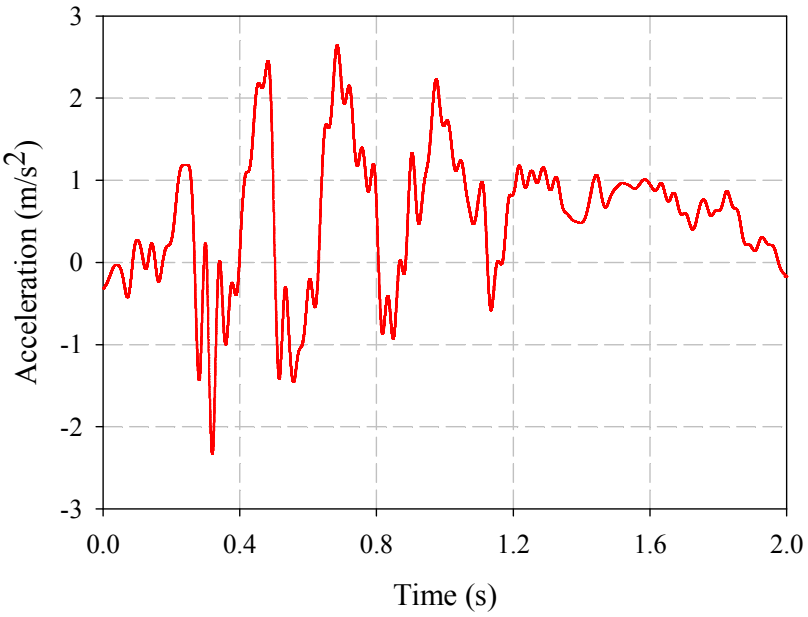

Figure 23 – Roundabout acceleration versus time.

7. AGGRESSIVE DRIVING CONDITIONS

The braking event, along with all other aggressive driving conditions, only needed the neck angle to be monitored since this is the chosen indicator for keeping airway patency. The neck forces and head accelerations, which will be analyzed in the crash analysis, are not presented for the aggressive driving conditions because they are negligible when being compared to the thresholds or suggested thresholds for neck forces and head accelerations to induce injury. The aggressive driving conditions are a good depiction of where the equilibrium states for the different restraint methods are. The initial portion of the simulation is generally where the sudden changes in speed and direction are and towards the end of the simulation the whole system is returning to rest.

7.1 Braking

Figure 24, below, shows the relationship between neck angle and time for the braking event. All three configurations show a similar pattern but are offset from each other by a certain amount and some have more pronounced drops and increases in neck angle. Initially, the neck angle drops to the minimum neck angle experienced, followed by a sudden increase in neck angle after the brakes are applied and a return to an equilibrium state. The minimum neck angles observed are 93, 80 and 106 degrees for the PPD, no PPD, and HRS conditions, respectively. The neck angles at equilibrium for those same conditions are 99, 85 and 107 degrees respectively. The HRS was not expected to have this much of an effect on any of the aggressive driving conditions since it was initially intended to serve as some extra protection during crash events. However, since the HRS is similar to a snug hooded sweater, it is possible that the tension is enough to keep the head fully back in the cavity of the PPD instead of settling to a slightly lower angle. Although the HRS does provide the most favorable neck angle for an open airway, both the PPD and the HRS provide an adequate level of extension throughout the braking event to maintain patency in the airway based on the findings presented by Wilson et al. [44]. The no PPD condition, on the other hand, exhibits a resting position in flexion. This means that without the PPD the infants head would have a tendency to fall forward and potentially increase the risk of airway obstruction and other respiratory difficulties.

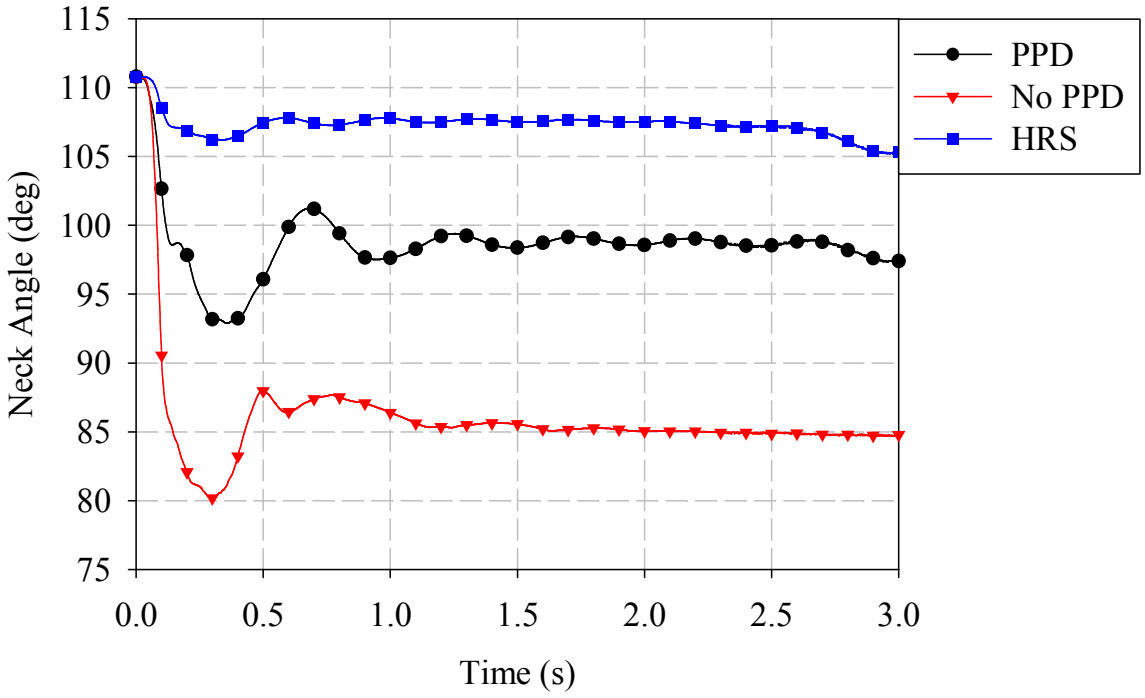

Figure 24 – Neck angle versus time for braking event.

7.2 Sharp Turn

The sharp turn event is not very different when comparing neck angles against those obtained in the braking event. However, there are a few small differences that seem to indicate it provides a larger disturbance for the infant. Where the braking event dropped abruptly followed by a small increase and a settling to an equilibrium state by 1.25 seconds in all configurations the equilibrium state doesn't appear to be reached with larger oscillations continuing through the entire duration of the simulation for the PPD scenario. Not only is the equilibrium state taking longer to reach in all configurations, but, it is being reached from a higher degree of neck flexion. That means that the neck angle is lower than the equilibrium state until it reaches it; increasing the risk for respiratory difficulties, even if only by a minor amount. The final neck angle for all three cases is the same as the one predicted for the braking event, which serves to reassure that this is in fact the equilibrium state for the given scenario. The neck angle response for all three configurations exposed to the sharp turn event can be found in Figure 25.

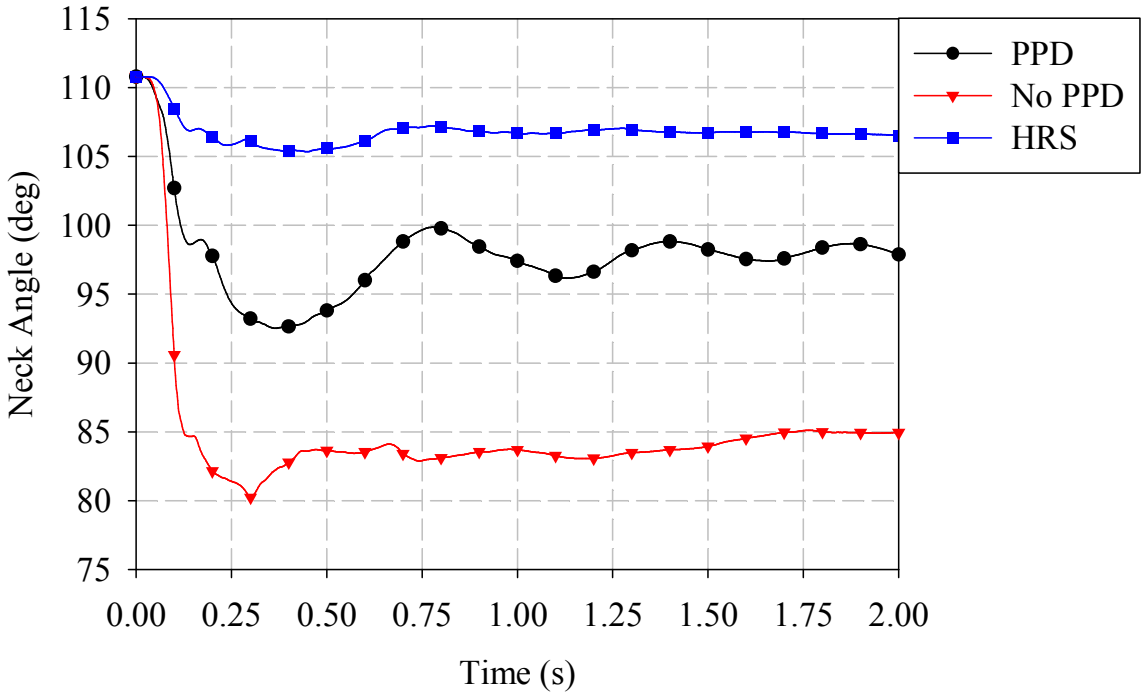

Figure 25 – Neck angle versus time for sharp turn event.

7.3 Roundabout

The roundabout is a slightly different event than the other two because it consists of a constant lateral acceleration generated by driving at a constant speed in a circular path whereas the accelerations in the other two aggressive driving events stemmed from braking and turning or a combination of the two. Once again, the no PPD condition has the highest degree of neck flexion of all three configurations. Something that is different about this event is that the neck angle gets progressively worse the longer the vehicle is in the turn. Instead of reaching a plateau, the responses show that the infant is able to overcome the initial disturbance introduced when entering the roundabout and reach their equilibrium. After the initial minimum all three configurations so a minor rebound to a local maximum before returning to a resting position. Final neck angle values for the PPD, no PPD, and HRS configurations are 97 degrees, 84 degrees, and 103 degrees.

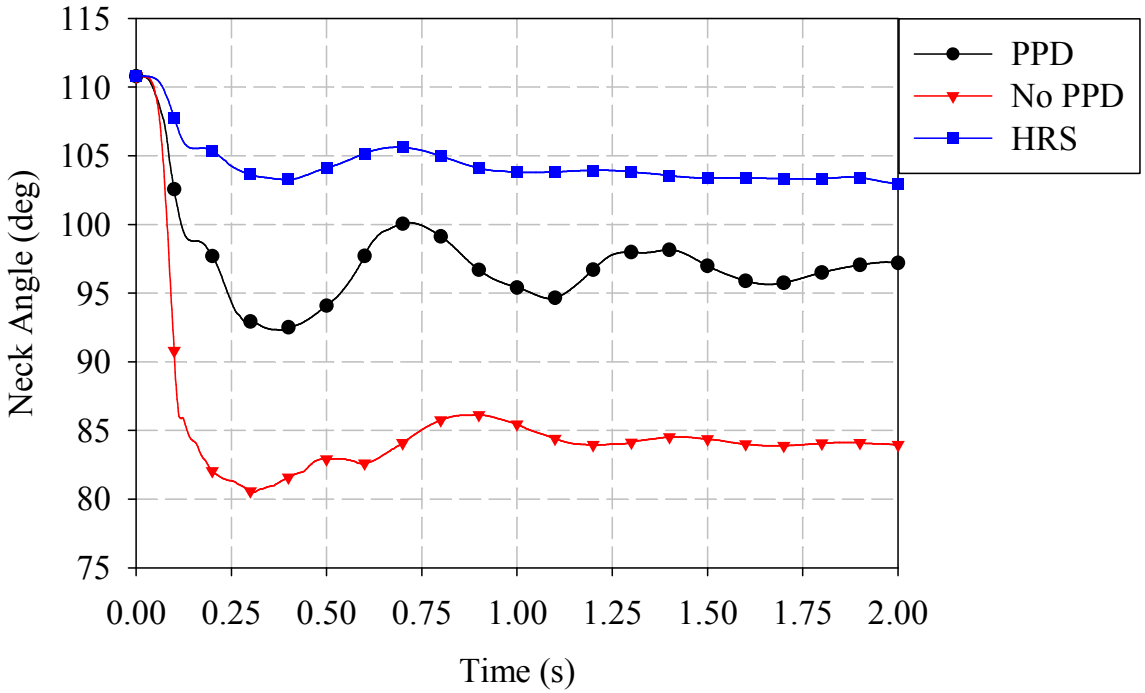

Figure 26 – Neck angle versus time for the roundabout event.

7.4 Discussion

Although the disturbances for the various driving conditions were not too extreme, the initial behaviour in all three scenarios is slightly different. The HRS configuration proves to be the most successful in keeping a good degree of neck extension while the no PPD configuration is the only configuration with the neck of the infant in flexion throughout the simulation. These plots are also good indicators of the final resting position of the various configurations and what neck angle could be expected at the end of the crash simulations if the model was returned to rest. The resting angles for the PPD, no PPD, and HRS configurations are 98 degrees, 85 degrees, and 105 degrees respectively. Indicating that the HRS configuration has the best ability to reduce the frequency of respiratory difficulties based on the data presented earlier by Wilson et al. [44].

The HRS and PPD were originally expected to have much more similar results; however, the HRS manages to provide a better level of airway opening via a larger neck angle throughout the various events. This is as a result of just the slightest resistance to movement provided by the HRS fabric encompassing the head. The events are not as violent as the crash events (which will be discussed in more detail later) and so a large amount of effort is not required to keep the head back in the seat. However, the PPD is able to provide some lateral support but no back to front support for the head movement. Meanwhile the HRS does provide some restriction to movement in all directions to prevent the head from bouncing around freely. With no PPD or HRS present the head has a tendency to slouch forward with only gravitational acceleration as an input and so any type of disturbance will generally manage to make that worse. Implementation of the HRS in every day driving conditions is easily duplicated by having the infant wear a hoodie and keeping it snug. However, if it is not coupled with the PPD then there is already an initial tendency for the head to slouch and the hoodie would only then prevent the situation from getting worse.

8. PPD CRASH PERFORMANCE

The PPD and the HRS were evaluated in 5 different conditions as mentioned in the previous section. The performance of these two devices will be evaluated relative to the current configuration of infants in CRSs, positioning within the seat with no add-ons. The children are generally discharged from the hospital with rolled towels placed to either side and in the crotch region to prevent some of the movement; these towels are not, however, considered to be able to provide support in the event of a collision. There is nothing preventing the rolled towels from being thrown out of the seat because of the lack of restraint system for those towels which are not intended to be placed behind the infants for that reason. Although the improvement of conditions to prevent respiratory complications, via more neutral and slightly extended neck, are the main function of the PPD it is still important to evaluate it considering head accelerations and neck forces experienced by the child as a result of these dynamic events to ensure that the safety of the child is not compromised in the event of a car accident. The condition with HRS denotes a configuration where both the PPD and the HRS are present. All of the head accelerations and force outputs were filtered at 1000 Hz frequency according to the SAE J211 recommendations for ATDs in a crash test. Section 8 will cover the performance of the PPD relative to the no PPD condition (or the current status quo). The HRS condition will be considered in section 9 further in the document.

8.1 Front Crash

The first event to be considered is the front crash event. Before jumping to any numerical considerations a qualitative assessment of the various configurations will be considered. Figure 27 shows a side by side comparison of a head on view of the PPD at various moments in the frontal impact simulation. The green block behind the infant in the No PPD configuration represents the foam that is provided with the CRS by the manufacturer. The moment just prior to peak head acceleration can be observed from the picture corresponding to 130 ms, at 150 ms mark the neck extension is greatest (just after the acceleration peak), at 190 ms the largest amount of compression in the neck is observed and 250 ms shows the final state in the simulation. It is important to note from the first images side by side that the neck is visible in both configurations with the PPD

and with the HRS coupled with PPD, while in the no PPD configuration the neck is not visible indicating that the head is slouching and the neck is closest to flexion in this configuration. The second frame looks quite similar across all three configurations with no significant differences between all three. The last two frames are also similar, other than the no PPD conditions appears to show a smaller neck angle. Although this section will only cover the PPD versus no PPD conditions, the qualitative observations presented below will also show the HRS condition but the behaviour will be discussed in section 8 along with the remainder of the HRS evaluation.

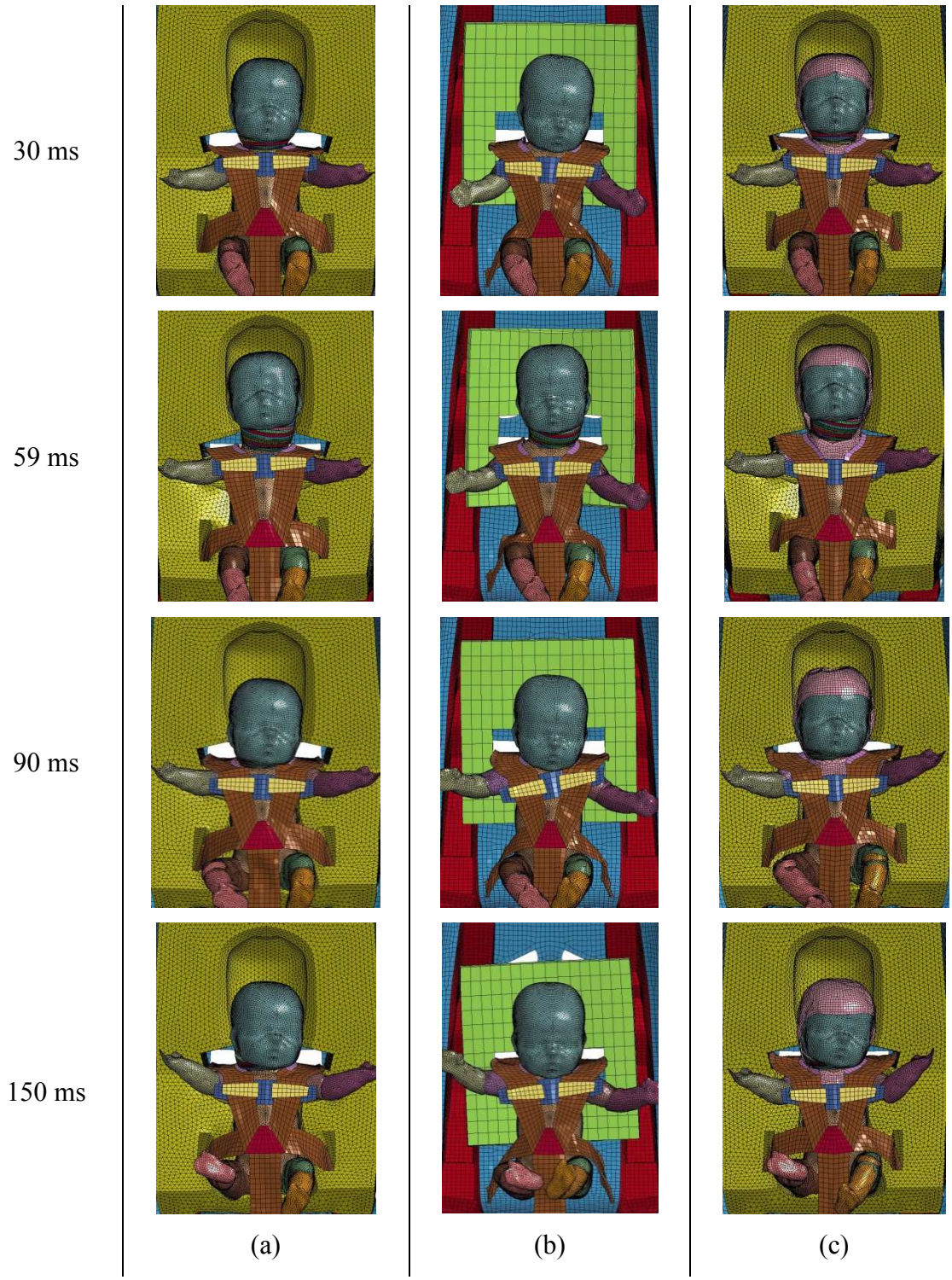

Figure 27 – Qualitative comparison of the front crash condition, from a frontal view, with (a) PPD, (b) No PPD, and (c) PPD and HRS.

8.1.1 Neck Angle

The initial resting neck angle for the ATD model was 110 degrees. The initial portion of the curves shows the infant ATD settling into the seat, ending at 0.1 seconds. In this belt tightening portion of the simulation it is important to note that the infant is simply settling into the seat and the trends observed show that the configuration of CRS with no PPD induces the highest amount of neck flexion along with the steepest declining slope, indicating that it has a much higher tendency to cause neck flexion. Although the neck begins flexing later than in the configuration with the PPD this is due to the later contact with the material behind the ATD in the simulation. During the crash event portion (starting at 0.1 seconds and ending at 0.25 seconds) of the simulation, the neck angle continues to drop, followed by an increase in neck angle to a maximum and then a return towards a more neutral position. Although the curves are similar in shape, the condition with the PPD provides a larger degree of neck extension than the condition with no PPD. It is also important to note that towards the end of the simulation the configuration with the PPD is increasing towards a higher degree of neck extension whereas the no PPD condition seems to have found a state of equilibrium at a neck angle of 90 degrees.

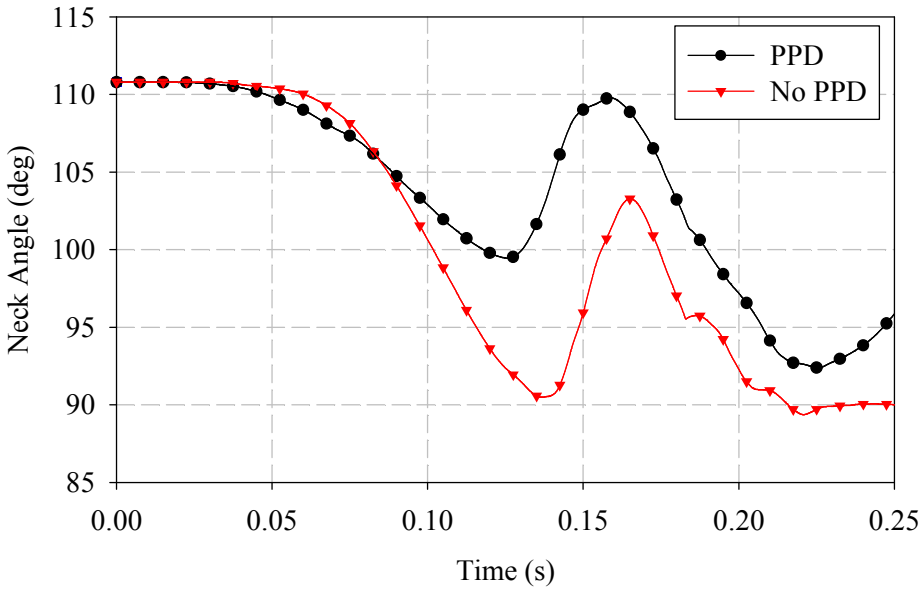

Figure 28 – Neck angle versus time for all three CRS configurations – frontal impact.

8.1.2 Head accelerations

Head accelerations are an important aspect of crash analysis because they are used to evaluate the severity of an impact and used to determine the head injury criterion (*HIC*). Equation 1 uses the resultant head acceleration response to calculate the *HIC* either over an interval (t_1-t_2) of 15 ms or 36 ms. According to both the CMVSS 213 and the Federal Motor Vehicle Safety Standard (FMVSS) 213, the peak head accelerations experienced in a crash test by an ATD should not exceed 80 g's for a period of more than 3 ms [65,66], while the *HIC* should not exceed 660 for any 12 month old (or younger) infant [67].

$$HIC_{t_2-t_1} = \left[\frac{1}{t_2-t_1}\int_{t_1}^{t_2} a_{resultant} \cdot dt\right]^{2.5} \cdot (t_2 - t_1) \quad \text{Equation 1}$$

Figure 29 shows the head accelerations as a function of time for both configurations. All three plots have very similar profiles once again with peaks occurring at 155 ms into the simulation. The peak head accelerations for the PPD and No PPD conditions are 80 g's and 90 g's, respectively. The duration of these peaks is pretty consistent across both of the simulations; lasting roughly 50 ms. There is a second disturbance that can be observed at 80 ms. These peaks correspond to the time when the ATD head contacts the chest clasp during the simulation. Since both entities are rigid, when they come into contact the accelerations are distorted. Although these spikes were not filtered out by the SAE J211 specifications, they should not be considered as something that would affect the infant but should be noted as another one of the limitations of the model. Another difference between the No PPD condition and the PPD condition is the variation in the initial peak. Both configurations experience an initial peak between 40 and 60 g's at the 40 ms mark. However, the No PPD configuration exhibits a higher initial peak, and experiences a more significant drop in acceleration than the PPD configuration (dropping from 55 g's to roughly 18 g's instead of dropping from 40 to 30 g's). This could be one of the reasons that, despite the higher peak accelerations, the *HIC* value is lower in the no PPD condition. The HIC_{36} sees a small increase of 0.6 percent for the PPD configuration with a value of 350.6. The HIC_{36} for the no PPD condition is 348.6. Since the variation in *HIC* is very small both configurations can be considered to be very similar when analysing using these values. If, however, considering peak head accelerations the PPD configuration proves to have an improvement in performance. It

could also be noted that the no PPD configuration is the only configuration that does not adhere to the CMVSS and FMVSS standards previously mentioned that state that all head accelerations should not exceed 80 g's. The components of head acceleration for both configurations can be found in Appendix A. The values presented in the appendix are similar to the resultant head accelerations with the main direction of acceleration being the x direction.

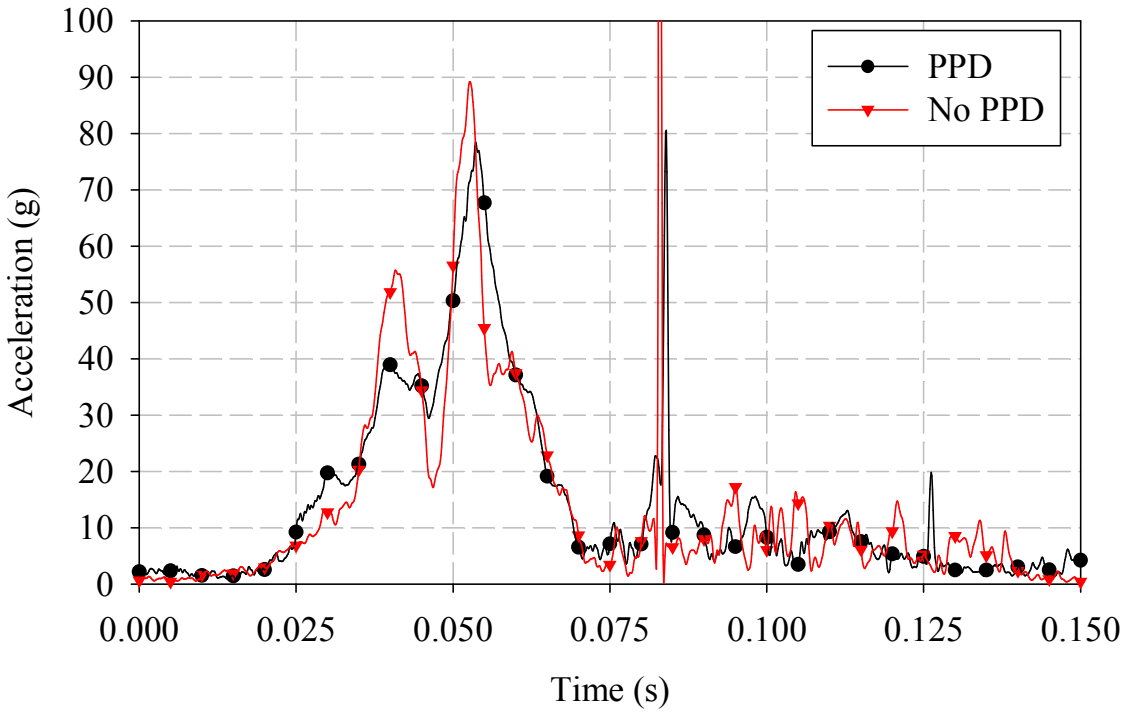

Figure 29 – Head accelerations versus time – frontal impact.

8.1.3 Tensile Neck Forces

Neck injuries are also common injuries in crash scenarios, especially in the low birth weight and preemie babies because of the lack of development previously mentioned. The model was updated to allow easy extraction of tensile neck forces. These forces will be presented for the front crash scenario because they are easier to read and very similar in nature to the resultant neck forces (aside from overall magnitude). Figure 30 illustrates the tensile forces in both the upper and lower neck joints.

When considering the tensile forces, the PPD condition and the no PPD condition exhibit almost identical peak tensile loads. Peak loads experienced at the upper joint were 190 N and 205 N for the PPD and no PPD configurations respectively and 200 N in both configurations at the lower neck joint. Although the reduction in neck load is definitely desirable, one drawback from the introduction of the PPD is that the forces experienced in the neck ramp up to their peak forces earlier and stay there for approximately 40 ms. The condition with no PPD has a higher peak force but the duration that the peak is held for approximately 25 ms. The peak neck forces predicted by the model, again, cannot not be considered as absolute values, but, are a good indication of the region of loading that could be expected for a child. All three configurations surpass the minimum force for failure found by Luck et al. [15] (142 N), but stay below the average force for failure (205.5 N). The numbers quoted previously were for a spine with no ligaments or muscles, and when considering the work by Duncan [14] where tests were completed with the ligamentous and muscular spine, all three configurations are well within the minimum failure force of 400 N found in that study. The resultant neck forces and shear components of force can both be found in Appendix A under the Front Crash Section.

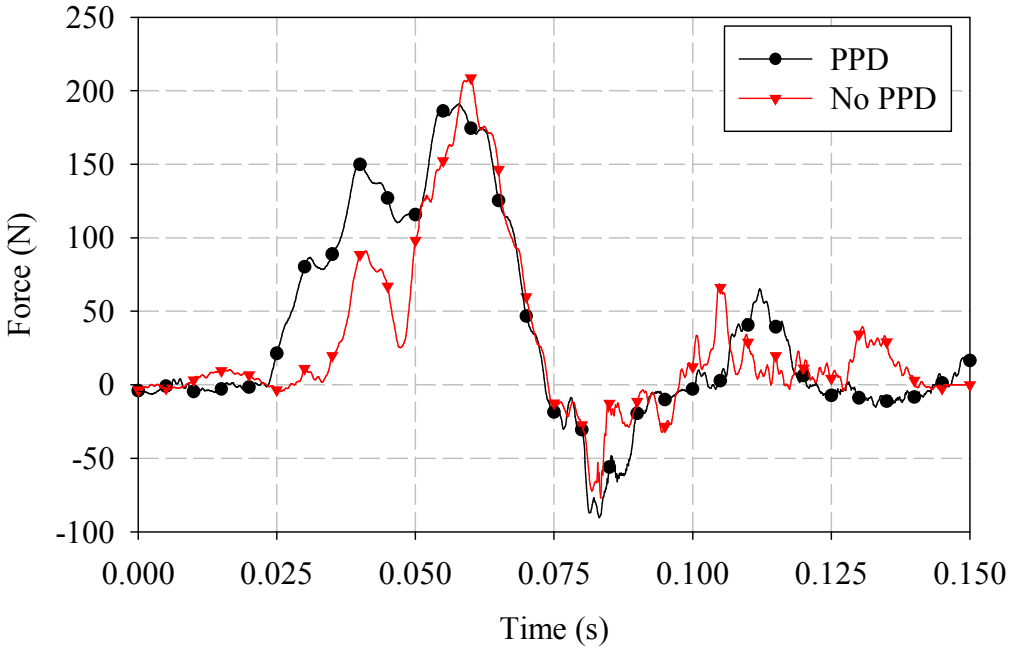

(a)

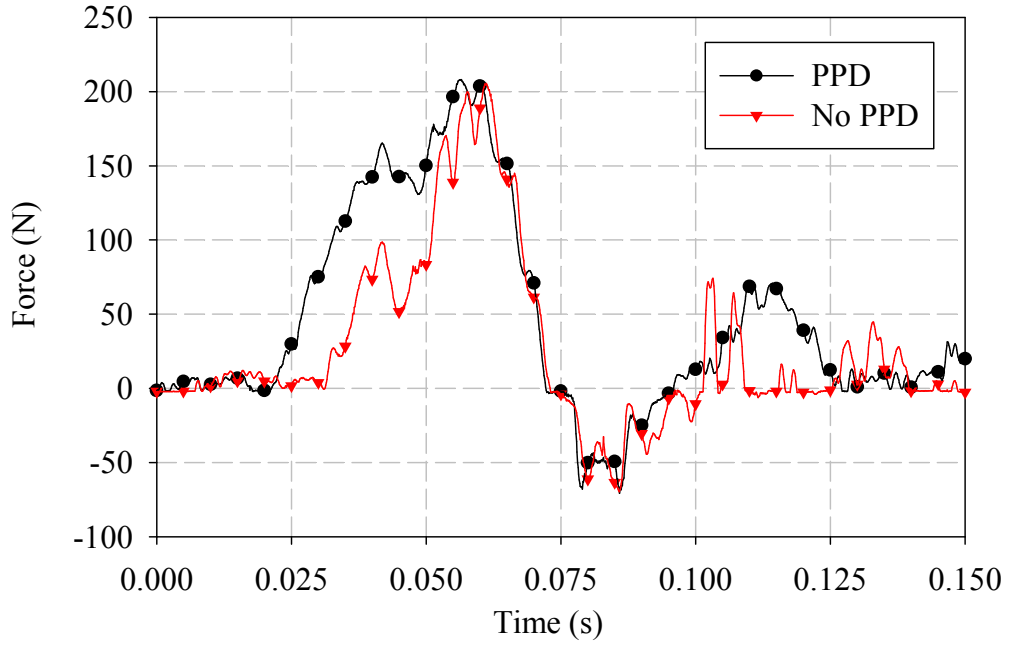

(b)

Figure 30 – Neck tensile forces – front impact (a) upper neck joint and (b) lower neck joint.

8.2 Side Crash

The second event to be considered was side impact with the kinematic displacement response illustrated in Figure 31. Different times from those selected in the front crash were chosen to be shown because of the different nature of the event and timing of certain moments. The maximal lateral displacement observed after the first peak in head acceleration occurs at 150 ms. At 175 ms the maximal lateral head displacement after the second acceleration peak can be observed. The full rebound of the infant within the restraints occurs at 210 ms and this is generally where the head started to contact the chest clasp and experience the smallest neck angles. The 250 ms mark showed the final positioning at the end of the simulation.

In the first two frames it appears that the no PPD condition has the least amount of lateral head and torso motion. This is because the foam of the PPD allows for more side to side movement of the child since the foam is being crushed by the weight of the ATD. However, the position of the head relative to the torso seems to be much more neutral, in terms of neck angle, in the configurations with PPD and HRS than when no PPD is present. This appears to be true at all instances of time, especially in the last two frames when the PPD has brought the ATD back to its starting configuration while the no PPD configuration is exhibiting a larger amount of lateral displacement of the head. In the third frame, all configurations have reached the largest amount of slouching. However, in the last frame the configuration with PPD is returning to a larger degree of neck extension while the other two configurations appear to not have changed from the previous image. Although the HRS condition is shown alongside the other two configurations, the remaining results will also be analyzed separately.

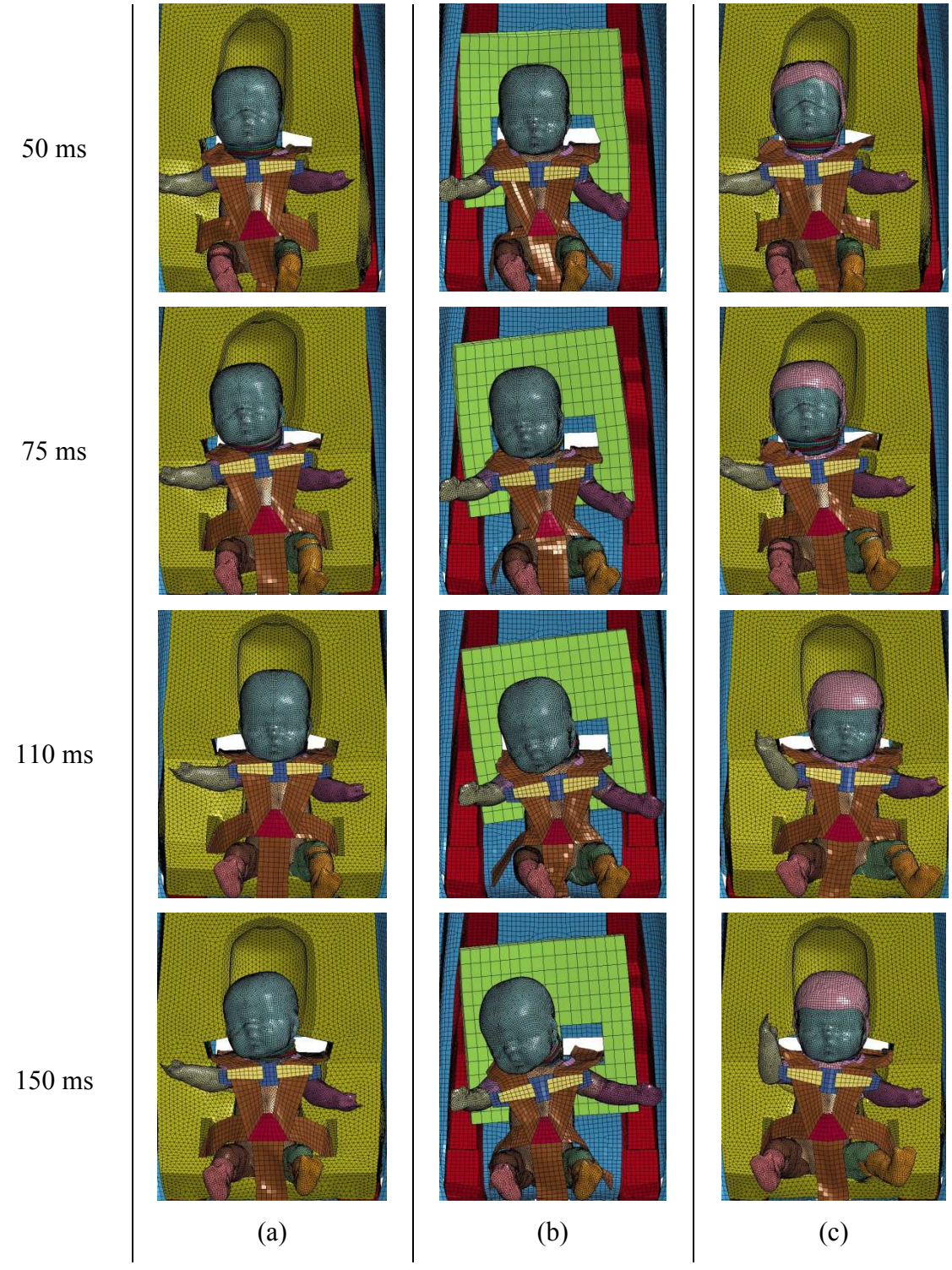

Figure 31 – Head on view of side impact simulation in all three configurations, (a) PPD (b) No PPD (c) HRS.

8.2.1 Neck Angle

There was a much larger degree of neck flexion in the side crash simulations. Previously the frontal impact showed a minimum degree of neck flexion with a value of 90 degrees and only in the worst case scenario (with no PPD). Figure 32, below, shows the no PPD condition reaching a minimum of 75 degrees at the end while the condition with PPD has a minimum of 82 degrees. Once again, throughout the simulation both configurations have a very similar neck angle profile but offset by a certain amount after the start of the acceleration pulse. The PPD provides an improvement of 5 degrees of neck extension when compared to the no PPD configuration during the crash pulse. At the end, this benefit becomes even larger with an increase in neck angle of over 10 degrees resulting in a small degree of neck extension instead of the final position in flexion observed when no PPD is present. Both scenarios show a trend towards a larger neck angle at the end of the simulation, however, the no PPD condition ends with a smaller upward slope than both other configurations and already has the most flexion (77 degrees). The PPD condition ends with a neck angle of 91 degrees while the no PPD condition shows the child with a final neck angle of 77 degrees.

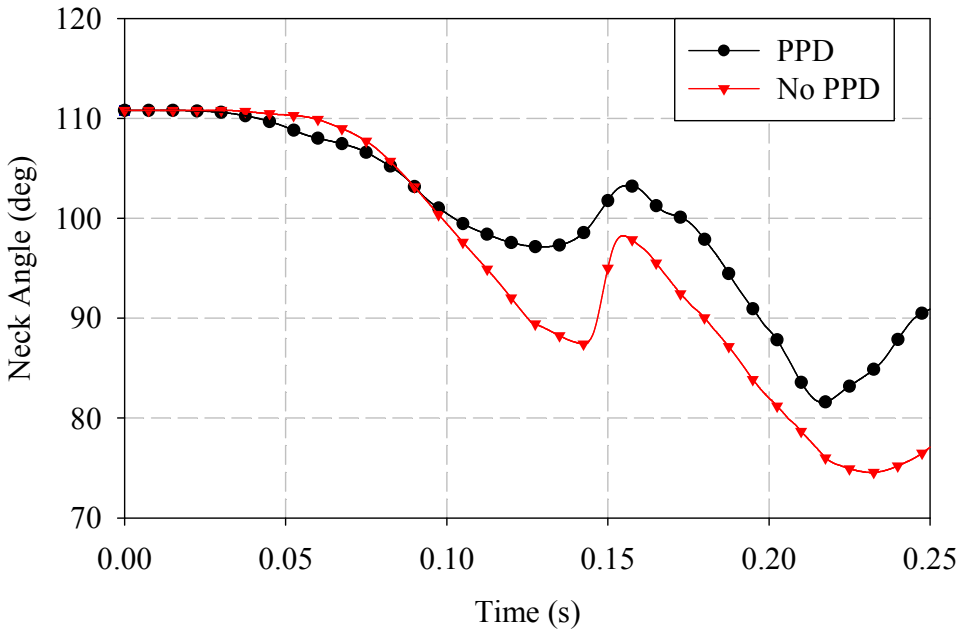

Figure 32 – Neck angle versus time – side impact.

8.2.2 Head Acceleration

For the side crash condition, all three peak head accelerations were below the CMVSS and FMVSS recommended 80 g's. The largest and most notable difference is the abundance of peaks in the no PPD configuration. The multiple peaks are due to the frequent contact of the head with the chest clasp. Since the neck angles are significantly lower, compared to the frontal impact simulation, the head will contact the chest clasp more often. The peaks that occur as a result of head and chest clasp contact are at 26 ms and between 106 ms and 130 ms. Aside from those previously mentioned no other head accelerations are influenced by this limitation to the model. The sharp peaks are generated by rigid on rigid contact in the model, which is one of the limitations of the model. The rigid contact interfaces provide unrealistic spikes in recorded accelerations and the accelerations generated by this contact can be ignored for the purpose of analysis. This becomes evident when considering the components of head acceleration found in Appendix B where the sharp peaks later in the simulation are present in the Z direction while the loading direction is the Y directions. The Y component of acceleration should account for the largest contribution of the head acceleration, which is not the case for the previously mentioned peaks. The no PPD condition had a peak head acceleration of 76 g's, while the PPD condition on the other hand had a peak head acceleration of 69 g's. Another interesting observation is that the no PPD condition experiences some oscillations in its peak with two small peaks both before and after the maximum peak of roughly 70 g's. There is then a brief drop to a near zero value and a second significant peak above 60 g's. The PPD condition had a short peak head acceleration, as a result the *HIC* values for the PPD configuration were lower than those observed with no PPD present. For the PPD and no PPD conditions the *HIC* values were 206.9 and 391.5 respectively. The introduction of the PPD causes a reduction in peak head acceleration of 9.2 percent and a reduction in *HIC* of 47.2 percent. The change in HIC is a significant improvement in the performance of the CRS system as a whole when experiencing a side impact.

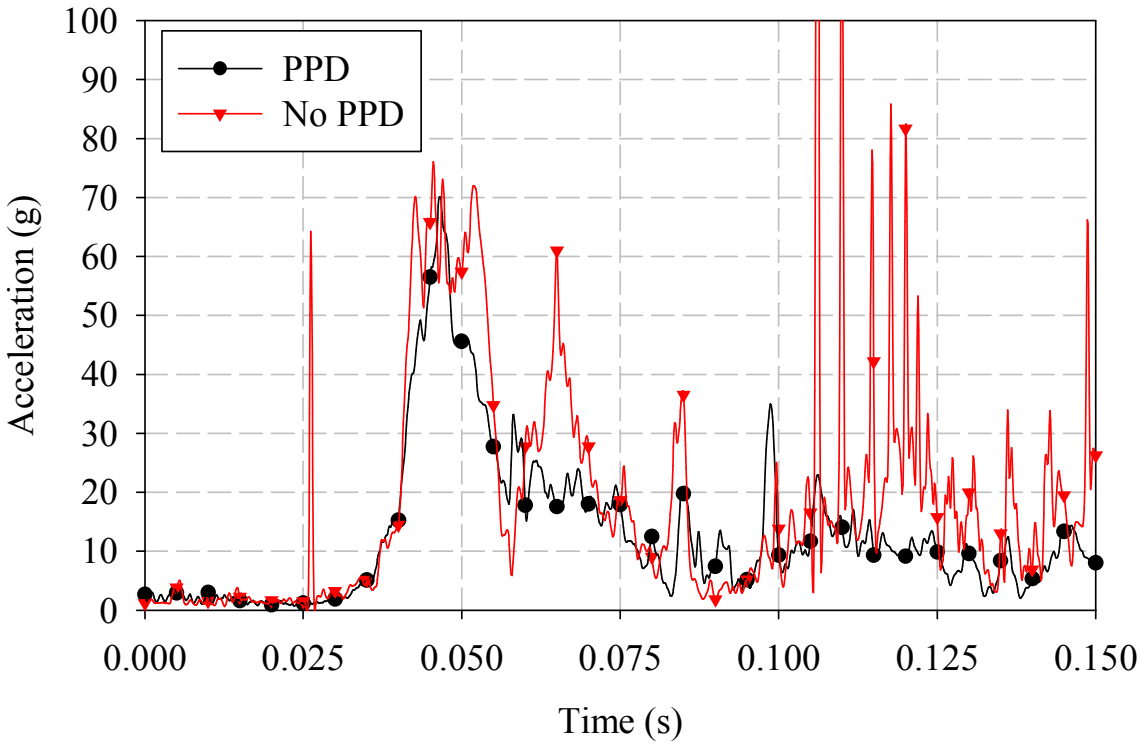

Figure 33 – Head accelerations versus time – side impact.

8.2.3 Neck Tensile Force

When considering the tensile neck loads, the PPD reduces the neck loads if comparing to the status quo of no PPD. These observations can be seen in Figure 34 on page 71. At the upper neck joint the introduction of the PPD reduces the peak tensile force in the joint by 41.9 percent from 155 N to 90 N. AS a result of the increased head accelerations observed earlier after 100 ms, the forces experienced by the upper neck joints are also magnified, as can be observed in Figure 34. The artificial peak observed at the end of the response is due to the rigid contact between the head of the infant and the chest clasp. However, prior to 100 ms the neck force response has none of these effects. Other than magnitude, both curves have a somewhat similar profile with the PPD introducing slightly larger forces in the early stages of the crash event while the second peak for the no PPD condition is greater than all forces seen with the PPD, along with a longer duration at that peak. At the lower neck joint, the peak tensile force is reduced by 37.7 percent from 225 N to 140 N. The response at the lower neck joint seems to be

significantly more violent when no PPD is present, with forces experienced are doubled at some points with the later stages of the simulations being quite similar. It is important to note that the peak head tensile forces observed at the lower neck joint when the PPD is present occur in the final moments of the simulation over a brief period of time. The first two peaks observed in the PPD condition are 90 N and 75 N respectively, while those observed in the no PPD condition are 180 N and 225 N respectively (both of which are at least double those observed with the PPD present).

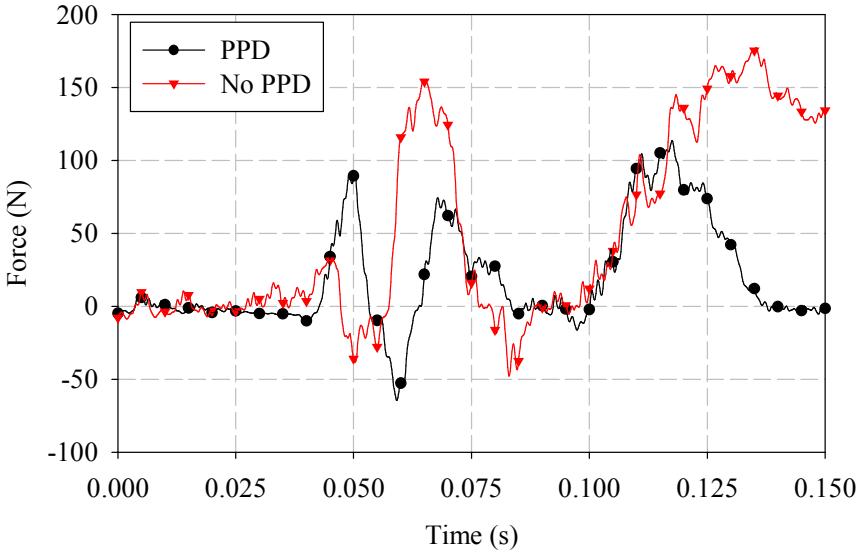

(a)

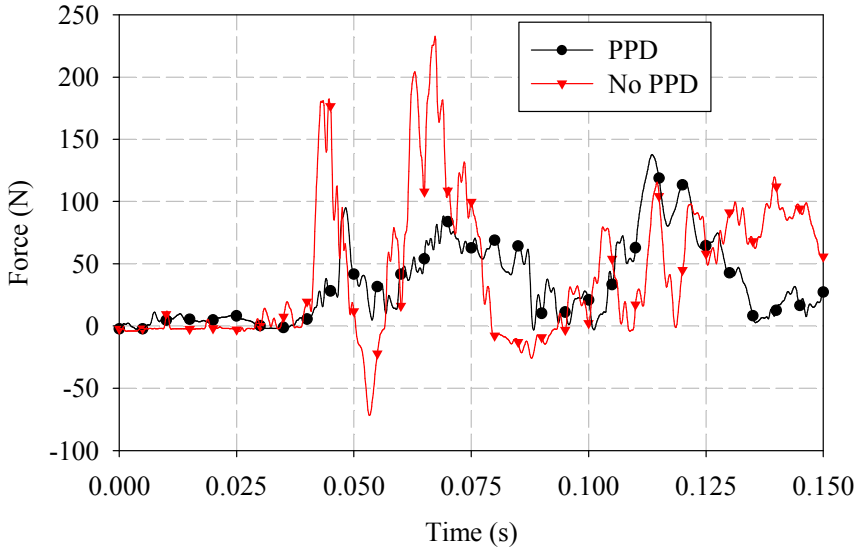

(b)

Figure 34 – Neck tensile forces – side impact (a) upper neck joint (b) lower neck joint.

8.3 Discussion

When comparing the PPD to no PPD conditions in the frontal impact simulations it can be observed from various aspects that the PPD provides a generally positive impact on the ability of the CRS to protect the infant from respiratory complication as well as reduce the severity of the impact on the child.

A neck angle of 90 degrees is considered a neutral neck position. Anything below is considered flexion and anything above is considered extension. In the study by Wilson et al. [44], any degree of flexion below 90 degrees induces closing pressure whereas any extension above 90 degrees requires some external force to close the airway. The neutral position did not induce airway collapse, however, it was still somewhat prone to it because regular respiration was strong enough to overcome the pressure required to close the airway. Another point to consider is one of the limitations of the model. The infant ATD is composed of rigid components as is the chest clasp. This means that if the infant head is resting at a neutral position of 90 degrees and does not seem to be moving it is because the head has come into contact with the torso or the chest clasp. Since all of these entities are rigid there is no allowance for further flexion of the neck in the model, whereas in real life there would be. Therefore, any minimum values obtained from the simulations could be lower in a real life scenario. This is why it is very important to note that the configuration with the PPD has a neck angle with an upward trend at the end of the simulation. This means that, when the crash event is coming to an end the PPD configuration is returning to a neck angle in its resting position, while, the no PPD condition is not.

Although the no PPD condition does not meet the CMVSS standard for peak head acceleration it is important to remember that the values obtained from the simulations are not perfect and can only be used as indicators of the region where the head accelerations could be. That being said, this is still a worrisome result that shows that there still needs to be some research done on the safety of using the CRSs currently available for infants born either prematurely or at a low birth weight.

The PPD and the no PPD both stay well within the average tensile loads at failure found by both Duncan [14] and Luck et al. [15], except on one occasion. The lower neck

tensile forces exceed the average tensile loads at failure found by Luck et al. [15] by a margin of 20 N. Once again, these values are not absolute values but the fact that all of the predictions show that they are within the limits set out by Luck et al. [15] means that these are conservative values since those results were based on skeletal testing and not cadaver testing like Duncan [14] performed. The addition of the PPD to the setup greatly reduces the tensile loads experience in a side crash event and only slightly in the frontal impact situation. When also considering the resultant neck forces and shear neck forces; the PPD is always performing better than the status quo with no PPD. This means that the PPD provides adequate support in both crash conditions and does not pose a risk to the infant in frontal or side impact events.

9. HRS CRASH PERFORMANCE

The crash performance of the PPD was already evaluated relative to the condition with no PPD present. The performance from a health safety perspective and crash performance were generally positive in the crash scenarios. As a result the HRS configuration will be compared to the PPD condition to determine its potential effectiveness in further protecting the child. The qualitative comparison was previously discussed and the quantitative results will follow.

9.1 Front Crash

9.1.1 Neck Angle

Both configurations show a very similar neck angle profile. However, the condition with HRS present is offset three to four degrees higher than the PPD only configuration for the majority of the simulation. The lowest neck and observed for the PPD and HRS configurations are 93 and 96 degrees respectively, which means there is a 3.2 percent increase in neck angle for the HRS configuration. The final neck angles are very similar with values of 96 and 97 for the PPD and HRS respectively. Both configurations show a tendency to return to a higher degree of neck extension which is definitely favorable for the infant. Both configurations can be considered to be consistent since the improvements are not significant when introducing the HRS. Figure 35 shows the neck angle as a function of time for both mentioned configurations.

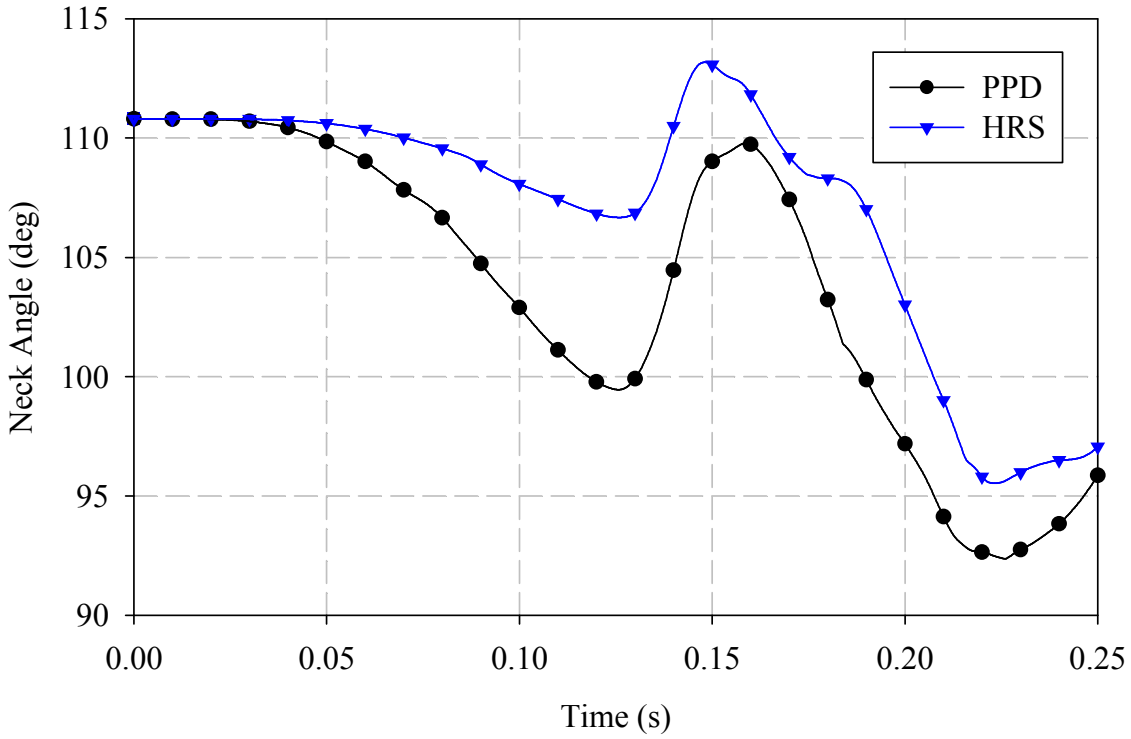

Figure 35 – Neck angle versus time – front impact.

9.1.2 Head Acceleration

When examining the head acceleration results it is evident that both the PPD and the HRS configurations have similar performance levels. The largest observable difference, obtained from Figure 36 below, is the difference in peak head acceleration experienced by the ATD in either configuration. The peak head accelerations for the PPD and HRS are 78 g's and 70 g's respectively. This constitutes a 10.3 percent decrease in peak head acceleration when the HRS is introduced. Although the peak head acceleration is reduced the *HIC* results are very similar, with the HRS exhibiting a larger *HIC* value. With the PPD the HIC_{36} value is 350.6 while the introduction of the HRS increased the value to 363.1. This represents an increase of 3.6 percent which indicates no significant change to performance when considering *HIC*. Head acceleration components show very similar results and can be found in Appendix A.

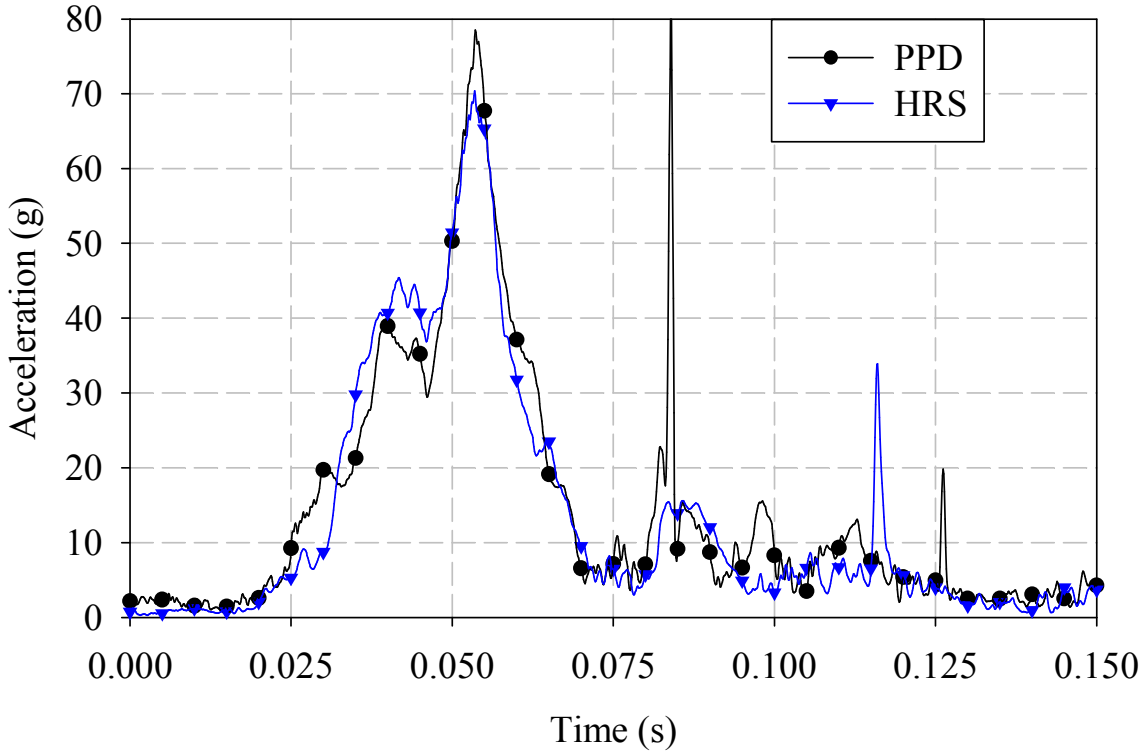

Figure 36 – Resultant head accelerations versus time – frontal impact.

9.1.3 Neck Tensile Forces

The neck tensile forces are once again quite similar in terms of profile but different when considering magnitude, the results are presented in Figure 37. There are two peaks at both the upper and lower neck joints and the first peak is consistent for both configurations at both locations. However, there is a decrease of the second peak in neck tensile force with the introduction of the HRS of 26.3 percent and 23.8 percent at the upper and lower neck joint, respectively. The introduction of the HRS allows for a decrease of roughly 25 percent of the tensile neck forces experienced which is very favorable for the safety of the infant. The resultant and shear neck forces can be found in Appendix A. The resultant forces show similar behaviour while the shear forces remain at a more consistent level in the frontal impact situation.

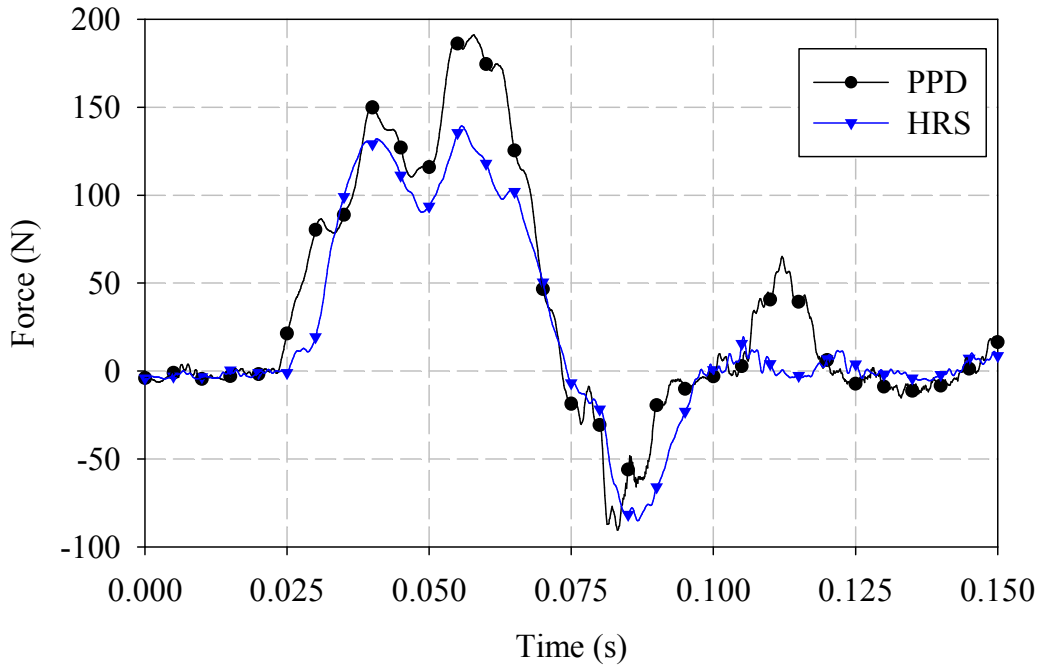

(a)

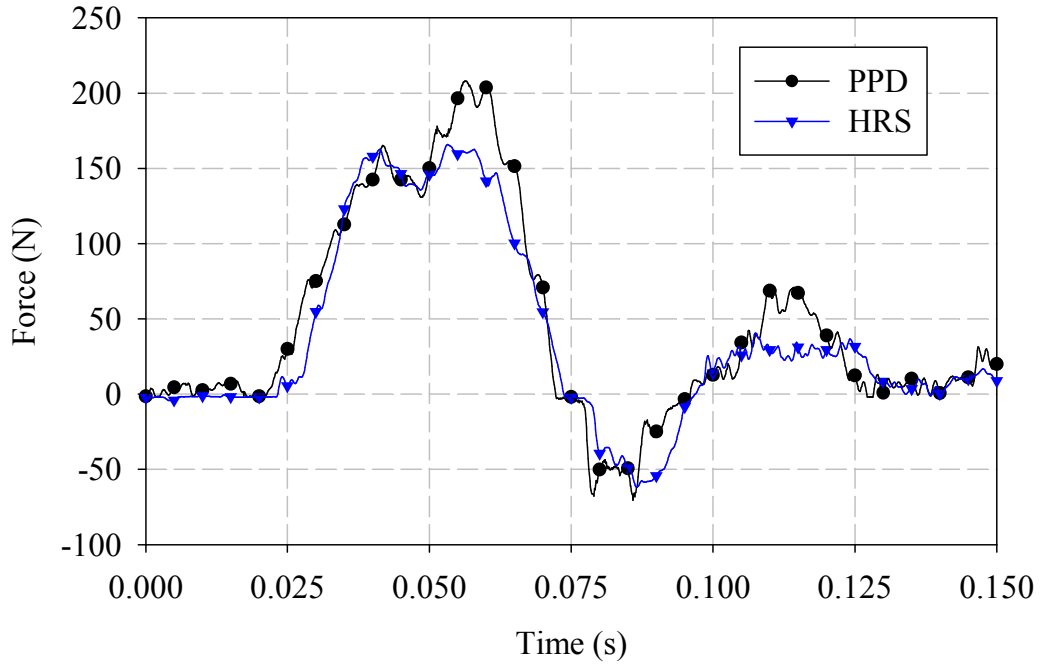

(b)

Figure 37 – Neck tensile forces – frontal impact (a) upper neck joint (b) lower neck joint.

9.2 Side Crash

9.2.1 Neck Angle

The neck angle profiles are similar again for both configurations with some slightly different behaviour from that observed in the frontal impact situation. Figure 38 illustrates the angle time response. With the HRS implemented, a larger degree of neck extension (or lower level of neck flexion occurs) is observed until both responses meet at their minimum neck angle of 82 degrees at 0.22 seconds. After that coincident minimum the PPD configuration seems to show a quicker recovery to a final neck angle of 92 degrees which appears to be continuing to rise while the HRS configuration rises slower to a final neck angle of 86 degrees, but also appears to be continuing to rise. This means that the PPD has less time spent in a position of neck flexion than the HRS and that the HRS finishes the simulation with neck flexion while the ATD has slight neck extension in the PPD.

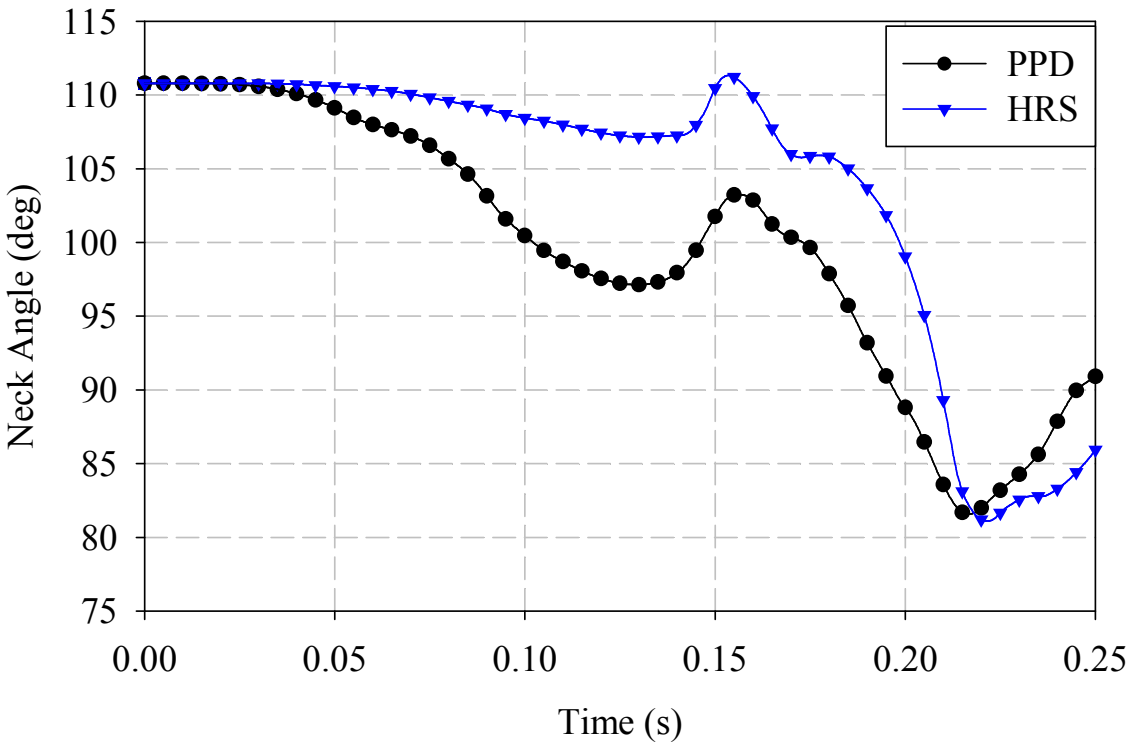

Figure 38 – Neck angle versus time – side impact.

9.2.2 Head Accelerations

The HRS did not provide any extra protection from severe head accelerations in the lateral direction as it did with the front crash condition, these observations can be found in Figure 39, below. The reason behind this is that it is composed of cloth material and it is only effective when in tension and has no resistance to bending. The peak acceleration observed at roughly 115 ms after implementing the HRS is also due to the rigid contact between the head and chest clasp. The *HIC* with HRS present is 229.3 while with the PPD it is 206.5. Although the HRS did increase the peak head acceleration slightly the duration of the peak was not long and so the *HIC* values are quite similar with the increase in head accelerations and *HIC* being 14.2 percent and 11.0 percent respectively.

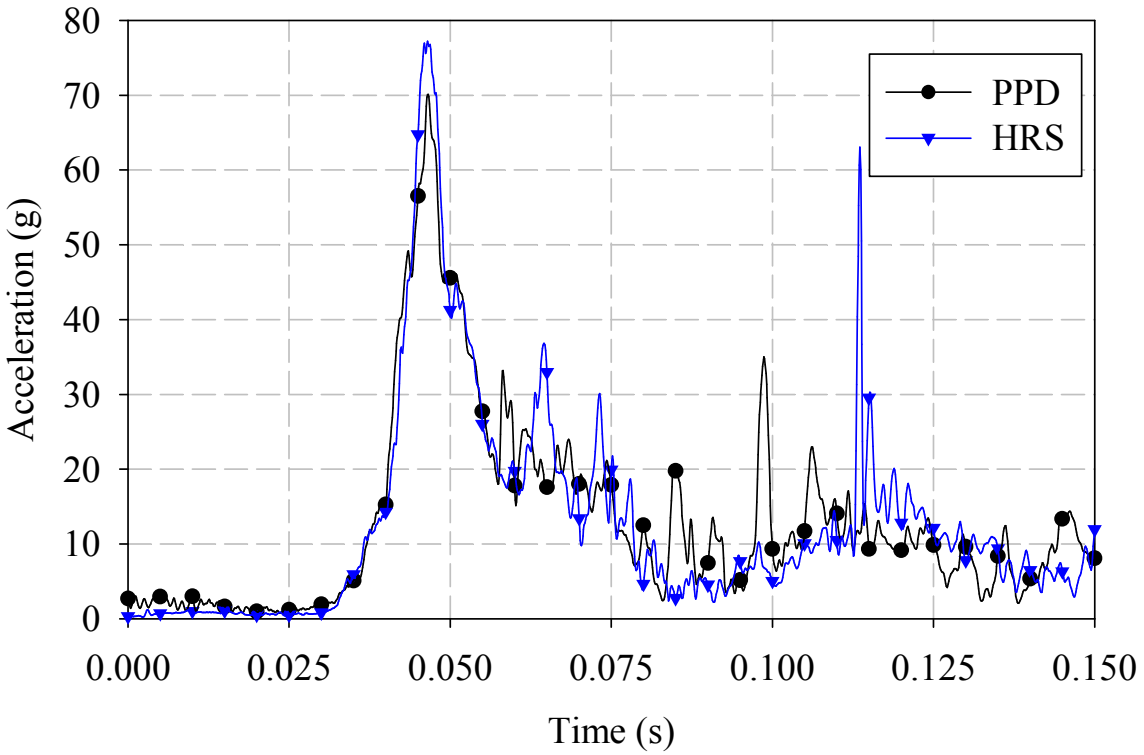

Figure 39 – Resultant head accelerations versus time – side impact.

9.2.3 Neck Tensile Forces

At the upper neck joint, the tensile loads experienced by the joints are quite consistent. Generally the compressive forces are larger in the upper neck joints with the HRS configuration. However, the largest force observed is 115 N for the PPD and 110 N for the HRS. Therefore the upper neck joint experiences the same conditions with both configurations. The lower neck joint is much the same, with the exception that there are not many compressive forces acting on the lower neck joint throughout the event. The resultant neck forces observed are higher by 10.7 percent at the upper neck joint and lower by 7.2 percent at the lower neck joint with the HRS other than the difference in peak force the forces experienced are very similar throughout the simulation. The shear behaviour is almost identical to the resultant behaviour since it accounts for a larger portion of the resultant force than the tensile loads do. The tensile loads can be found in Figure 40, while the resultant and shear force plots can be found in Appendix B.

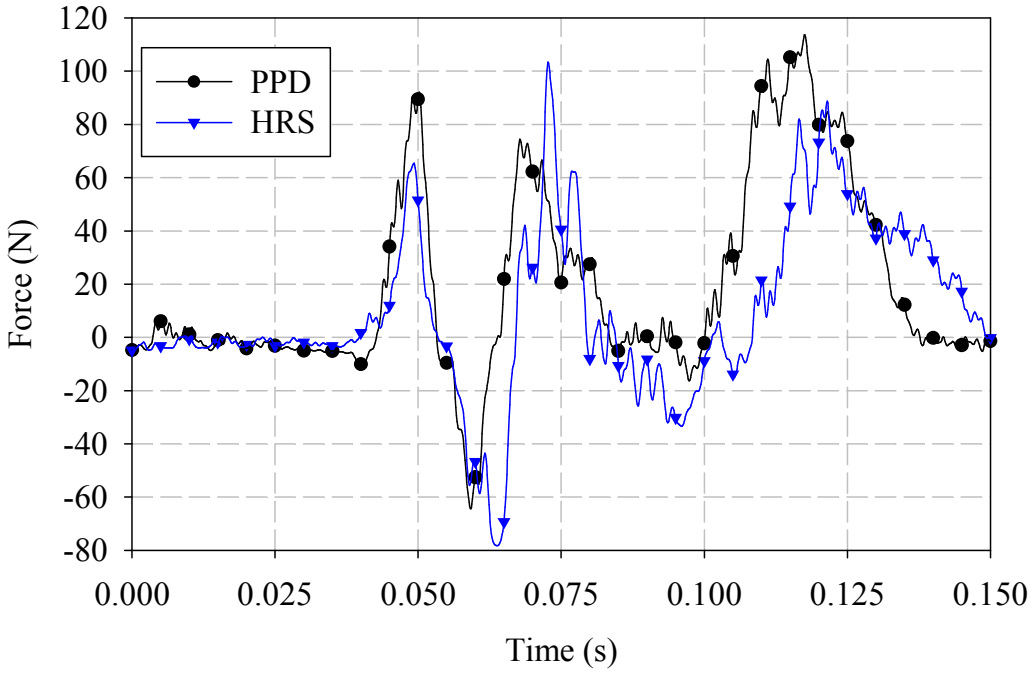

(a)

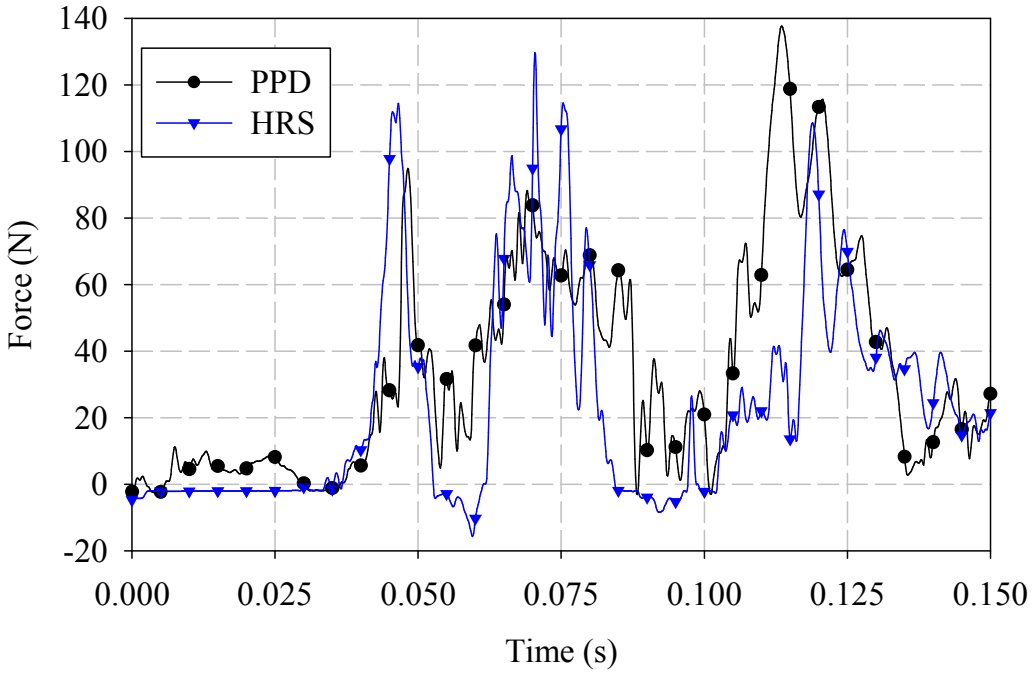

(b)

Figure 40 – Neck tensile forces – side impact (a) upper neck joint (b) lower neck joint.

9.3 Discussion

The addition of the HRS did not prove to have significant advantages or disadvantages when judging the performance based on neck angle and head acceleration data. The changes in those two parameters were generally within 10 percent and generally provided a slight benefit. The neck angle was always ending in an upward trend, returning to the resting position that provides an adequate level of neck extension. The only point of worry would be the neck angle at the end of the side impact simulation because the neck is still in flexion, but with an upward trend. It is expected it would return to the resting position found in the aggressive driving conditions but that is not guaranteed. The head accelerations are well within the limits set out by the CMVSS and there is no significant change between the PPD and HRS configurations.

However, the HRS proves to have some merit on the basis that it could be used as a load limiting device. In the tensile force graphs, there are two peaks. At both the upper and lower neck joint there are two tensile force peaks. In both instances the first peak is consistent between the PPD and HRS configuration. However, at the second peak the HRS only returns to the level of loading of the first peak, whereas the PPD configuration experiences a higher second peak. This shows that the HRS does not allow the loads in the neck to surpass a certain level which is very desirable. With the right material, a neck loading threshold could be determined and once those loads are reached the HRS would start to fail allowing for the HRS to absorb some of the energy associated with the crash events.

The HRS performs better in the front crash scenario because all of the fabric is being loaded in tension. However during a side impact one side of the HRS material is simply loaded in bending and the material has no resistance to bending. The HRS should be further investigated to see how the effects of the side impact can be mitigated through the use of the HRS. Although the rear impact was not studied in this thesis work, the HRS would be a good potential candidate to improve the safety of the infant in the case of such an event. In a rear collision, the infant's head would be thrown out of the seat, which would be a very detrimental scenario for the infant with its undeveloped neck. However,

if the HRS is present it would again be loaded in tension and reduce the amount of head excursion experienced by the infant while providing some additional support to the neck.

Figure 41 is a good graphical representation of the HRS in action taking in some of the shock from the frontal impact. The load path is in the direction the head is moving during the impact. As a result the HRS is limiting the load experienced by the neck joints, as previously observed in Figure 37 and is also able to limit the amount of head excursion. When attempting to find similar results with the side impact it is not possible. The HRS is not capable of restraining the head as well in a lateral direction because of the slack introduced by one of the sides not receiving any load. To improve the performance of the HRS this issue need to be addressed in order to have the material loaded in tension no matter what type of loading the system is experiencing. Only then will the HRS be able to perform to its full potential in all situations.

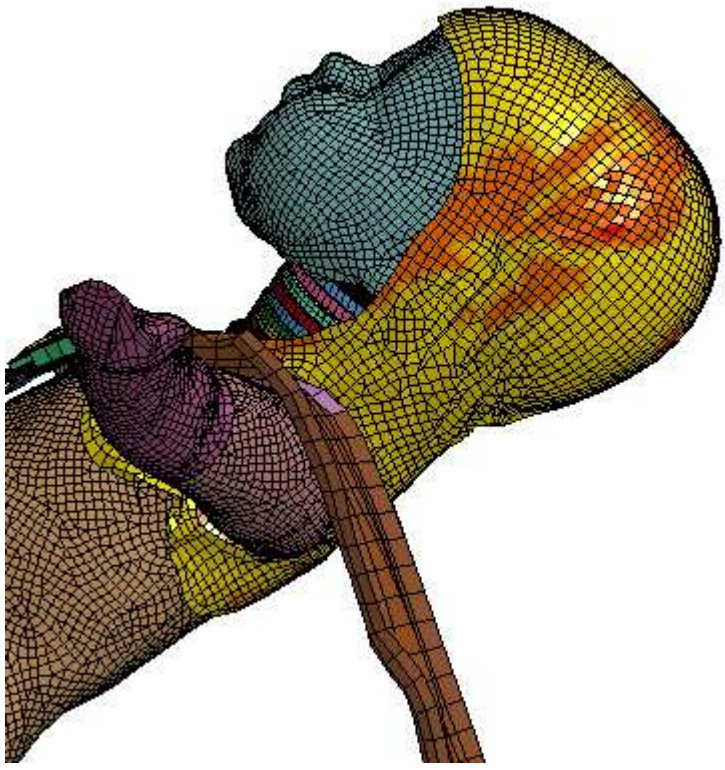

Figure 41 – The component of stress in the x direction shown over the surface of the HRS.

10. **CONCLUSIONS**

Prematurely born and low birth weight infants are a vulnerable population. The lack of development of musculature and bones makes them very vulnerable to respiratory complications and injuries when subjected to impacts and shaking induced by car maneuvers or any other type of disturbance. Studies have been undertaken to try and determine the source of the respiratory difficulties, because of the large social and economic burden posed by keeping these infants in hospitals longer than they generally need to be.

Two devices, the PPD and the HRS, were studied in various conditions to determine the potential contributions of these designs to the well-being of low birth weight and premature infants in CRSs. The study concluded that:

1) The presence of the PPD and the HRS improved the neck angle for all aggressive driving conditions by an average of 15 percent and 23.6 percent, respectively. The PPD and HRS conditions also assure an appropriate and acceptable level of neck extension throughout the entire events while the no PPD condition exhibited constant flexion of the neck towards the end of the events.

2) In the front crash event, both prototypes provide an improvement when it comes to the neck angle. Both the PPD and the HRS provide a 3-10 degree improvement over the no PPD condition throughout the entire simulation. There is never any neck flexion as both the PPD and HRS provide angles above 90 degrees for the duration of the simulation creating a good environment for airway patency while the no PPD configuration sees a resting place towards the end of roughly 90 degrees (corresponding to a neutral neck angle). The PPD and HRS also provide an 11 percent and 20 percent decrease in peak head acceleration, with the values dropping below 80 g's which is the threshold for failure according to the CMVSS and

FMVSS standards, while the no PPD condition leads to a peak head acceleration of 90 g's. Although the no PPD configuration leads to the highest peak head accelerations, the *HIC* was higher with the PPD and HRS by a margin of 0.6-11 percent depending on the configuration of the CRS. Forces in the neck are similar in the no PPD and PPD configurations. However, the presence of the HRS is able to reduce the peak neck tensile loads at both the upper and lower neck by 26.3 percent and 23.8 percent respectively.

3) The side crash event proved to be more harmful as a disturbance to the infant based on the neck angles observed from the ATD. All three configurations experienced some degree of neck flexion and only the PPD configuration returned to a neutral neck angle before the end of the simulation. However, both the PPD and HRS had a rising neck angle at the time of termination. The configuration involving the HRS seemed to have little to no effect on the side crash protection since the PPD and HRS head acceleration responses followed each other closely. The no PPD condition had a similar peak in acceleration but a much longer duration of elevated head accelerations than the other two configurations, along with a secondary peak rising above 60 g's and a third peak reaching roughly 35 g's. The neck forces experience in the presence of the PPD and the HRS were reduced by 40 percent in the upper neck joints and by 45 percent in the lower neck joints when comparing to the no PPD configuration.

The purpose of the PPD was to provide respiratory stability for the at risk preemie and low birth weight infants without compromising the crash performance of the CRS. The PPD is able to provide an appropriate neck angle and positioning for the infant in all of the studied scenarios and most other driving scenarios that could disrupt the infant. The introduction of the PPD in the CRS did not hinder the performance in both front and side impact events.

The HRS was being investigated to see whether or not simply dressing these vulnerable infants in a tightened hooded sweater could impact the response of the child in every day driving conditions and crash events. The introduction of the HRS does impact the performance of a CRS in a side crash but it is able to improve the response of the system through reduced neck loads, better neck angle and lower head accelerations in the front crash scenario. In a front crash situation it reduces the peak head acceleration by 10.3 percent, has similar *HIC* values, reduces the loads passing through the neck by 26.3 percent and 28.3 percent (at the upper and lower neck joints, respectively) and improves the neck angle by 3.2 percent. The HRS is better suited for protection in a frontal crash. A tight hoodie will also help reduced the amount of motion during every day and aggressive driving conditions. It proved to have additional protection against neck flexion in all aggressive driving scenarios.

11. **LIMITATIONS OF THE STUDY**

There are certain limitations to the study that need to be discussed in order to be considered in future investigations that could come as a result of the finding in this study. Although the limitations are present in the study, they are consistently present in all of the configurations studied and in all scenarios investigated. The limitations are:

1) The infant dummy model is constructed of only rigid components which does not allow for accurate contact to be represented when it is coming in contact with harder surfaces and it does not allow for a full range of motion of the child. Where there would be deformation in a real life scenario, the simulations show an immediate stop and rebound at the contact interface. This is most noticeable when the head of the infant is coming into contact with the chest clasp which also consists of a rigid entity. This issue is most noticeable when there is no PPD present because the neck angle is the lowest in that configuration and the head is more prone to coming in contact with the chest clasp. In this case the full neck flexion is not able to be captured because in a real life scenario there could be some deformation at the chin and the head would not be as likely to rebound because of the softer contact.

This leads to an inability of the model to estimate the full extent neck flexion experienced by the infant and the performance gains of the PPD and HRS would generally improve without this limitation.

2) Another limitation to the model is the lack of the presence of the manufacturer's CRS cloth cover in the simulations. Although this does provide a small layer of material between the infant and the CRS it is not a significant source of energy absorption or cushioning for the infant and its implementation would be rather difficult because of the lack of stiffness in the material and its loose fit over the CRS.
3) Although the infant dummy was validated in from some aspects, the response of this dummy was never compared to an experimental response of an ATD of this size in a physical crash simulation. The problem here is that an ATD of this size is not readily available for testing and there is no ATD that exists with the complex joints and possibilities of movement present in this numerical model. It would be important to try and replicate these simulation results with physical experiments to confirm the accuracy of the model.

REFERENCES

[1] Transport Canada (2013). *Canadian Motor Vehicle Traffic Collision Statistics 2011.* Transport Canada: Ottawa, Ontario; 1-6.

[2] Weber, K., (2000). *Crash protection for child passengers: a review of best practice.* UMTRI Research Review, 31(3).

[3] Wegner, M.V. and Girasek, D.C., (2003). *How readable are child safety seat installation instructions?* Pediatrics, 111(3): p. 588-591.

[4] Howson, C.P., Kinney, M.V., and Lawn, J.E., (2012). *Born Too Soon: The Global Action Report on Preterm Births*, March of Dimes, The Partnership for MAternal, Newborn & Child Health, Save the Children, World Health Organization: Geneva.

[5] Canadian Institute for Health Information (2011). *Highlights of 2009-2010 Selected Indicators Describing the Birthing Process in Canada.* Canadian Institue for Health Information: Ottawa, ON; 1-7.

[6] Muraskas, J. and Parsi, K., (2008). *The cost of saving the tiniest lives: NICUs versus prevention.* Virtual Mentor, 10(10): p. 655.

[7] Phibbs, C.S. and Schmitt, S.K., (2006). *Estimates of the cost and length of stay changes that can be attributed to one-week increases in gestational age for premature infants.* Early human development, 82(2): p. 85-95.

[8] Russell, R.B., Green, N.S., Steiner, C.A., Meikle, S., Howse, J.L., Poschman, K., Dias, T., Potetz, L., Davidoff, M.J., and Damus, K., (2007). *Cost of hospitalization for preterm and low birth weight infants in the United States.* Pediatrics, 120(1): p. e1-e9.

[9] SMARTRISK, (2009). *The Economic Burden of Injury in Canada*, SMARTRISK: Toronto, ON. p. 1-5.

[10] Decina, L. and Lococo, K., (2003). *Misusse of Child Restraints*, U.S. Department of Transportation/National Highway Traffic Safety Administration: Washington, DC.

[11] Turner, C.H., (2006). *Bone strength: current concepts.* Annals of the New York Academy of Sciences, 1068(1): p. 429-446.

[12] Burdi, A.R., Huelke, D.F., Snyder, R.G., and Lowrey, G., (1969). *Infants and children in the adult world of automobile safety design: Pediatric and anatomical considerations for design of child restraints.* Journal of Biomechanics, 2(3): p. 267-280.

[13] Howard-Salsman, K.D., (2006). *Car seat safety for high-risk infants.* Neonatal Network: The Journal of Neonatal Nursing, 25(2): p. 117-129.

[14] Duncan, J.M., (1874). *Laboratory note: on the tensile strength of the fresh adult foetus.* British medical journal, 2(729): p. 763-764.

[15] Luck, J.F., Nightingale, R.W., Loyd, A.M., Prange, M.T., Dibb, A.T., Song, Y., Fronheiser, L., and Myers, B.S., (2008). *Tensile mechanical properties of the perinatal and pediatric PMHS osteoligamentous cervical spine.* Stapp car crash journal, 52: p. 107.

[16] Ouyang, J., Zhu, Q., Zhao, W., Xu, Y., Chen, W., and Zhong, S., (2005). *Biomechanical assessment of the pediatric cervical spine under bending and tensile loading.* Spine, 30(24): p. E716-E723.

[17] Van Ee, C.A., Nightingale, R., Camacho, D., Chancey, V., Knaub, K., Sun, E., and Myers, B., (2000). *Tensile properties of the human muscular and ligamentous cervical spine.* Stapp car crash journal, 44: p. 85-102.

[18] Myers, B.S., Van Ee, C.A., Camacho, D.L., Woolley, C., and Best, T., (1995). *On the structural and material properties of mammalian skeletal muscle and its relevance to human cervical impact dynamics*. in *Proceedings: Stapp Car Crash Conference*: Society of Automotive Engineers SAE.

[19] Myers, B.S. and Winkelstein, B.A., (1995). *Epidemiology, classification, mechanism, and tolerance of human cervical spine injuries.* Critical Reviews™ in Biomedical Engineering, 23(5-6).

[20] Roche, C. and Carty, H., (2001). *Spinal trauma in children.* Pediatric radiology, 31(10): p. 677-700.

[21] Scheidler, M.G., Shultz, B.L., Schall, L., and Ford, H.R., (2000). *Risk factors and predictors of mortality in children after ejection from motor vehicle crashes.* Journal of Trauma-Injury, Infection, and Critical Care, 49(5): p. 864-868.

[22] Howard, A., Rothman, L., McKeag, A.M., Pazmino-Canizares, J., Monk, B., Comeau, J.L., Mills, D., Blazeski, S., Hale, I., and German, A., (2004). *Children*

in side-impact motor vehicle crashes: seating positions and injury mechanisms. Journal of Trauma-Injury, Infection, and Critical Care, 56(6): p. 1276-1285.

[23] Apple, J., Kirks, D., Merten, D., and Martinez, S., (1987). *Cervical spine fractures and dislocations in children.* Pediatric radiology, 17(1): p. 45-49.

[24] Bohn, D., Armstrong, D., Becker, L., and Humphreys, R., (1990). *Cervical spine injuries in children.* Journal of Trauma and Acute Care Surgery, 30(4): p. 463-469.

[25] Brown, R.L., Brunn, M.A., and Garcia, V.F., (2001). *Cervical spine injuries in children: a review of 103 patients treated consecutively at a level 1 pediatric trauma center.* Journal of pediatric surgery, 36(8): p. 1107-1114.

[26] Cirak, B., Ziegfeld, S., Knight, V.M., Chang, D., Avellino, A.M., and Paidas, C.N., (2004). *Spinal injuries in children.* Journal of pediatric surgery, 39(4): p. 607-612.

[27] Kokoska, E.R., Keller, M.S., Rallo, M.C., and Weber, T.R., (2001). *Characteristics of pediatric cervical spine injuries.* Journal of pediatric surgery, 36(1): p. 100-105.

[28] Nightingale, R.W., Winkelstein, B.A., Van Ee, C.A., and Myers, B.S., (1998). *Injury mechanisms in the pediatric cervical spine during out-of-position airbag deployments*. in *Annual Proceedings/Association for the Advancement of Automotive Medicine*: Association for the Advancement of Automotive Medicine.

[29] Dietrich, M., Kedzior, K., and Zagrajek, T., (1991). *A biomechanical model of the human spinal system.* Proceedings of the Institution of Mechanical Engineers, Part H: Journal of Engineering in Medicine, 205(1): p. 19-26.

[30] Givens, T.G., Polley, K.A., Smith, G.F., and Hardin, W.D., (1996). *Pediatric cervical spine injury: a three-year experience.* Journal of Trauma-Injury, Infection, and Critical Care, 41(2): p. 310-314.

[31] Nitecki, S. and Moir, C.R., (1994). *Predictive factors of the outcome of traumatic cervical spine fracture in children.* Journal of pediatric surgery, 29(11): p. 1409-1411.

[32] Bass, J.L., Mehta, K.A., and Camara, J., (1993). *Monitoring premature infants in car seats: implementing the American Academy of Pediatrics policy in a community hospital.* Pediatrics, 91(6): p. 1137-1141.

[33] Bull, M.J. and Engle, W.A., (2009). *Safe Transportation of Preterm and Low Birth Weight Infants at Hospital Discharge.* Pediatrics, 123: p. 1424-1429.

[34] Bull, M.J. and Stroup, K.B., (1985). *Premature infants in car seats.* Pediatrics, 75(2): p. 336-339.

[35] Kinane, T.B., Murphy, J., Bass, J.L., and Corwin, M.J., (2006). *Comparison of Respiratory Physiologic Features When Infants Are Placed in Car Safety Seats or Car Beds.* Pediatrics, 118(2): p. 522-527.

[36] Merchant, J.R., Worwa, C., Porter, S., Coleman, J., and Deregnier, R.A.O., (2001). *Respiratory instability of term and near-term healthy newborn infants in car safety seats.* Pediatrics, 108(3): p. 647-652.

[37] Ojadi, V.C., Petrova, A., Mehta, R., and Hegyi, T., (2005). *Risk of cardio-respiratory abnormalities in preterm infants placed in car seats: a cross-sectional study.* BMC pediatrics, 5(1): p. 28.

[38] Willett, L.D., Leuschen, M.P., Nelson, L.S., and Nelson Jr, R.M., (1986). *Risk of hypoventilation in premature infants in car seats.* The Journal of pediatrics, 109(2): p. 245-248.

[39] Willett, L.D., Leuschen, M.P., Nelson, L.S., and Nelson Jr, R.M., (1989). *Ventilatory changes in convalescent infants positioned in car seats.* The Journal of pediatrics, 115(3): p. 451-455.

[40] Salhab, W.A., Khattak, A., Tyson, J.E., Crandell, S., Summer, J., Goodman, B., Fisher, L., and Robinson, K., (2007). *Car seat or car bed for very low birth weight infants at discharge home.* J Pediatr, 150(3): p. 224-228.

[41] Tonkin, S.L., Vogel, S.A., Bennet, L., and Gunn, A.J., (2006). *Apparently life threatening events in infant car safety seats.* BMJ, 333(7580): p. 1205-1206.

[42] Cote, A., Bairam, A., Deschenes, M., and Hatzakis, G., (2008). *Sudden infant deaths in sitting devices.* Archives of Disease in Childhood, 93(5): p. 384-389.

[43] Reber, A., Wetzel, S.G., Schnabel, K., Bongartz, G., and Frei, F.J., (1999). *Effect of combined mouth closure and chin lift on upper airway dimensions during routine magnetic resonance imaging in pediatric patients sedated with propofol.* Anesthesiology, 90(6): p. 1617-1623.

[44] Wilson, S.L., Thach, B.T., Brouillette, R.T., and Abu-Osba, Y.K., (1980). *Upper airway patency in the human infant: influence of airway pressure and posture.* J Appl Physiol, 48(3): p. 500-504.

[45] Lacourt, G. and Polgar, G., (1971). *Interaction between nasal and pulmonary resistance in newborn infants.* Journal of applied physiology, 30(6): p. 870-873.

[46] Polgar, G. and Kong, G.P., (1965). *The nasal resistance of newborn infants.* The Journal of pediatrics, 67(4): p. 557-567.

[47] Swyer, P.R., Reiman, R., and Wright, J.J., (1960). *Ventilation and ventilatory mechanics in the newborn: methods and results in 15 resting infants.* The Journal of pediatrics, 56(5): p. 612-622.

[48] Thach, B. and Taeusch Jr, H., (1976). *Sighing in newborn human infants: role of inflation-augmenting reflex.* Journal of applied physiology, 41(4): p. 502-507.

[49] (1996). *Safe transportation of premature and low birth weight infants.* Pediatrics, 97(5): p. 758-760.

[50] Elder, D.E., Russell, L., Sheppard, D., Purdie, G.L., and Campbell, A.J., (2007). *Car seat test for preterm infants: comparison with polysomnography.* Archives of Disease in Childhood-Fetal and Neonatal Edition, 92(6): p. F468-F472.

[51] Insurance Institute for Highway Safety, (2014). Safety Belts and Child Restraints. http://www.iihs.org/iihs/topics/laws/safetybeltuse (Accessed: September, 2014).

[52] CPSafety, (2013). Car Seat Types and Styles. http://www.cpsafety.com/articles/csstypes.aspx (Accessed: September, 2014).

[53] Shorten, G., Armstrong, D., Roy, W., and Brown, L., (1995). *Assessment of the effect of head and neck position on upper airway anatomy in sedated paediatric patients using magnetic resonance imaging.* Pediatric Anesthesia, 5(4): p. 243-248.

[54] Tonkin, S.L., McIntosh, C.G., Hadden, W., Dakin, C., Rowley, S., and Gunn, A.J., (2003). *Simple Car Seat Insert to Prevent Upper Airway Narrowing in Preterm Infants: A Pilot Study.* Pediatrics, 112(4): p. 907-913.

[55] McIntosh, C.G., Tonkin, S.L., and Gunn, A.J., (2013). *Randomized controlled trial of a car safety seat insert to reduce hypoxia in term infants.* Pediatrics, 132(2): p. 326-331.

[56] Bull, M.J., Stroup, K.B., Stout, J., Doll, J.P., Jones, J., and Feller, N., (1990). *Establishing special needs car seat loan program.* Pediatrics, 85(4): p. 540-547.

[57] Bondy, M., Altenhof, W., Chen, X., Snowdon, A., and Vrkljan, B., (2012). *Development of a finite element/multi-body model of a newborn infant for restraint analysis and design.* Computer methods in biomechanics and biomedical engineering, 17(2): p. 149-162.

[58] Humanetics Innovative Solutions, (2011). *Q0 User's Manual*. Humanetics Innovative Solutions, Plymouth, Michigan, U.S.A.

[59] Chen, X., (2012) *Development of a restraint device for low birth-weight infants*, in *Mechanical Engineering*University of Windsor: Windsor, ON, Canada.

[60] Stockman, I., Bohman, K., and Jakobsson, L., (2013). *Kinematics and Shoulder Belt Position of Child Anthropomorphic Test Devices during Steering Manoeuvres.* Traffic Injury Prevention, (just-accepted).

[61] Stockman, I., Bohman, K., Jakobsson, L., and Brolin, K., (2013). *Kinematics of child volunteers and child anthropomorphic test devices during emergency braking events in real car environment.* Traffic injury prevention, 14(1): p. 92-102.

[62] HANS Performance Products, (2004). *Hans Owner's Manual*, Atlanta, Georgia, U.S.A.

[63] Kapoor, T., (2008) *Methods to Mitigate Injuries to Toddlers in a Vehicle Crash*, in *Mechanical Engineering*University of Windsor: Windsor, ON, Canada.

[64] Kapoor, T., Altenhof, W., Howard, A., Rasico, J., and Zhu, F., (2008). *Methods to mitigate injuries to toddlers in a vehicle crash.* Accid Anal Prev, 40(6): p. 1880-1892.

[65] Department of Transportation - Government of Canada (2013). Canadian Motor Vehicle Safety Standard 213: Child Restraint Systems. http://laws-lois.justice.gc.ca/eng/regulations/SOR-2010-90/page-5.html (Accessed: July, 2014)

[66] National Highway Traffic Safety Administration - US Department of Transportation, (2013). Federal Motor Vehicle Safety Standard 213: Child Restraint Systems. http://www.nhtsa.gov/ (Accessed: July 2014).

[67] Kleinberger, M., Sun, E., Eppinger, R., Kuppa, S., and Saul, R., (1998). *Development of Improved Injury Criteria for the Assessment of Advanced Automotive Restraint Systems*, National Highway Traffic Safety Administration.

APPENDIX A – FRONT CRASH RESULTS

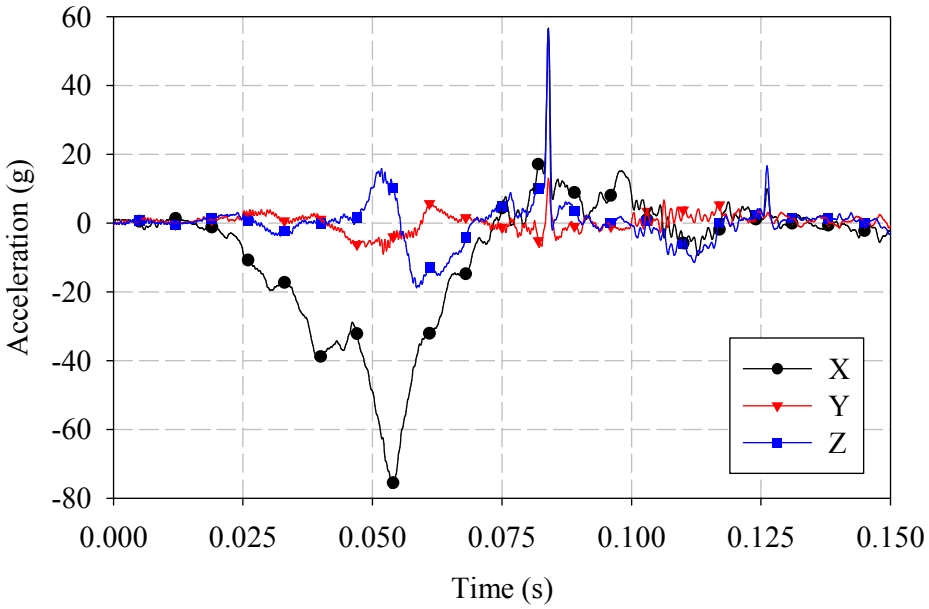

Figure A-1 – PPD condition head acceleration components.

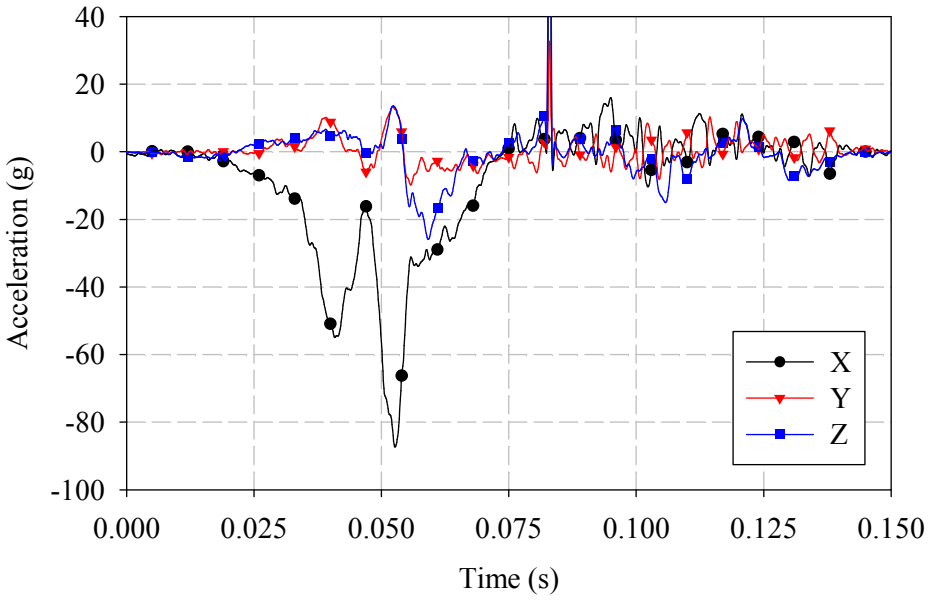

Figure A-2 – No PPD condition head acceleration components. (X, Y, and Z directions correspond to the global coordinate system previously defined in Figure 11.)

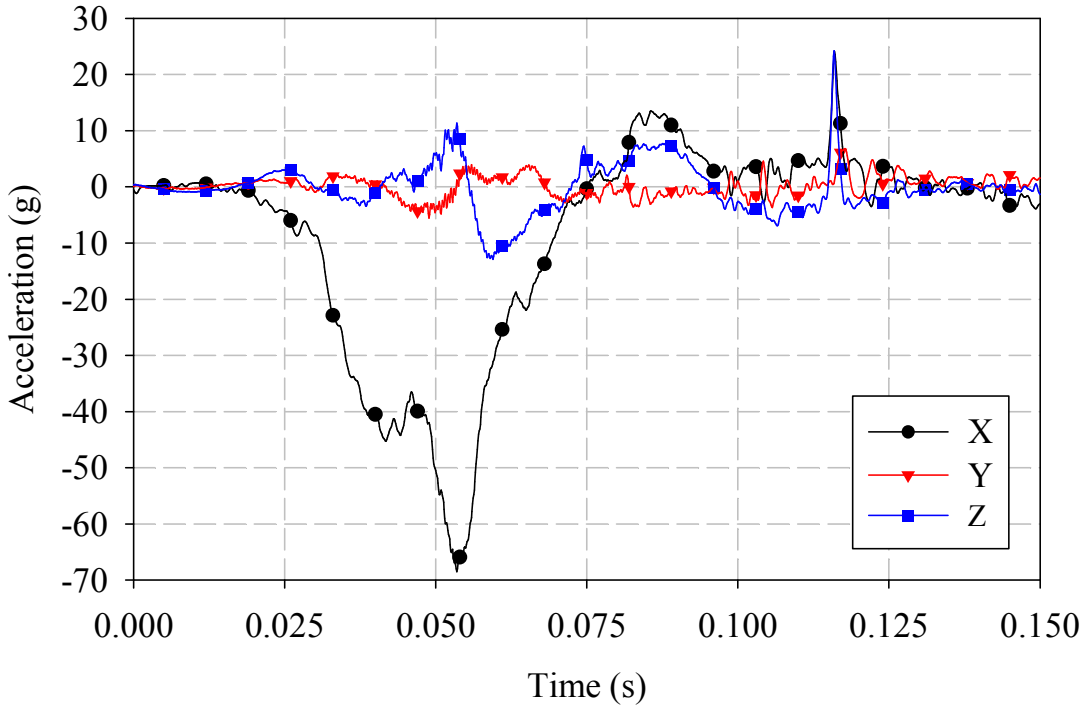

Figure A-3 – HRS condition head acceleration components.

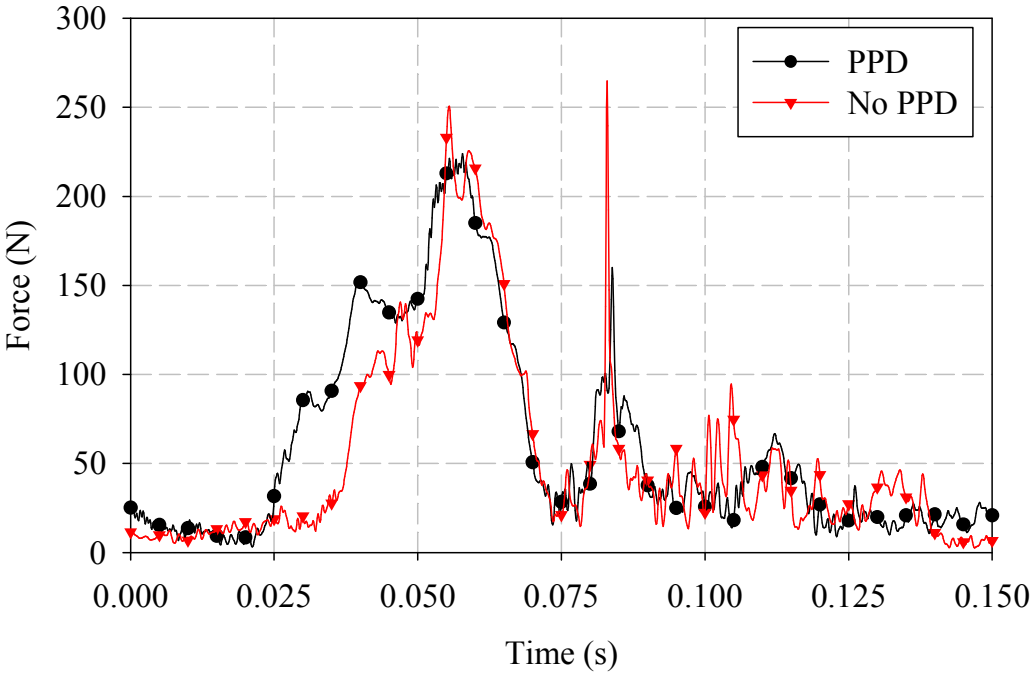

(a)

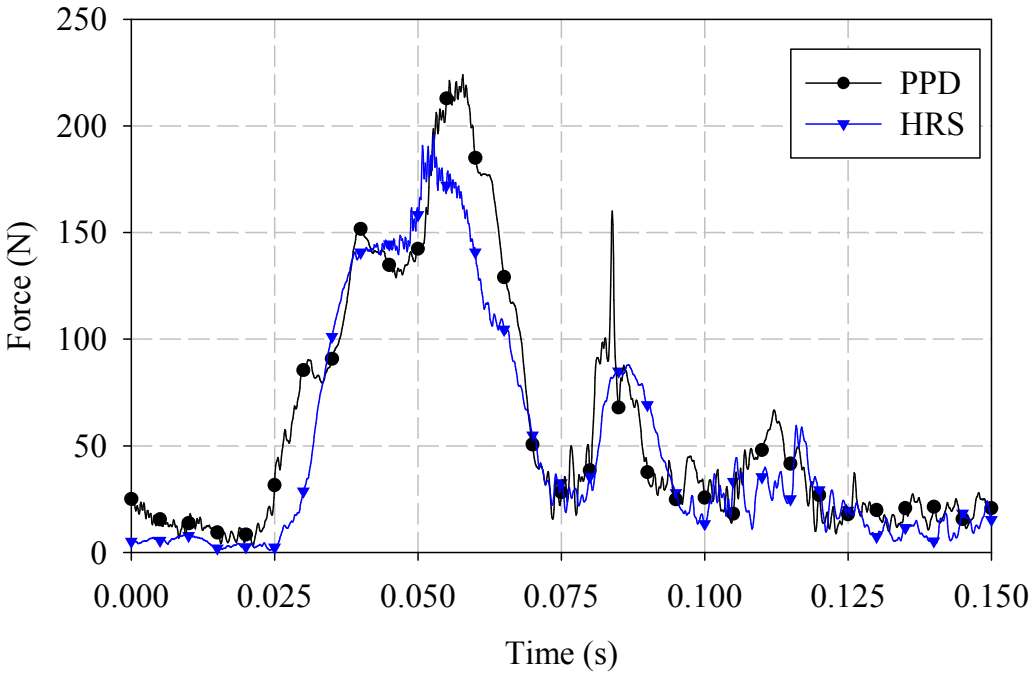

(b)

Figure A-4 – Resultant upper neck forces (a) PPD vs. No PPD and (b) PPD vs. HRS.

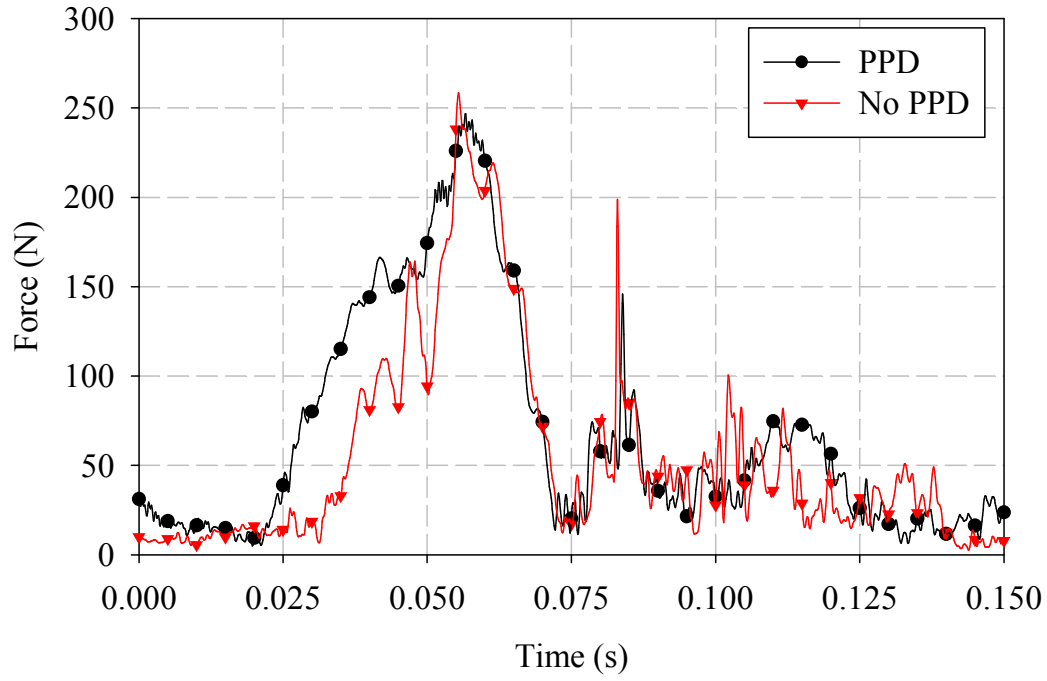

(a)

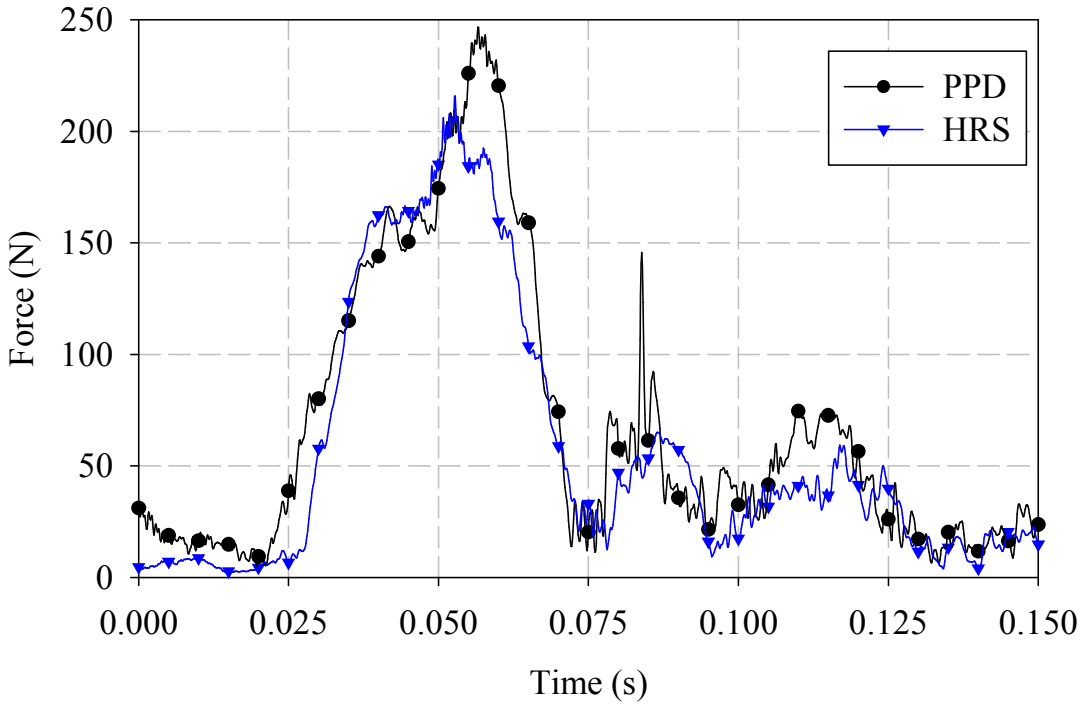

(b)

Figure A-5 – Resultant lower neck forces (a) PPD vs. No PPD and (b) PPD vs. HRS.

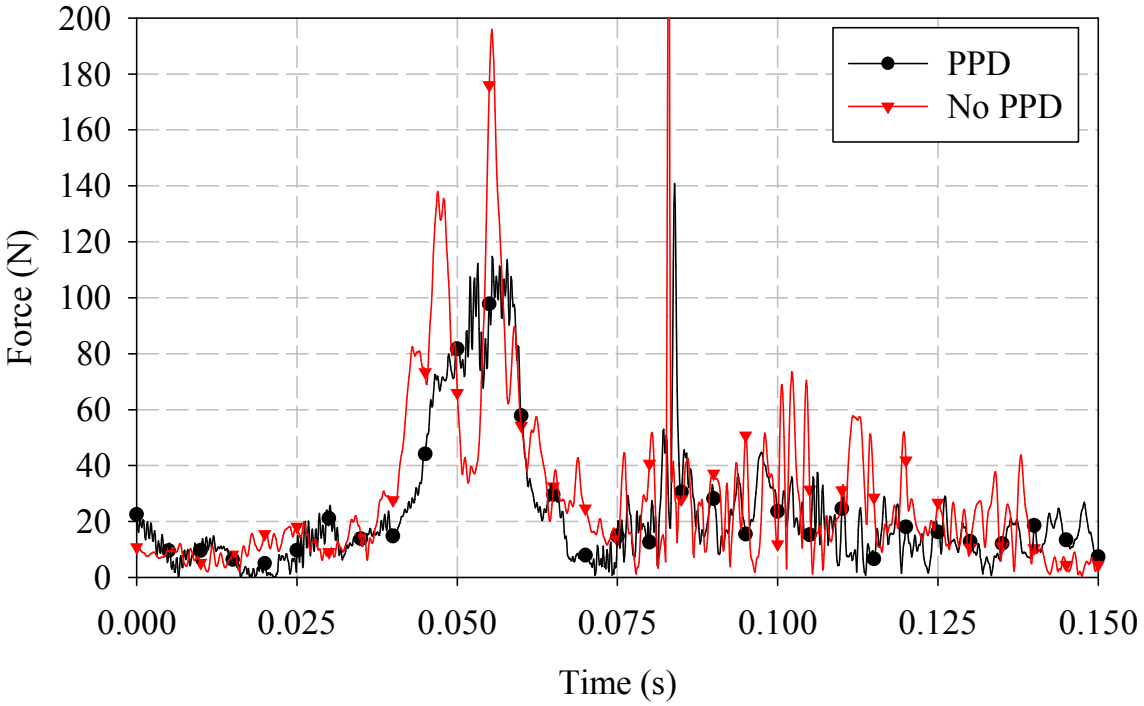

(a)

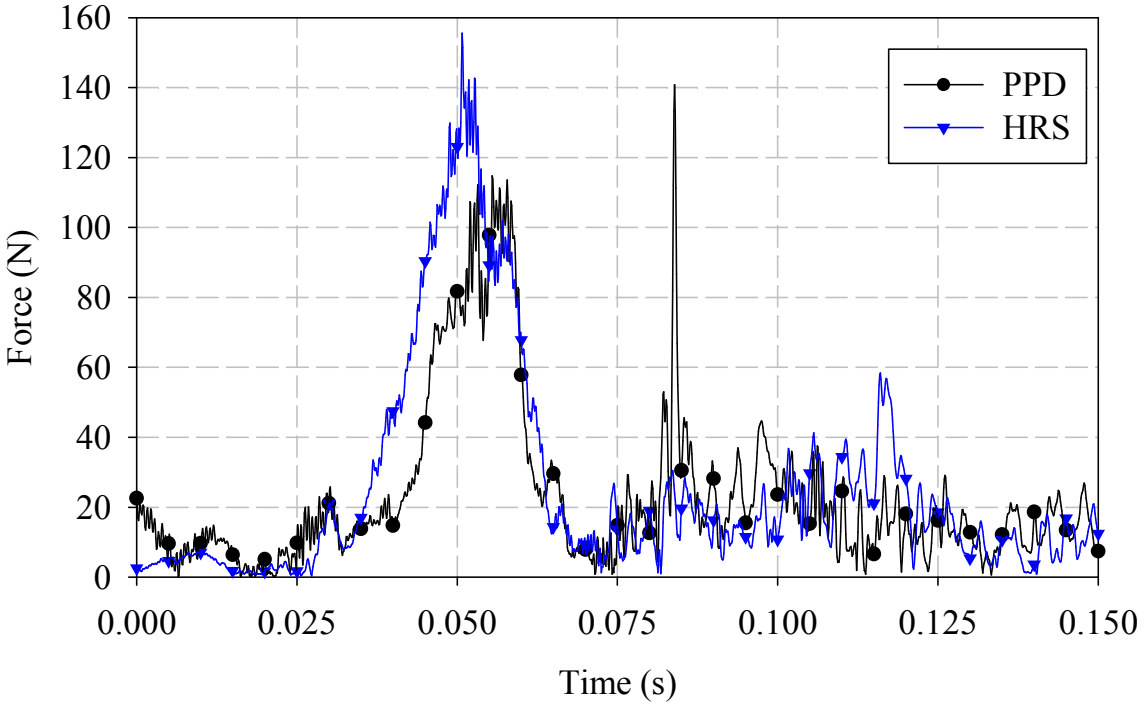

(b)

Figure A-6 – Shear upper neck forces (a) PPD vs. No PPD and (b) PPD vs. HRS.

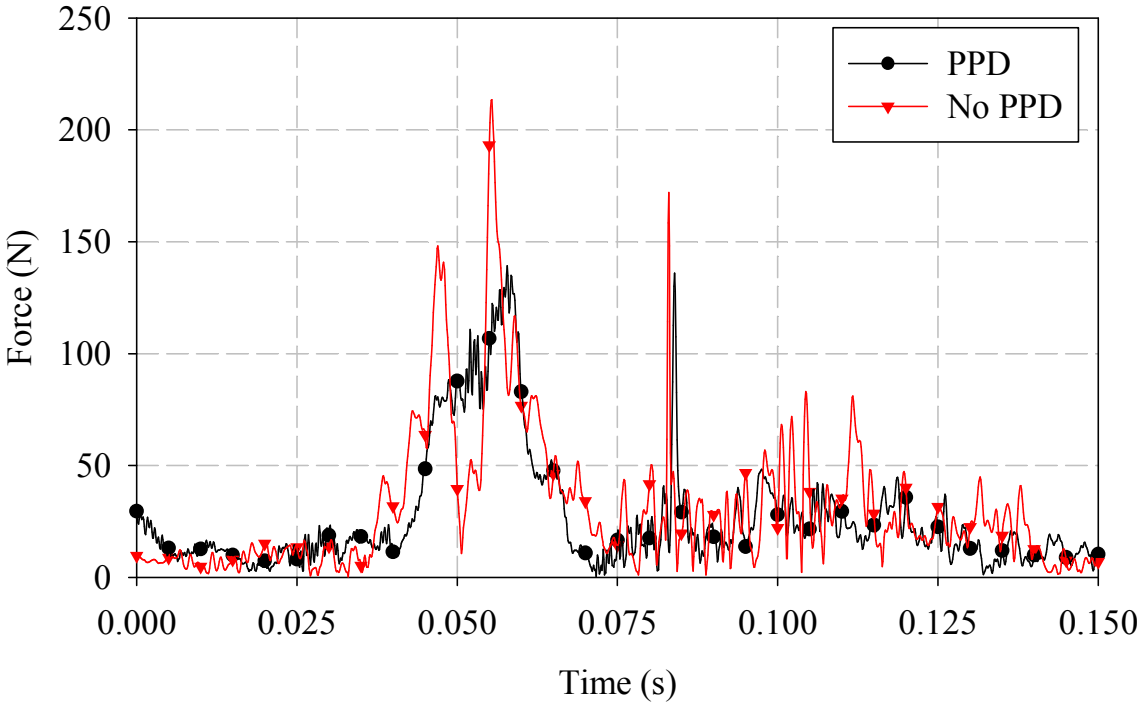

(a)

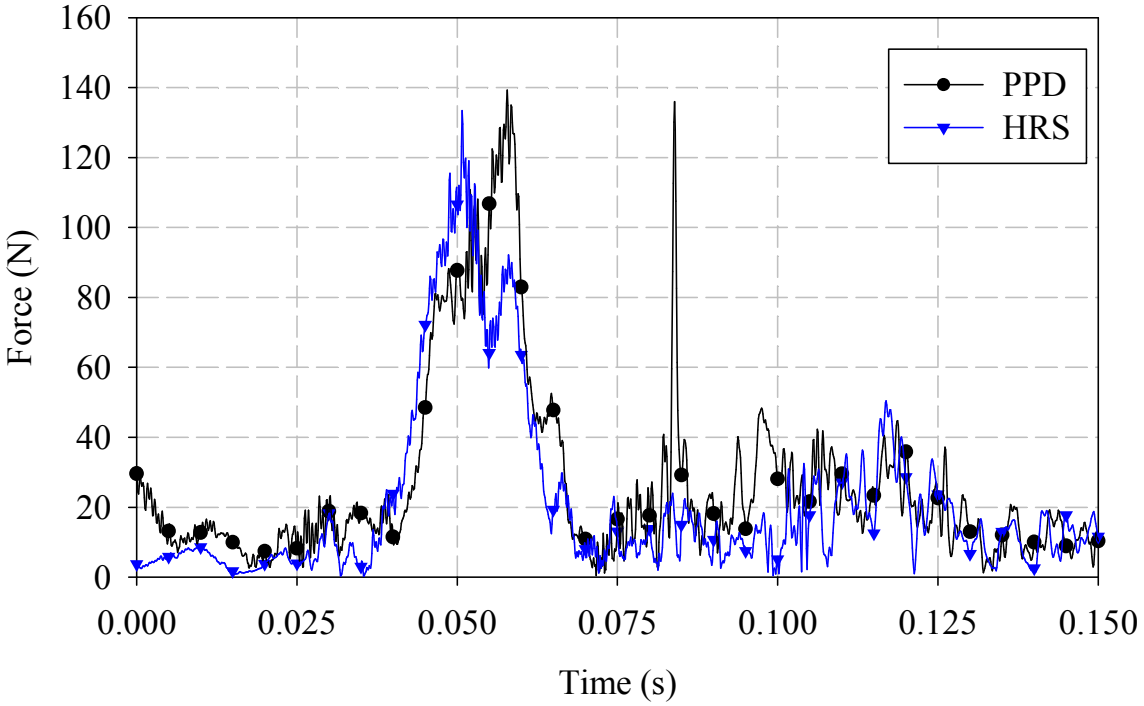

(b)

Figure A-7 – Shear lower neck forces (a) PPD vs. No PPD and (b) PPD vs. HRS.

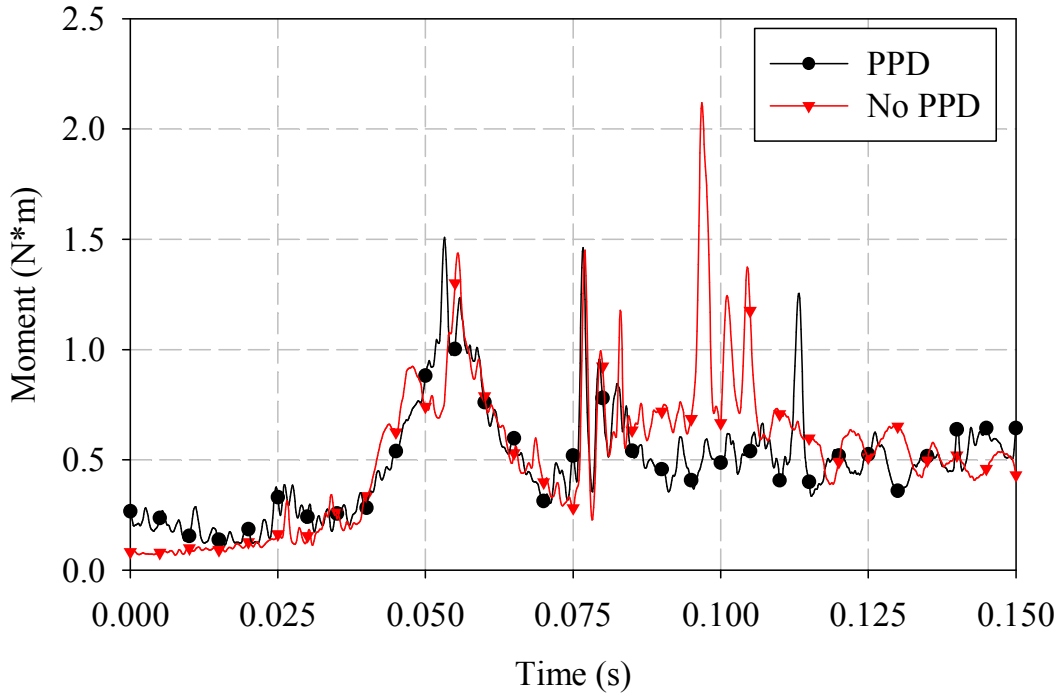

(a)

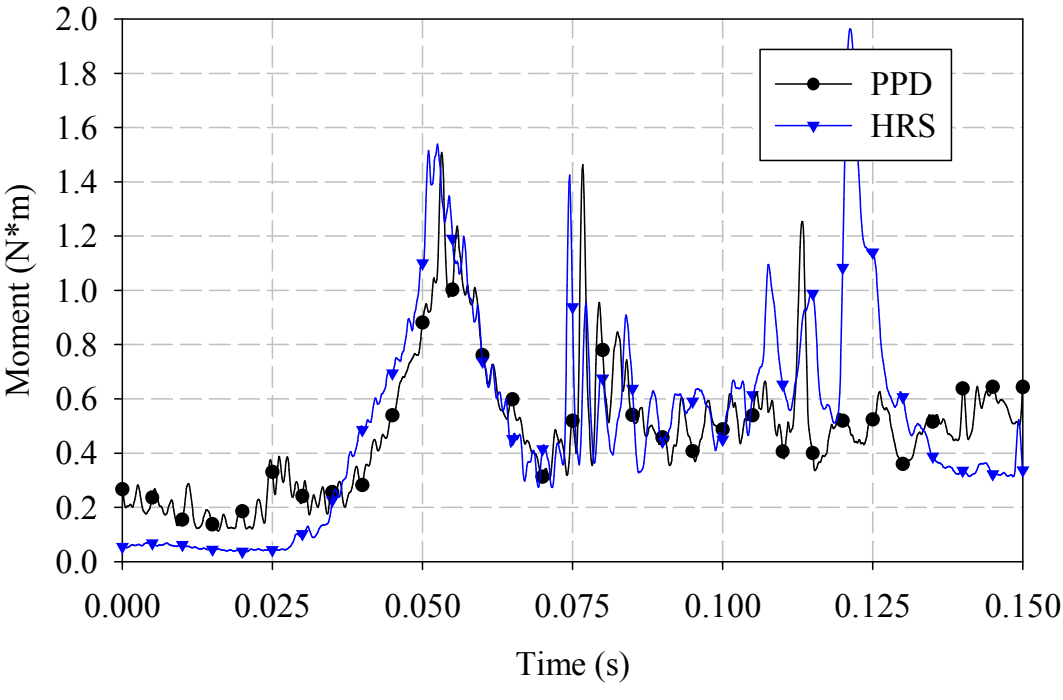

(b)

Figure A- 8 – Upper neck moments (a) PPD vs. No PPD and (b) PPD vs. HRS.

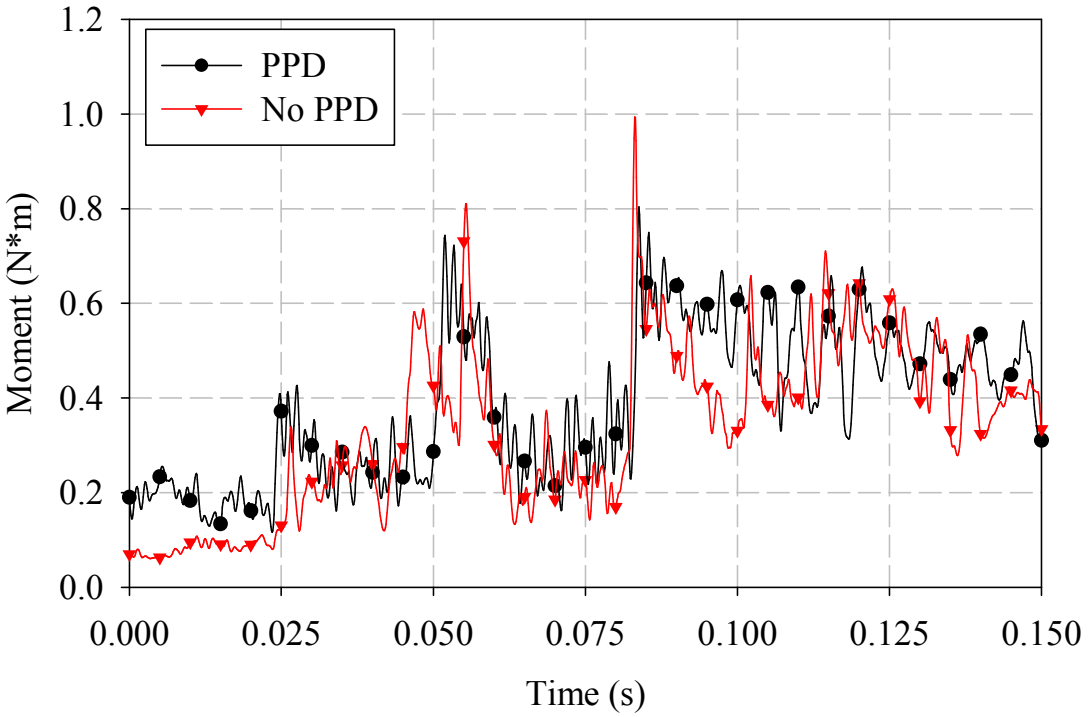

(a)

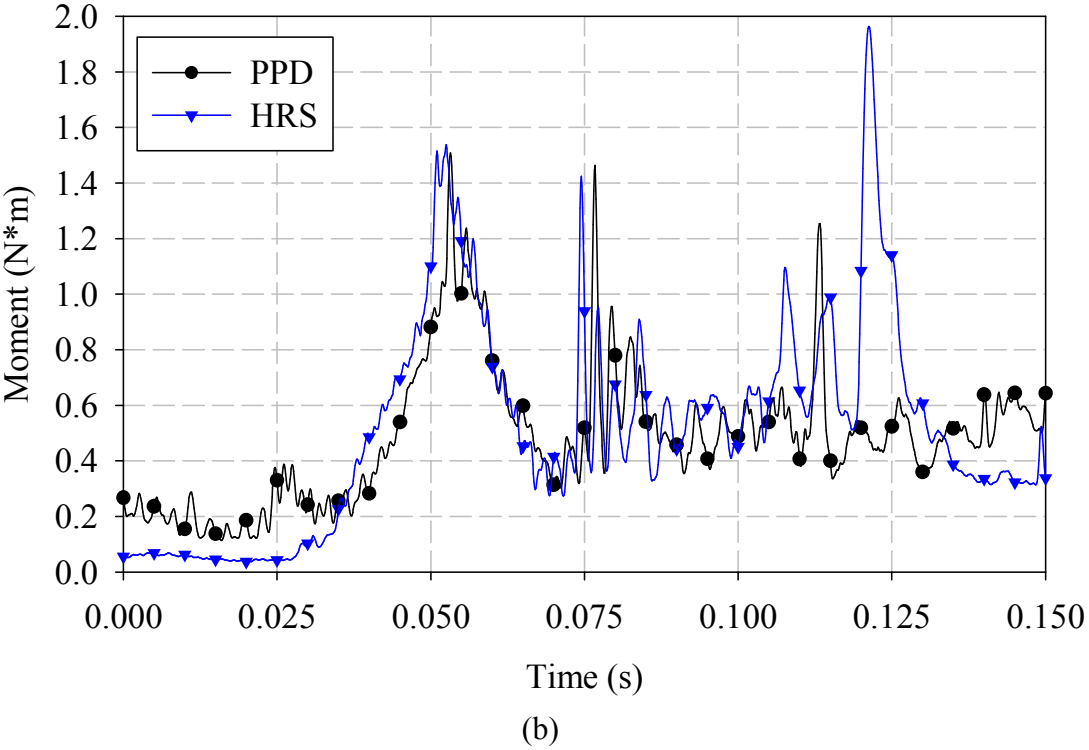

(b)

Figure A-9 – Lower Neck moments (a) PPD vs. No PPD and (b) PPD vs. HRS.

APPENDIX B – SIDE CRASH RESULTS

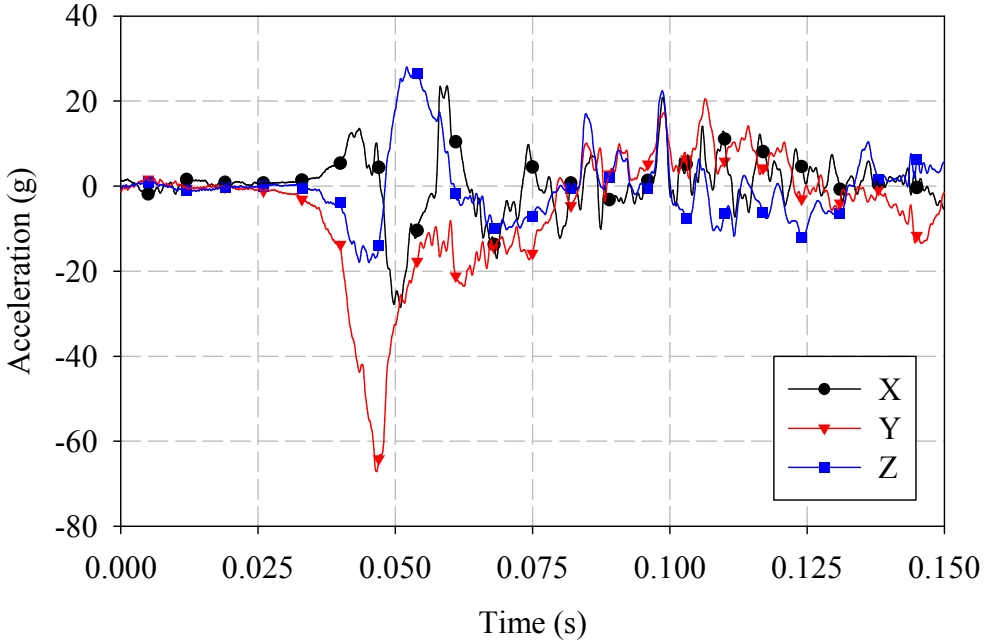

Figure B-1 – PPD condition head acceleration components.

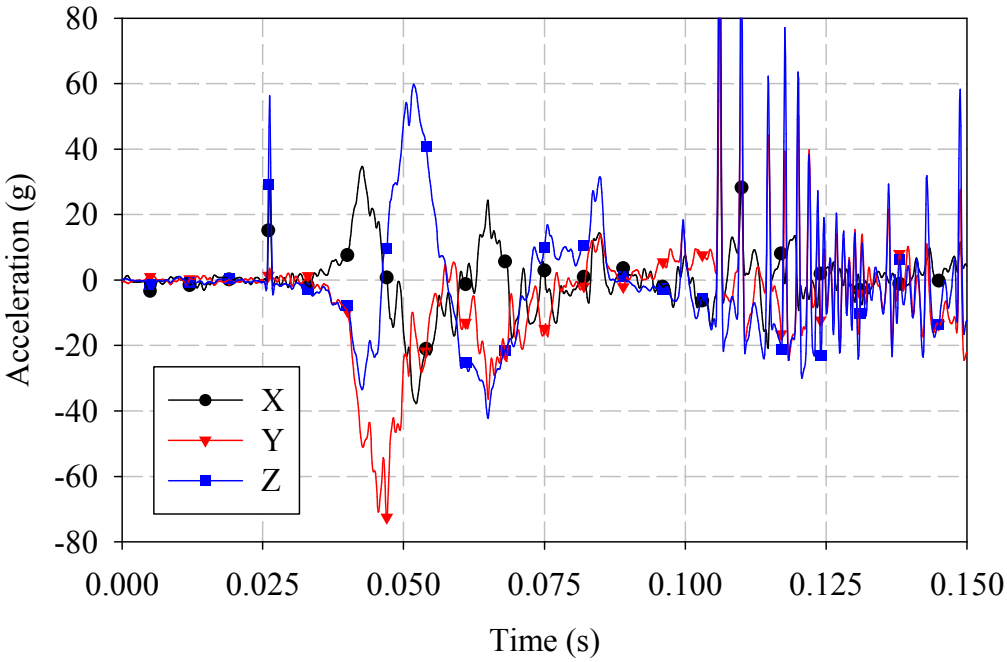

Figure B-2 – No PPD condition head acceleration components.

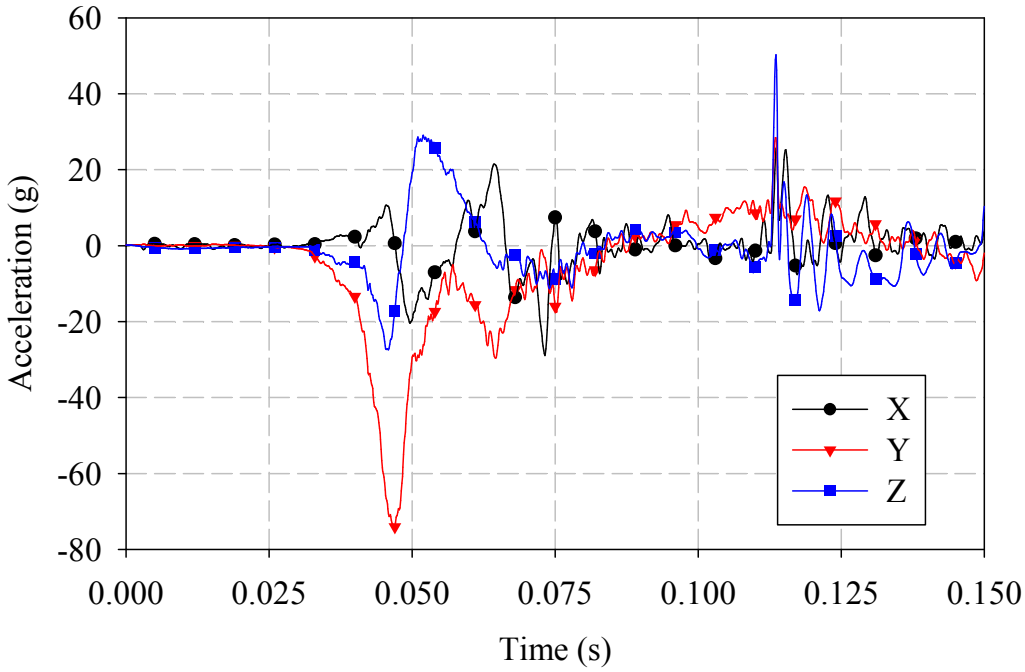

Figure B-3 – HRS condition head acceleration components.

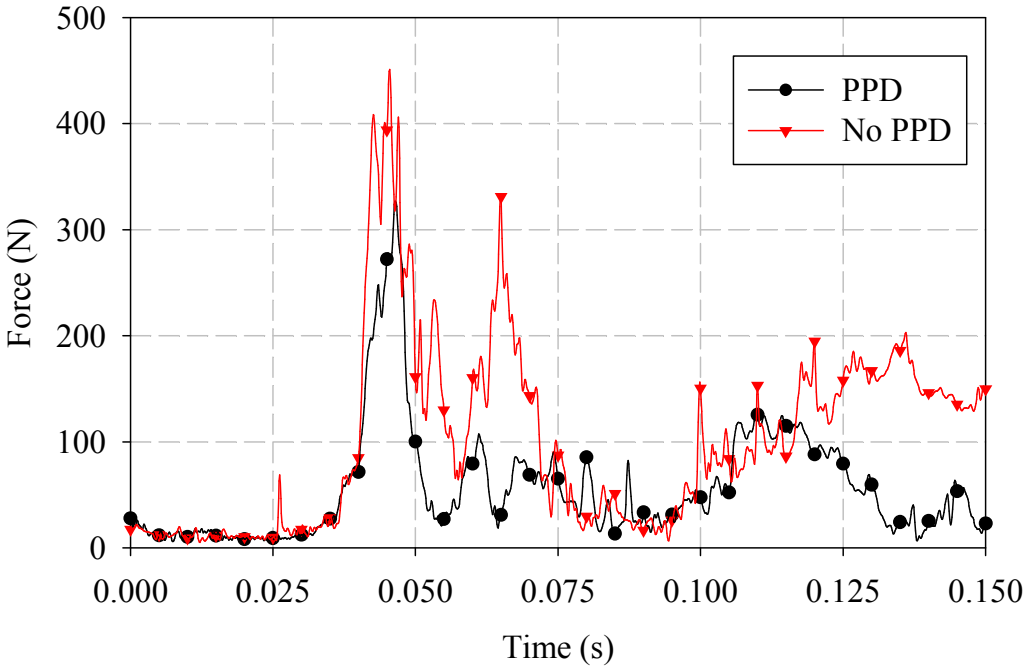

(a)

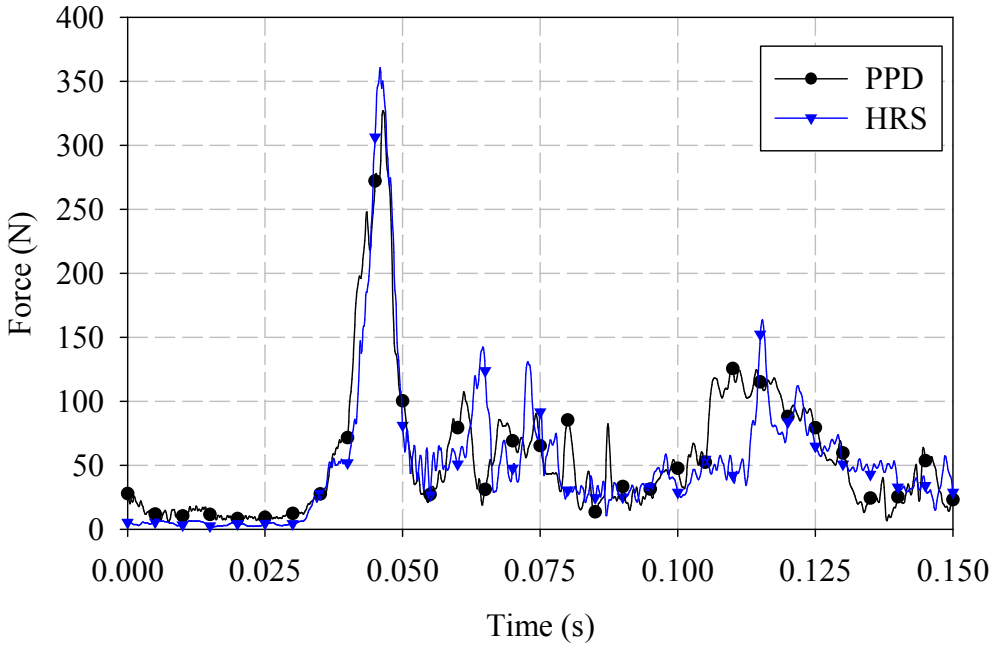

(b)

Figure B-4 – Resultant upper neck forces (a) PPD vs. No PPD and (b) PPD vs. HRS.

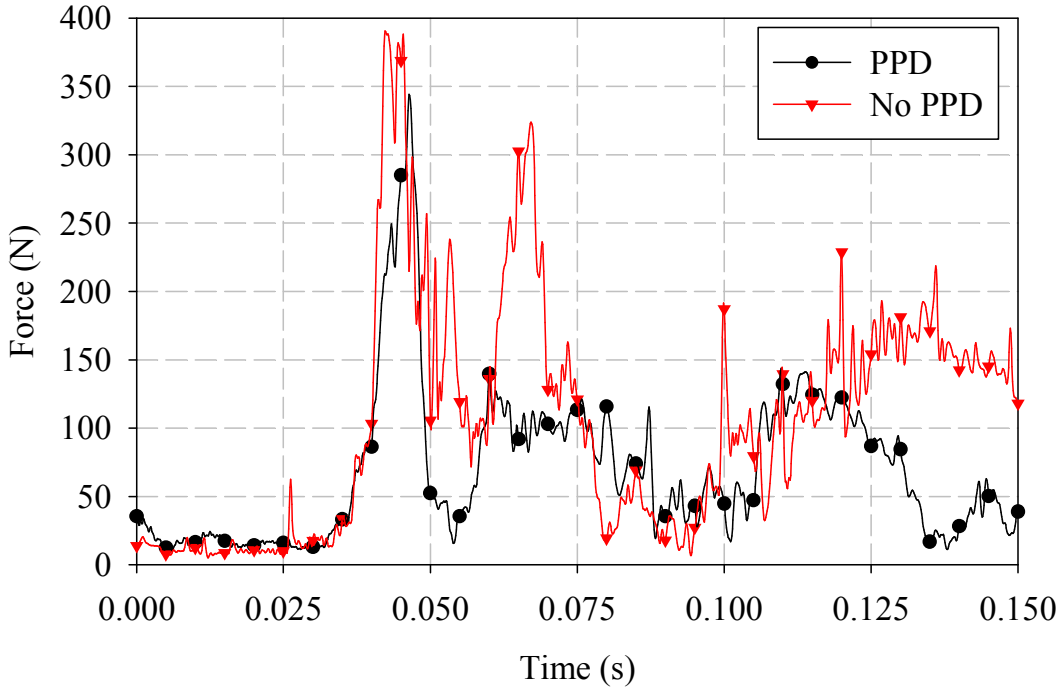

(a)

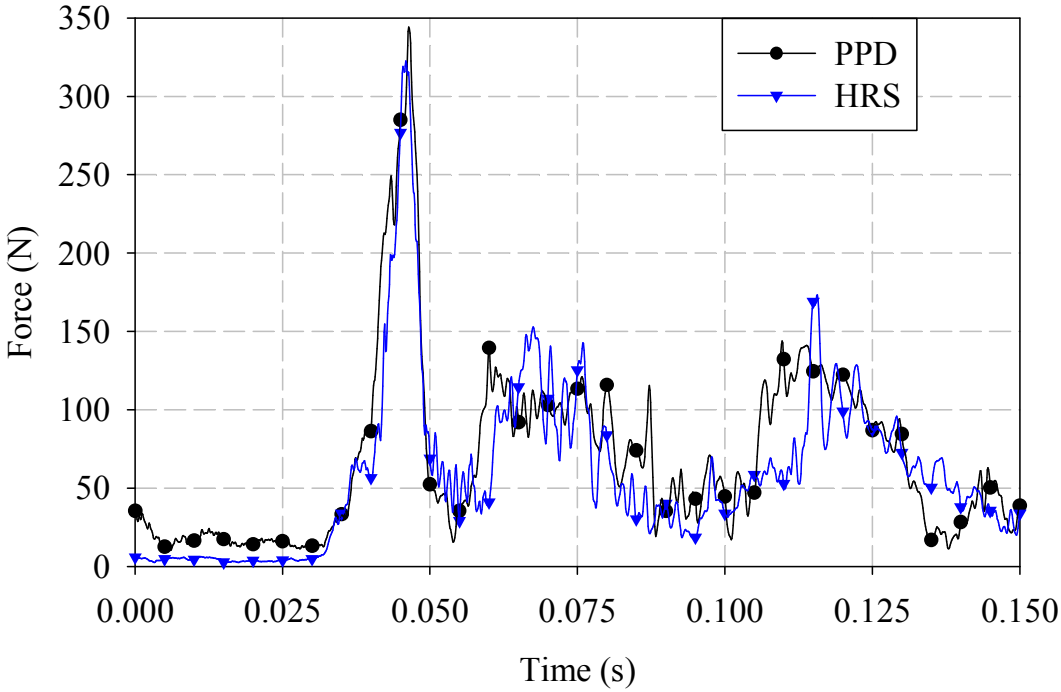

(b)

Figure B-5 – Resultant lower neck forces (a) PPD vs. No PPD and (b) PPD vs. HRS.

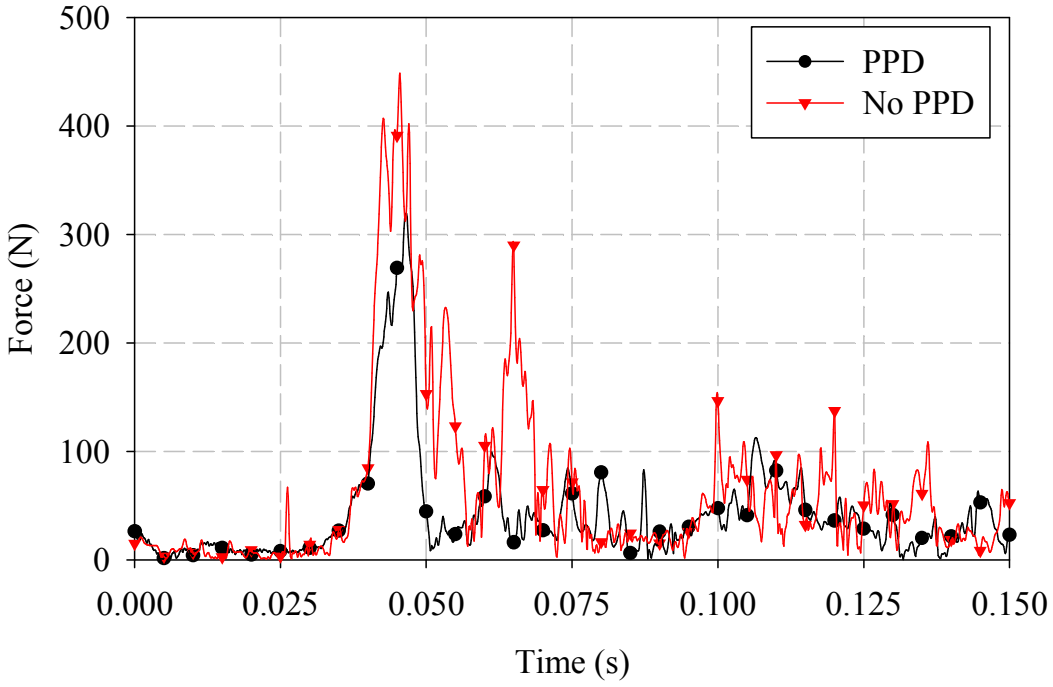

(a)

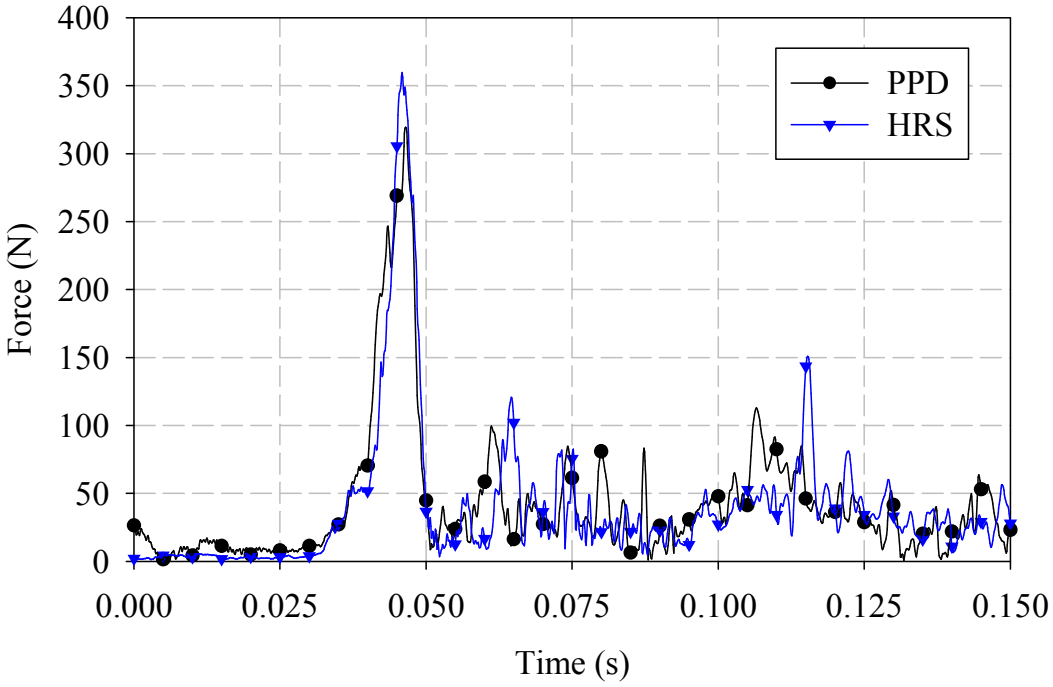

(b)

Figure B-6 – Shear upper neck forces (a) PPD vs. No PPD and (b) PPD vs. HRS.

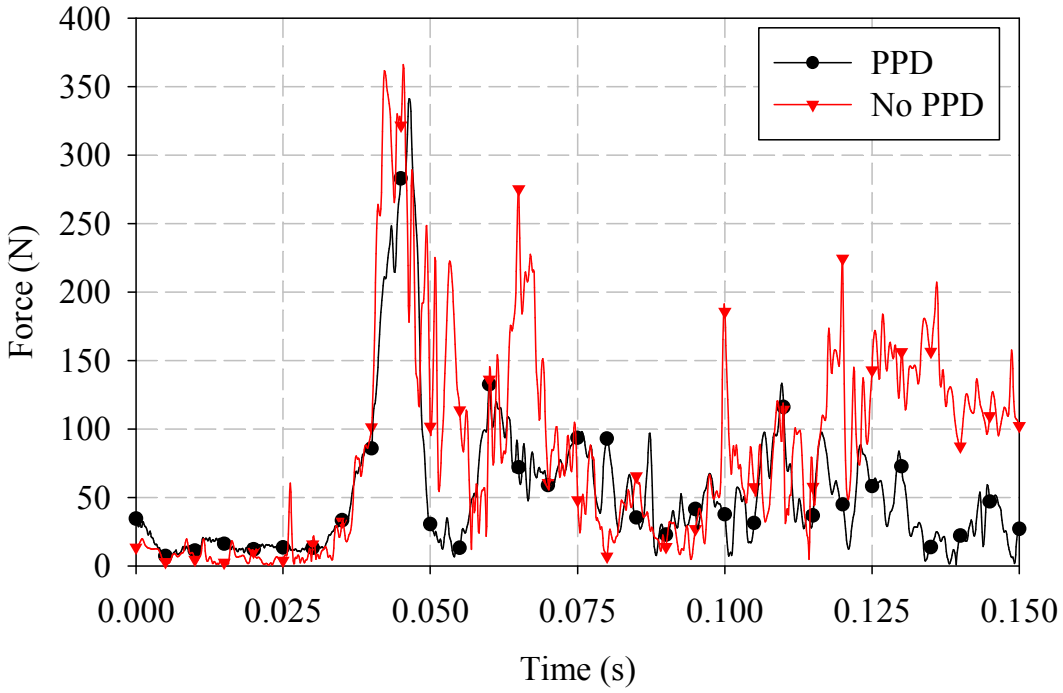

(a)

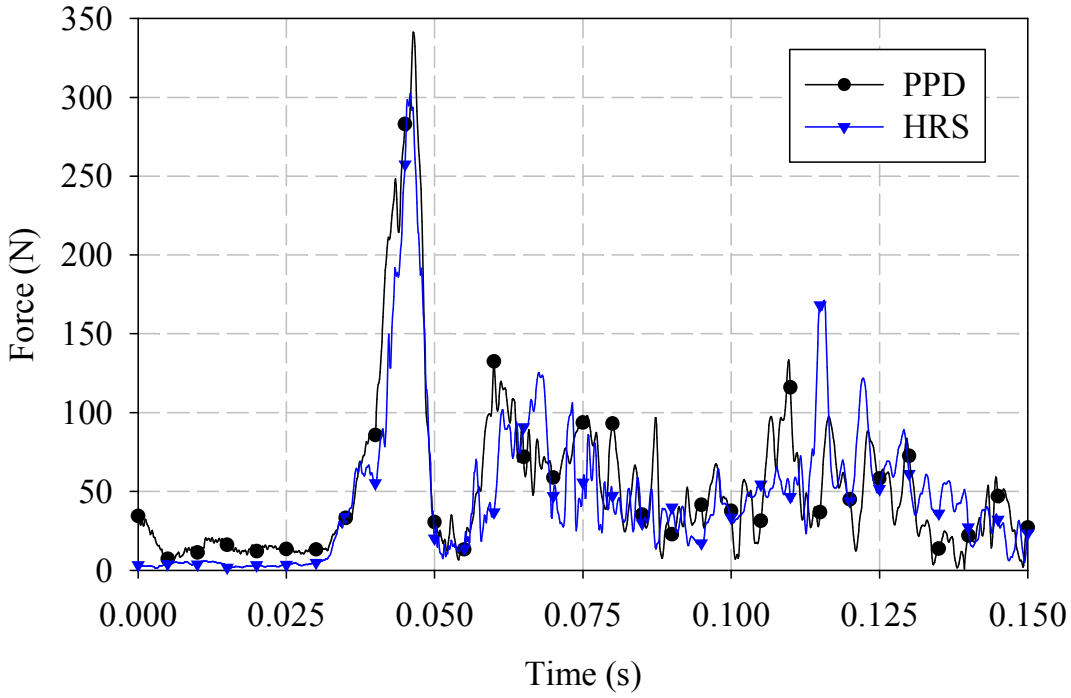

(b)

Figure B-7 – Shear lower neck forces (a) PPD vs. No PPD and (b) PPD vs. HRS.

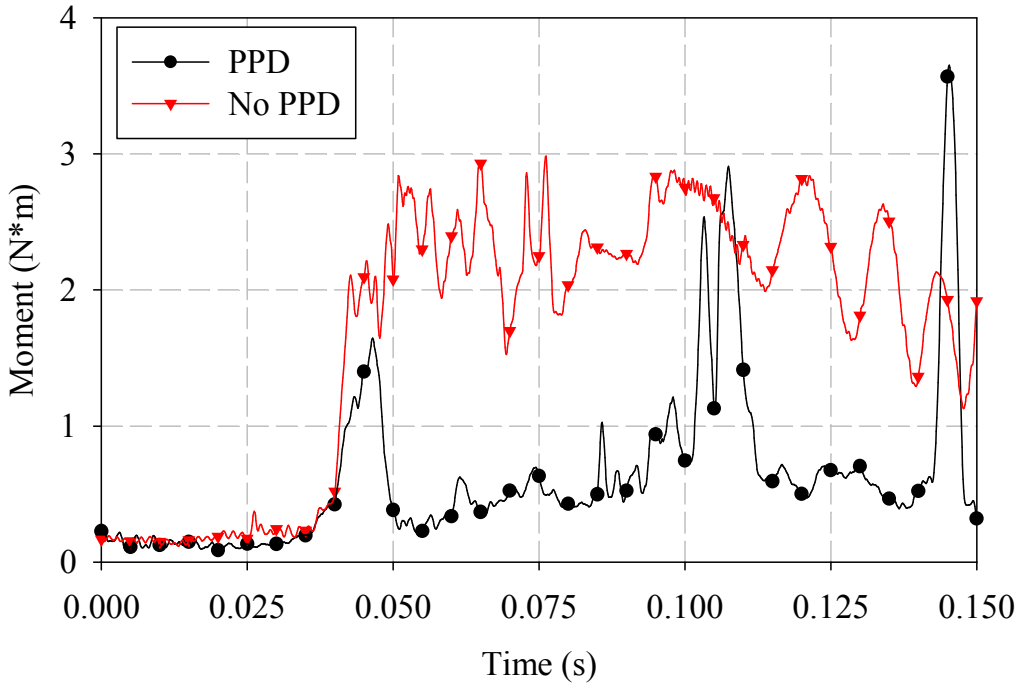

(a)

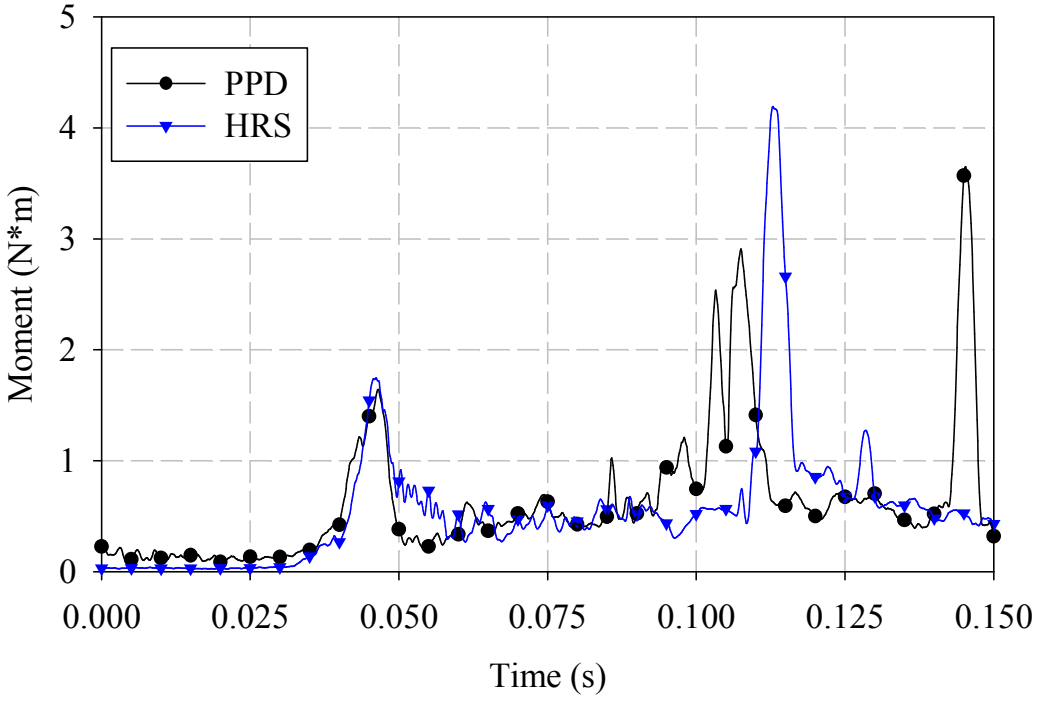

(b)

Figure B-8 – Upper neck moments (a) PPD vs. No PPD and (b) PPD vs. HRS.

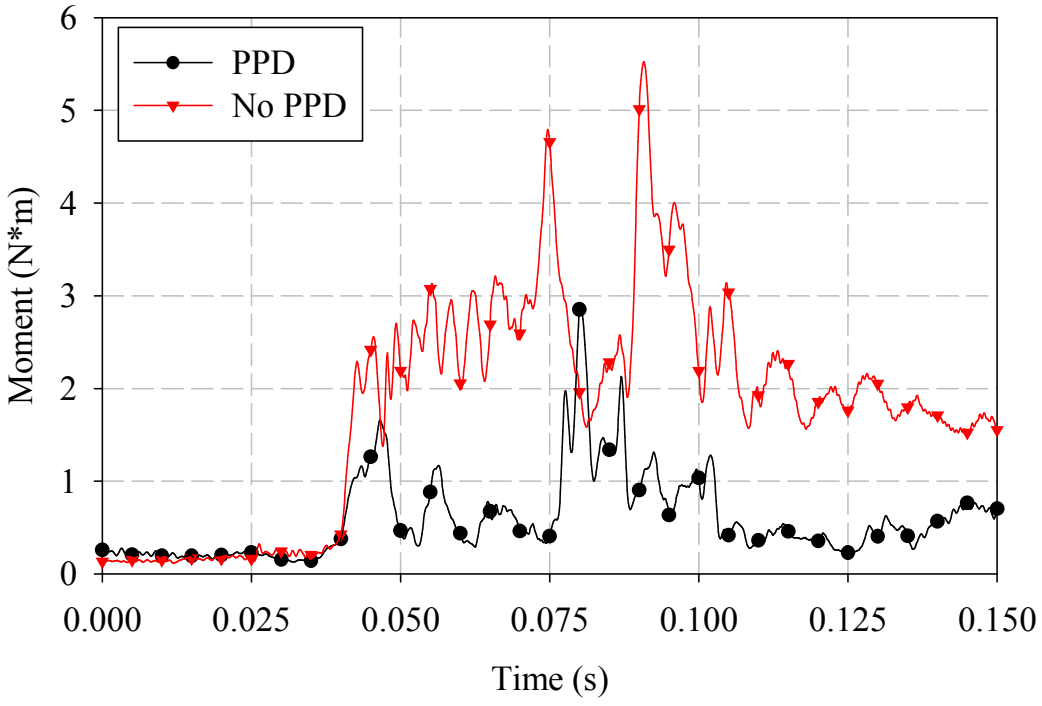

(a)

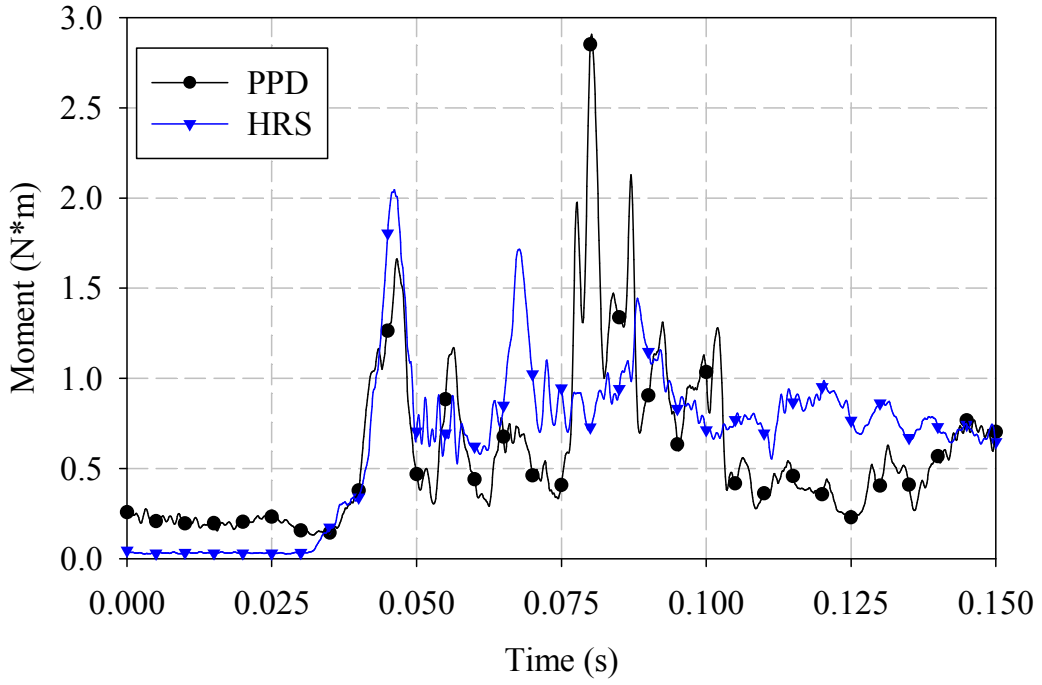

(b)

Figure B-9 – Lower neck moments (a) PPD vs. No PPD and (b) PPD vs. HRS.

APPENDIX C – MATLAB CODE FOR OBTAINING NECK ANGLE DATA

```
clear all
clc
%% This input file was generated by Kazimierz Czubernat for the purpose of
%% extracting and manipulating node location data to obtain Neck Angle data to
%% incorporate into his thesis
%%
%% Before running this file the node data needs to be extracted manually from
%% LS-PREPOST (using same nodes as used in the DATABASE_HISTORY_NODES
%% card and the first 6 points (x, y and z coordinates) need to be plotted and then
%% exported to a .csv file containing a single x axis
data = dlmread('1Nodes.csv', ',',1,0);
time = data(:,1);
nosex = data(:,2);
earLx = data(:,3);
buttx = data(:,4);
neckBx = data(:,5);
neckFx = data(:,6);
earRx = data(:,7);
nosey = data(:,8);
earLy = data(:,9);
butty = data(:,10);
neckBy = data(:,11);
neckFy = data(:,12);
earRy = data(:,13);
nosez = data(:,14);
earLz = data(:,15);
buttz = data(:,16);
neckBz = data(:,17);
neckFz = data(:,18);
earRz = data(:,19);
```

```
%% All Variables are now defined and the midpoints need to be found for the two
%% points associated with the ear and the two points associated with the neck
earx = (earLx+earRx)/2;
eary = (earLy+earRy)/2;
earz = (earLz+earRz)/2;
neckx = (neckBx+neckFx)/2;
necky = (neckBy+neckFy)/2;
neckz = (neckBz+neckFz)/2;
%% Now we are left with 4 points of interest (the neck center, the butt,
%% the center of both ears and the nose
%%
%% These points will be used to generate two vectors which will in turn be
%% used to compute the neck angle
BUTT = [buttx butty buttz];
NECK = [neckx necky neckz];
EAR = [earx eary earz];
NOSE = [nosex nosey nosez];
V1 = (NOSE-EAR)';
V2 = (BUTT-NECK)';
V1V2 = (dot(V1,V2));
magV1 = norm(V1,'cols');
magV2 = norm(V2,'cols');
X = (V1V2./(magV1.*magV2));
ANGLE = [acos(X)*(180/pi)]';
plot (time, ANGLE);
expdata = [time, ANGLE];
dlmwrite ('AngleData.csv', expdata, ',');
```

APPENDIX D – PERMISSIONS

Above is the permission to reuse the content found in Figure 1 in any thesis or dissertation.

VITA AUCTORIS

Mr. Kazimierz Czubernat was born in 1989 in Wingham, Ontario. He graduated from L'Essor high school, Tecumseh, Ontario in 2007. He then went on to the University of Windsor to obtain his Bachelor of Applied Science in Mechanical Engineering in 2011. He is working towards his Master's degree in Mechanical Engineering at the University of Windsor in 2014.